

## Impact Factor:

ISRA (India) = 6.317  
ISI (Dubai, UAE) = 1.582  
GIF (Australia) = 0.564  
JIF = 1.500

SIS (USA) = 0.912  
ПИИИ (Russia) = 3.939  
ESJI (KZ) = 9.035  
SJIF (Morocco) = 7.184

ICV (Poland) = 6.630  
PIF (India) = 1.940  
IBI (India) = 4.260  
OAJI (USA) = 0.350

SOI: [1.1/TAS](#) DOI: [10.15863/TAS](#)

### International Scientific Journal Theoretical & Applied Science

p-ISSN: 2308-4944 (print) e-ISSN: 2409-0085 (online)

Year: 2022 Issue: 03 Volume: 107

Published: 22.03.2022 <http://T-Science.org>

QR – Issue



QR – Article



#### Denis Chemezov

Vladimir Industrial College  
M.Sc.Eng., Corresponding Member of International Academy of  
Theoretical and Applied Sciences, Lecturer, Russian Federation  
<https://orcid.org/0000-0002-2747-552X>  
[vic-science@yandex.ru](mailto:vic-science@yandex.ru)

#### Akbar Juraev

Navoi State Mining Institute  
PhD of Engineering, Republic of Uzbekistan

#### Ilya Yakovlev

Vladimir Industrial College  
Student, Russian Federation

#### Danil Sukhorukov

Vladimir Industrial College  
Student, Russian Federation

#### Artyom Gorechnin

Vladimir Industrial College  
Student, Russian Federation

#### Yuriy Mironov

Vladimir Industrial College  
Student, Russian Federation

#### Aleksey Kuzin

Vladimir Industrial College  
Student, Russian Federation

#### Vyacheslav Matveev

«Security Navigator» LLC  
Mechanic, Vladimir, Russian Federation

## REFERENCE DATA OF PRESSURE DISTRIBUTION ON THE SURFACES OF AIRFOILS HAVING THE NAMES BEGINNING WITH THE LETTER G (THE FIRST PART)

**Abstract:** The results of the computer calculation of air flow around the airfoils having the names beginning with the letter G are presented in the article. The contours of pressure distribution on the surfaces of the airfoils at the angles of attack of 0, 15 and -15 degrees in conditions of the subsonic airplane flight speed were obtained.

**Key words:** the airfoil, the angle of attack, pressure, the surface.

**Language:** English

**Citation:** Chemezov, D., et al. (2022). Reference data of pressure distribution on the surfaces of airfoils having the names beginning with the letter G (the first part). *ISJ Theoretical & Applied Science*, 03 (107), 701-784.

## Impact Factor:

ISRA (India) = 6.317	SIS (USA) = 0.912	ICV (Poland) = 6.630
ISI (Dubai, UAE) = 1.582	ПИИИ (Russia) = 3.939	PIF (India) = 1.940
GIF (Australia) = 0.564	ESJI (KZ) = 9.035	IBI (India) = 4.260
JIF = 1.500	SJIF (Morocco) = 7.184	OAJI (USA) = 0.350

Soi: <http://s-o-i.org/1.1/TAS-03-107-51> Doi:  <https://dx.doi.org/10.15863/TAS.2022.03.107.51>  
 Scopus ASCC: 1507.

### Introduction

Creating reference materials that determine the most accurate pressure distribution on the airfoils surfaces is an actual task of the airplane aerodynamics.

### Materials and methods

The study of air flow around the airfoils was carried out in a two-dimensional formulation by means of the computer calculation in the *Comsol Multiphysics* program. The airfoils in the cross section were taken as objects of research [1-19]. In this work,

the airfoils having the names beginning with the letter *G* were adopted. Air flow around the airfoils was carried out at the angles of attack ( $\alpha$ ) of 0, 15 and -15 degrees. The flight speed of the airplane in each case was subsonic. The airplane flight in the atmosphere was carried out under normal weather conditions. The geometric characteristics of the studied airfoils are presented in the Table 1. The geometric shapes of the airfoils in the cross section are presented in the Table 2.

**Table 1. The geometric characteristics of the airfoils.**

Airfoil name	Max. thickness	Max. camber	Leading edge radius	Trailing edge thickness
<i>G 3</i>	7.82% at 20.0% of the chord	4.0% at 30.0% of the chord	0.8462%	0.0%
<i>G 4</i>	6.68% at 20.0% of the chord	3.34% at 20.0% of the chord	0.8544%	0.24%
<i>G 5</i>	8.72% at 15.0% of the chord	3.41% at 30.0% of the chord	1.1895%	0.6%
<i>G 6</i>	10.0% at 20.0% of the chord	5.0% at 20.0% of the chord	1.7205%	0.0%
<i>GEMINI (smoothed)</i>	15.38% at 34.2% of the chord	2.2% at 37.9% of the chord	1.1754%	0.015%
<i>GIII BL0</i>	11.0% at 35.3% of the chord	0.74% at 15.2% of the chord	0.5686%	0.0359%
<i>GIII BL126</i>	8.77% at 45.1% of the chord	1.19% at 30.1% of the chord	0.3501%	0.036%
<i>GIII BL145</i>	8.26% at 45.1% of the chord	1.3% at 30.1% of the chord	0.2996%	0.037%
<i>GIII BL167</i>	8.29% at 45.1% of the chord	1.3% at 30.0% of the chord	0.3266%	0.036%
<i>GIII BL207</i>	8.32% at 40.0% of the chord	1.29% at 30.0% of the chord	0.3832%	0.036%
<i>GIII BL288</i>	8.45% at 40.0% of the chord	1.33% at 25.0% of the chord	0.5648%	0.036%
<i>GIII BL332</i>	8.49% at 35.0% of the chord	1.39% at 25.0% of the chord	0.7262%	0.036%
<i>GIII BL369</i>	8.53% at 35.0% of the chord	1.5% at 25.0% of the chord	0.9153%	0.036%
<i>GIII BL387</i>	8.55% at 35.0% of the chord	1.58% at 25.0% of the chord	1.0296%	0.036%
<i>GIII BL430</i>	8.51% at 34.9% of the chord	1.86% at 24.9% of the chord	1.4089%	0.036%
<i>GIII BL45</i>	10.45% at 35.2% of the chord	0.81% at 25.2% of the chord	0.51%	0.0369%
<i>GIII BL450</i>	8.42% at 34.9% of the chord	2.07% at 19.9% of the chord	1.671%	0.036%
<i>GIII BL75</i>	9.93% at 40.2% of the chord	0.92% at 30.2% of the chord	0.4589%	0.0369%
<i>GIII BL86</i>	9.71% at 40.1% of the chord	0.97% at 30.1% of the chord	0.4383%	0.0369%
<i>Gilroy</i>	8.6% at 20.0% of the chord	8.1% at 40.0% of the chord	1.1439%	0.4%
<i>GM15</i>	6.74% at 20.5% of the chord	4.76% at 49.3% of the chord	0.4483%	0.007%
<i>GM15 (smoothed)</i>	6.74% at 20.5% of the chord	4.76% at 49.3% of the chord	0.4483%	0.007%
<i>GMARTIN2</i>	13.47% at 20.0% of the chord	7.66% at 30.0% of the chord	1.2675%	0.0%
<i>GMARTIN3</i>	13.77% at 30.0% of the chord	6.89% at 30.0% of the chord	1.6865%	0.0%
<i>GMARTIN4</i>	15.49% at 30.0% of the chord	7.67% at 30.0% of the chord	1.3073%	0.0%
<i>GO-398B</i>	10.0% at 30.0% of the chord	6.32% at 30.0% of the chord	1.1708%	0.0%
<i>GO-436B</i>	11.08% at 30.0% of the chord	5.54% at 30.0% of the chord	1.1506%	0.0%
<i>GO-624B</i>	10.0% at 30.0% of the chord	2.71% at 0.0% of the chord	1.1014%	0.25%
<i>GO-7955</i>	10.0% at 30.0% of the chord	5.0% at 30.0% of the chord	0.9932%	0.5%
<i>GO-795B</i>	8.0% at 30.0% of the chord	4.0% at 30.0% of the chord	0.7812%	0.4%
<i>GOE 100 (SOPWITH)</i>	6.57% at 20.0% of the chord	3.59% at 40.0% of the chord	0.6102%	0.4%
<i>GOE 101</i>	6.9% at 30.0% of the chord	3.96% at 30.0% of the chord	0.6737%	0.0%
<i>GOE 10K</i>	3.85% at 50.0% of the chord	1.42% at 60.0% of the chord	1.6285%	0.0%
<i>GOE 113</i>	6.65% at 30.0% of the chord	3.09% at 40.0% of the chord	0.6055%	0.3%
<i>GOE 114 (MVA MK,1)</i>	9.54% at 30.1% of the chord	3.5% at 50.0% of the chord	0.6774%	0.0%
<i>GOE 115 (MVA MK,2)</i>	9.69% at 30.1% of the chord	3.73% at 40.0% of the chord	0.7549%	0.0%
<i>GOE 116 (MVA MK,3)</i>	9.3% at 40.0% of the chord	4.08% at 40.0% of the chord	0.6686%	0.35%
<i>GOE 117 (MVA MK,4)</i>	8.99% at 30.0% of the chord	4.57% at 40.0% of the chord	0.7396%	0.0%
<i>GOE 118 (MVA MK,7)</i>	8.64% at 30.0% of the chord	5.73% at 40.0% of the chord	0.5612%	0.21%
<i>GOE 11K</i>	7.45% at 50.0% of the chord	2.74% at 60.0% of the chord	1.5346%	0.0%
<i>GOE 121 (MVA H,1)</i>	6.64% at 20.0% of the chord	4.6% at 40.0% of the chord	0.8994%	0.2%
<i>GOE 122 (MVA H,2)</i>	7.3% at 30.0% of the chord	4.06% at 30.0% of the chord	0.8012%	0.25%
<i>GOE 123</i>	5.4% at 25.0% of the chord	5.7% at 40.0% of the chord	0.8395%	0.2%
<i>GOE 124 (MVA H,4)</i>	7.92% at 30.0% of the chord	5.56% at 40.0% of the chord	1.0691%	0.5%
<i>GOE 12K</i>	11.1% at 50.0% of the chord	4.08% at 60.0% of the chord	1.7637%	0.0%
<i>GOE 133 (MVA H,11)</i>	7.9% at 30.0% of the chord	4.32% at 30.0% of the chord	0.933%	0.2%
<i>GOE 134 (MVA H,12)</i>	9.45% at 30.0% of the chord	4.1% at 30.0% of the chord	0.9446%	0.9%
<i>GOE 137 (MVA H,15)</i>	8.59% at 30.0% of the chord	4.42% at 40.0% of the chord	0.823%	0.29%

**Impact Factor:**

<b>SISRA (India) = 6.317</b>	<b>SIS (USA) = 0.912</b>	<b>ICV (Poland) = 6.630</b>
<b>ISI (Dubai, UAE) = 1.582</b>	<b>ПИИИ (Russia) = 3.939</b>	<b>PIF (India) = 1.940</b>
<b>GIF (Australia) = 0.564</b>	<b>ESJI (KZ) = 9.035</b>	<b>IBI (India) = 4.260</b>
<b>JIF = 1.500</b>	<b>SJIF (Morocco) = 7.184</b>	<b>OAJI (USA) = 0.350</b>

GOE 13K	14.8% at 50.0% of the chord	5.45% at 60.0% of the chord	2.4025%	0.0%
GOE 14	9.89% at 30.0% of the chord	6.93% at 30.0% of the chord	2.1288%	0.13%
GOE 140 (MVA H,17)	8.78% at 30.0% of the chord	5.29% at 30.0% of the chord	0.912%	0.58%
GOE 142 (MVA H,19)	6.16% at 25.0% of the chord	3.85% at 35.0% of the chord	0.5504%	0.2%
GOE 143 (MVA H,20)	7.44% at 20.0% of the chord	3.79% at 30.0% of the chord	0.9288%	0.29%
GOE 144 (MVA H,21)	7.31% at 20.0% of the chord	4.72% at 40.0% of the chord	0.7757%	0.0%
GOE 147 (MVA H,6)	7.55% at 15.0% of the chord	3.76% at 30.0% of the chord	0.8051%	0.33%
GOE 14K	12.0% at 50.0% of the chord	2.7% at 50.0% of the chord	1.647%	0.0%
GOE 15	8.99% at 29.9% of the chord	7.75% at 29.9% of the chord	1.6324%	0.0%
GOE 155 (SSW D,1)	7.02% at 30.0% of the chord	5.28% at 40.0% of the chord	0.78%	0.4%
GOE 15K	15.0% at 50.0% of the chord	3.38% at 50.0% of the chord	1.9037%	0.0%
GOE 164 (MVA MK,10)	8.86% at 20.0% of the chord	6.64% at 40.0% of the chord	0.9319%	0.11%
GOE 165 (MVA MK,11)	12.12% at 20.1% of the chord	5.75% at 49.9% of the chord	0.8157%	0.12%
GOE 167 (V,KARMAN PROP,2)	10.09% at 30.0% of the chord	4.53% at 30.0% of the chord	0.9413%	0.9%
GOE 16K	18.15% at 50.0% of the chord	4.09% at 50.0% of the chord	2.3493%	0.0%
GOE 173 (ALBATROS 6020)	7.76% at 20.0% of the chord	5.91% at 40.0% of the chord	0.7843%	0.18%
GOE 174 (ALBATROS 5020)	8.58% at 20.0% of the chord	5.57% at 40.0% of the chord	0.9441%	0.29%
GOE 176 (ALBATROS 7020)	10.33% at 20.0% of the chord	5.55% at 40.0% of the chord	0.9451%	0.23%
GOE 177	7.7% at 20.0% of the chord	5.06% at 40.0% of the chord	0.6431%	0.2%
GOE 178	8.5% at 30.0% of the chord	4.4% at 40.0% of the chord	0.8552%	0.3%
GOE 180 (MVA H,26)	8.67% at 30.0% of the chord	4.44% at 40.0% of the chord	0.9595%	0.25%
GOE 182 (MVA H,27)	9.44% at 20.0% of the chord	5.26% at 40.0% of the chord	1.1779%	0.15%
GOE 184 (MVA H,29)	8.3% at 20.0% of the chord	5.28% at 40.0% of the chord	0.9835%	0.22%
GOE 187 (SCH-TTE-LANZ 2U10)	8.28% at 30.0% of the chord	4.84% at 30.0% of the chord	0.8399%	0.5%
GOE 188 (SCH-TTE-LANZ 3U10)	8.94% at 30.0% of the chord	4.39% at 30.0% of the chord	0.8955%	0.5%
GOE 190 (MVA MK,18)	12.67% at 20.1% of the chord	5.93% at 49.9% of the chord	1.4871%	0.0%
GOE 195	8.6% at 20.0% of the chord	5.1% at 50.0% of the chord	1.0727%	0.2%
GOE 198 (L,F,G, 5294)	7.77% at 20.0% of the chord	6.52% at 40.0% of the chord	1.3012%	0.85%
GOE 199 (L,F,G, 5406)	7.33% at 30.0% of the chord	5.18% at 30.0% of the chord	0.9237%	1.1%
GOE 207 (AVIATIK V8)	8.77% at 20.0% of the chord	6.63% at 30.0% of the chord	1.3698%	0.7500%
GOE 210 (DAIMLER)	6.63% at 30.0% of the chord	4.34% at 40.0% of the chord	0.7355%	0.16%
GOE 217 (MVA MK,12)	18.86% at 30.2% of the chord	6.32% at 59.9% of the chord	3.7948%	0.74%
GOE 222 (MVA H,33)	18.48% at 30.2% of the chord	7.17% at 50.0% of the chord	2.0426%	0.3%
GOE 223 (MVA H,34)	18.82% at 30.3% of the chord	5.7% at 50.1% of the chord	1.6158%	0.2%
GOE 225 (MVA H,35)	12.83% at 20.0% of the chord	7.63% at 49.9% of the chord	1.8234%	0.6%
GOE 226 (MVA H,36)	13.89% at 20.0% of the chord	8.07% at 49.9% of the chord	1.9959%	0.2%
GOE 227 (MVA H,37)	14.6% at 25.0% of the chord	7.85% at 50.0% of the chord	1.7179%	0.3%
GOE 228 (MVA H,38)	17.82% at 30.1% of the chord	6.99% at 50.0% of the chord	2.0011%	0.3%
GOE 229 (MVA H,39)	19.35% at 30.3% of the chord	5.91% at 50.1% of the chord	1.4383%	0.2%
GOE 233 (MVA CA4)	11.63% at 20.0% of the chord	8.21% at 49.9% of the chord	1.4716%	0.31%
GOE 234 (MVA CA5)	14.27% at 20.1% of the chord	9.16% at 49.9% of the chord	1.7654%	0.74%
GOE 235 (SCH-TTE-LANZ)	6.54% at 20.0% of the chord	3.54% at 40.0% of the chord	1.3269%	0.32%
GOE 238 (HANSA-BRANDENBURG)	9.8% at 30.0% of the chord	5.51% at 30.0% of the chord	1.4189%	0.0%
GOE 239 (MVA H,31)	11.22% at 20.0% of the chord	6.02% at 40.0% of the chord	1.3413%	0.42%
GOE 240 (KOLLER)	7.0% at 30.0% of the chord	5.16% at 40.0% of the chord	0.8284%	0.22%
GOE 241 (MVA PR,1)	18.82% at 30.1% of the chord	8.37% at 50.0% of the chord	2.6193%	0.4%
GOE 242 (MVA PR,2)	16.17% at 30.0% of the chord	7.51% at 50.0% of the chord	1.4144%	0.4%
GOE 243 (MVA PR,3)	18.91% at 30.1% of the chord	8.39% at 59.9% of the chord	3.5149%	0.3%
GOE 244 (MVA PR,4)	17.68% at 20.0% of the chord	9.98% at 49.9% of the chord	3.0152%	0.2%
GOE 255 (MVA CA,6)	18.57% at 30.4% of the chord	4.81% at 40.3% of the chord	1.5304%	0.5%
GOE 256 (JUNKERS E)	15.99% at 30.1% of the chord	4.71% at 40.1% of the chord	2.174%	0.25%
GOE 257	8.83% at 30.0% of the chord	4.08% at 30.0% of the chord	0.7999%	1.28%
GOE 264	6.42% at 20.0% of the chord	5.69% at 30.0% of the chord	0.7982%	0.64%
GOE 265	7.65% at 15.0% of the chord	7.25% at 40.0% of the chord	1.2222%	0.21%
GOE 269	6.59% at 30.0% of the chord	5.02% at 40.0% of the chord	1.0204%	0.58%
GOE 274 (DAIMLER V)	8.65% at 30.0% of the chord	4.85% at 30.0% of the chord	1.0113%	0.8%
GOE 275 (DAIMLER VI)	7.73% at 20.0% of the chord	4.71% at 30.0% of the chord	1.0714%	0.0%
GOE 276 (DAIMLER VII)	7.26% at 30.0% of the chord	4.03% at 30.0% of the chord	0.8108%	0.8%
GOE 277 (DAIMLER VIII)	8.34% at 30.0% of the chord	4.39% at 30.0% of the chord	0.8834%	0.32%
GOE 278 (DAIMLER IX)	7.44% at 30.0% of the chord	4.26% at 30.0% of the chord	0.9077%	0.2%
GOE 279 (DAIMLER X)	7.43% at 30.0% of the chord	4.73% at 40.0% of the chord	0.9657%	0.37%
GOE 280 (DAIMLER XI)	7.93% at 30.0% of the chord	4.55% at 30.0% of the chord	0.7111%	0.8%
GOE 281 (DAIMLER XII)	8.04% at 30.0% of the chord	4.54% at 40.0% of the chord	0.768%	0.52%
GOE 282 (DAIMLER XIII)	9.12% at 20.0% of the chord	5.02% at 40.0% of the chord	0.9287%	0.64%
GOE 284	17.6% at 30.2% of the chord	5.09% at 40.2% of the chord	3.0865%	0.59%
GOE 285	11.73% at 30.0% of the chord	3.72% at 30.0% of the chord	1.7117%	0.3%
GOE 286	9.35% at 30.0% of the chord	4.1% at 30.0% of the chord	1.0976%	0.5%
GOE 287	8.87% at 30.0% of the chord	4.88% at 40.0% of the chord	0.8427%	0.5%
GOE 288	17.3% at 30.2% of the chord	5.53% at 40.1% of the chord	2.5558%	0.59%

**Impact Factor:**

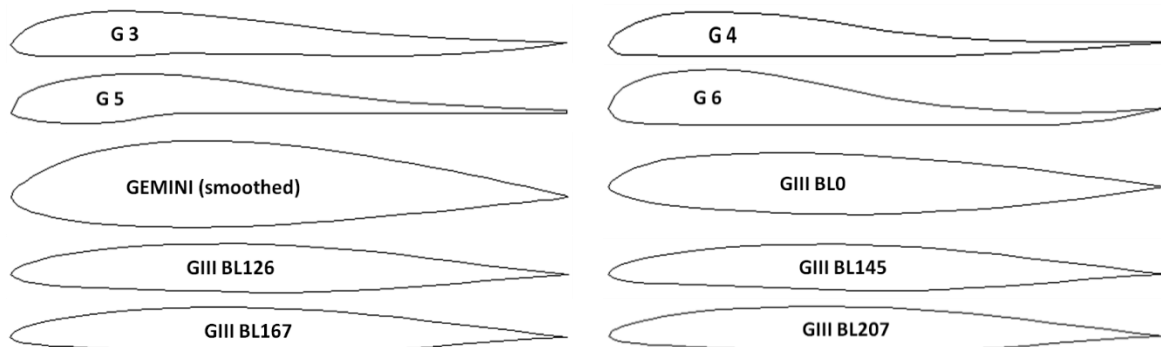
<b>ISRA (India)</b> = <b>6.317</b>	<b>SIS (USA)</b> = <b>0.912</b>	<b>ICV (Poland)</b> = <b>6.630</b>
<b>ISI (Dubai, UAE)</b> = <b>1.582</b>	<b>ПИИИ (Russia)</b> = <b>3.939</b>	<b>PIF (India)</b> = <b>1.940</b>
<b>GIF (Australia)</b> = <b>0.564</b>	<b>ESJI (KZ)</b> = <b>9.035</b>	<b>IBI (India)</b> = <b>4.260</b>
<b>JIF</b> = <b>1.500</b>	<b>SJIF (Morocco)</b> = <b>7.184</b>	<b>OAJI (USA)</b> = <b>0.350</b>

GOE 289 (MVA 289)	16.8% at 30.0% of the chord	6.12% at 40.0% of the chord	2.0069%	0.0%
GOE 290 (MVA 290)	17.51% at 30.3% of the chord	3.84% at 40.3% of the chord	2.6134%	0.6%
GOE 298	12.81% at 20.1% of the chord	4.53% at 40.1% of the chord	2.9101%	0.59%
GOE 29B	9.42% at 20.0% of the chord	6.55% at 30.0% of the chord	1.7223%	0.28%
GOE 300 (FRIEDRICHSHAFEN G20)	8.43% at 30.0% of the chord	6.69% at 30.0% of the chord	1.7904%	0.18%
GOE 301 (FRIEDRICHSHAFEN G13)	9.87% at 30.0% of the chord	6.48% at 40.0% of the chord	1.3725%	0.3%
GOE 303 (FRIEDRICHSHAFEN G03)	9.84% at 30.0% of the chord	5.88% at 40.0% of the chord	1.3128%	0.45%
GOE 304 (FRIEDRICHSHAFEN G02)	8.98% at 30.0% of the chord	6.32% at 40.0% of the chord	1.6525%	0.23%
GOE 308 (MVA H,40)	8.09% at 30.0% of the chord	5.04% at 30.0% of the chord	0.839%	0.0%
GOE 309 (MVA H,41)	8.43% at 30.0% of the chord	4.67% at 30.0% of the chord	0.7504%	0.4%
GOE 310 (MVA H,42)	8.14% at 30.0% of the chord	4.81% at 40.0% of the chord	0.8482%	0.0%
GOE 311 (MVA H,43)	8.44% at 20.0% of the chord	6.07% at 40.0% of the chord	0.8651%	0.42%
GOE 314 (HANSA-BRANDENBURG)	8.03% at 30.0% of the chord	4.69% at 30.0% of the chord	1.1653%	0.0%
GOE 315 (HANSA-BRANDENBURG III,5)	8.08% at 30.0% of the chord	4.1% at 30.0% of the chord	1.0559%	0.0%
GOE 316 (HANSA-BRANDENBURG IV,5)	9.08% at 30.0% of the chord	4.24% at 30.0% of the chord	1.0459%	0.42%
GOE 318 (HANSA-BRANDENBURG VI,5)	9.13% at 30.0% of the chord	4.32% at 30.0% of the chord	0.9949%	0.4%
GOE 319 (HANSA-BRANDENBURG II)	10.24% at 30.0% of the chord	5.76% at 30.0% of the chord	1.8855%	0.11%
GOE 320 (HANSA-BRANDENBURG II,1)	12.32% at 30.0% of the chord	6.19% at 30.0% of the chord	2.4739%	0.53%
GOE 321 (HANSA-BRANDENBURG III,1)	11.15% at 30.0% of the chord	5.14% at 30.0% of the chord	1.5254%	0.43%
GOE 322 (HANSA-BRANDENBURG IV,1)	13.06% at 30.0% of the chord	6.02% at 30.0% of the chord	1.4689%	0.6%
GOE 323 (HANSA-BRANDENBURG V,1)	11.04% at 30.0% of the chord	5.17% at 30.0% of the chord	1.5893%	0.11%
GOE 324 (HANSA-BRANDENBURG)	13.12% at 30.0% of the chord	5.94% at 30.0% of the chord	2.2189%	0.24%
GOE 325 (PFALZ 54)	8.2% at 20.0% of the chord	4.67% at 30.0% of the chord	0.8395%	0.3%
GOE 326 (PFALZ 55)	8.18% at 30.0% of the chord	4.72% at 40.0% of the chord	0.9193%	0.3%
GOE 328	8.2% at 30.0% of the chord	4.35% at 30.0% of the chord	1.0403%	0.5%
GOE 329 (PFALZ 58)	10.16% at 30.0% of the chord	5.53% at 30.0% of the chord	1.1333%	0.6%
GOE 330 (PFALZ 59)	10.2% at 30.0% of the chord	5.76% at 40.0% of the chord	1.0371%	0.1%
GOE 331 (PFALZ 60)	10.64% at 30.0% of the chord	6.86% at 40.0% of the chord	1.5909%	0.26%
GOE 332 (PFALZ 61)	11.78% at 30.0% of the chord	6.36% at 40.0% of the chord	1.4504%	0.3%
GOE 335 (D,F,W.)	6.85% at 20.0% of the chord	4.8% at 40.0% of the chord	0.6993%	0.0%
GOE 336 (MVA H,44)	8.95% at 30.0% of the chord	5.4% at 30.0% of the chord	1.0029%	0.3%
GOE 342	5.4% at 20.0% of the chord	6.22% at 40.0% of the chord	0.8803%	0.3%

**Note:**

G 3, G 4, G 5, G6 (F. Gale' (Italy));  
 GIII BL0 (Grumman/Gulfstream GIII transonic airfoils);  
 Gilroy (B. Gilroy (USA));  
 GM15 (Gilbert Morris – F1C class free flight flapper);  
 GOE 10K (Gottingen 10K airfoil).

**Table 2. The geometric shapes of the airfoils in the cross section.**



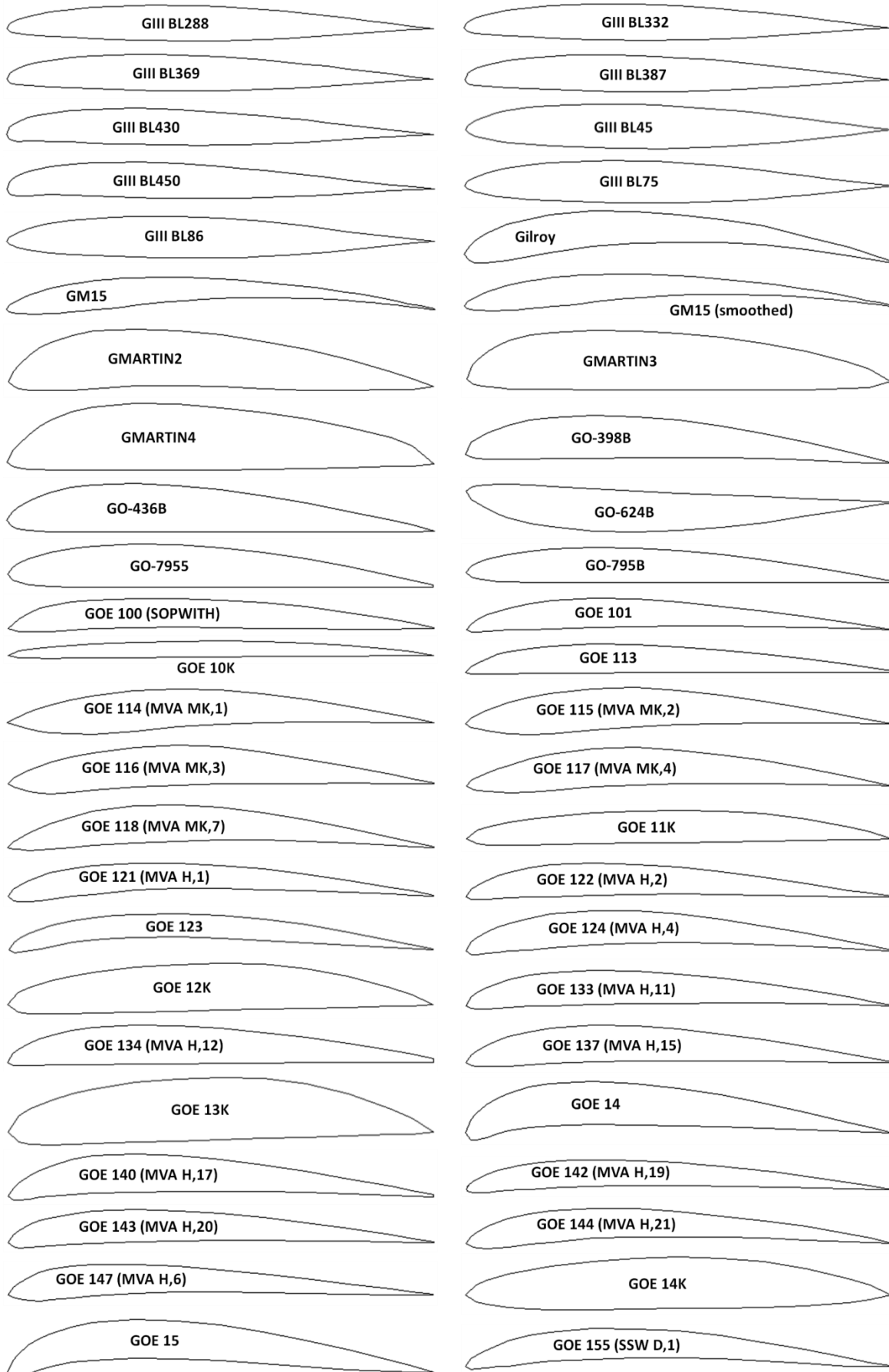


**Impact Factor:**

**ISRA (India) = 6.317**  
**ISI (Dubai, UAE) = 1.582**  
**GIF (Australia) = 0.564**  
**JIF = 1.500**

**SIS (USA) = 0.912**  
**ПИИЦ (Russia) = 3.939**  
**ESJI (KZ) = 9.035**  
**SJIF (Morocco) = 7.184**

**ICV (Poland) = 6.630**  
**PIF (India) = 1.940**  
**IBI (India) = 4.260**  
**OAJI (USA) = 0.350**

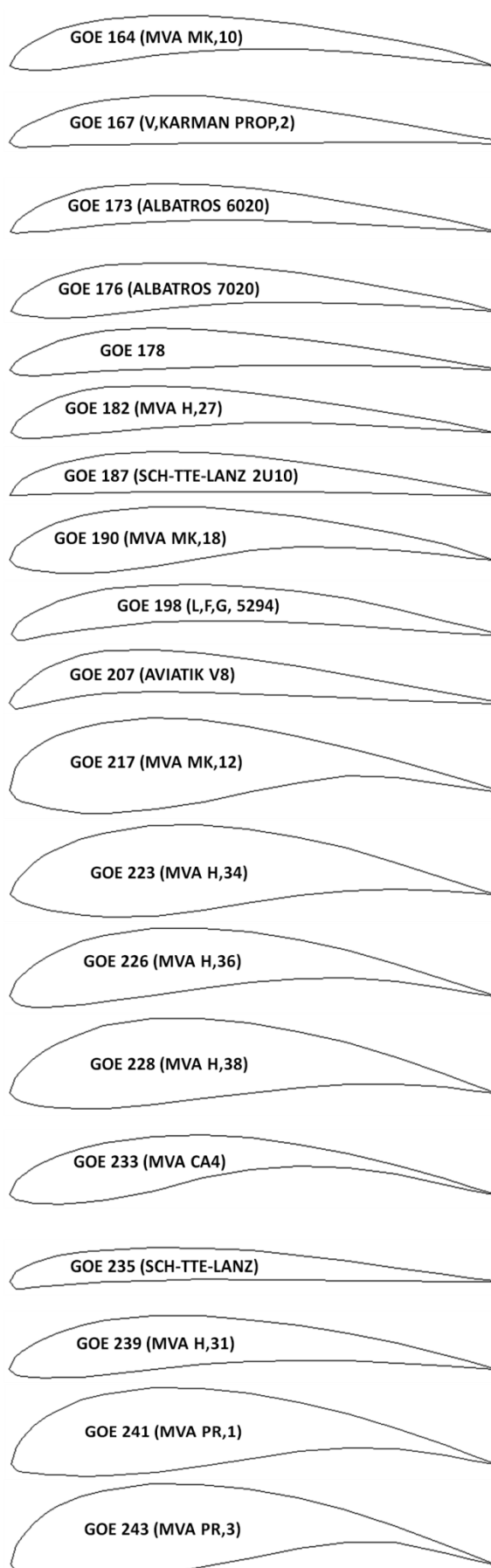
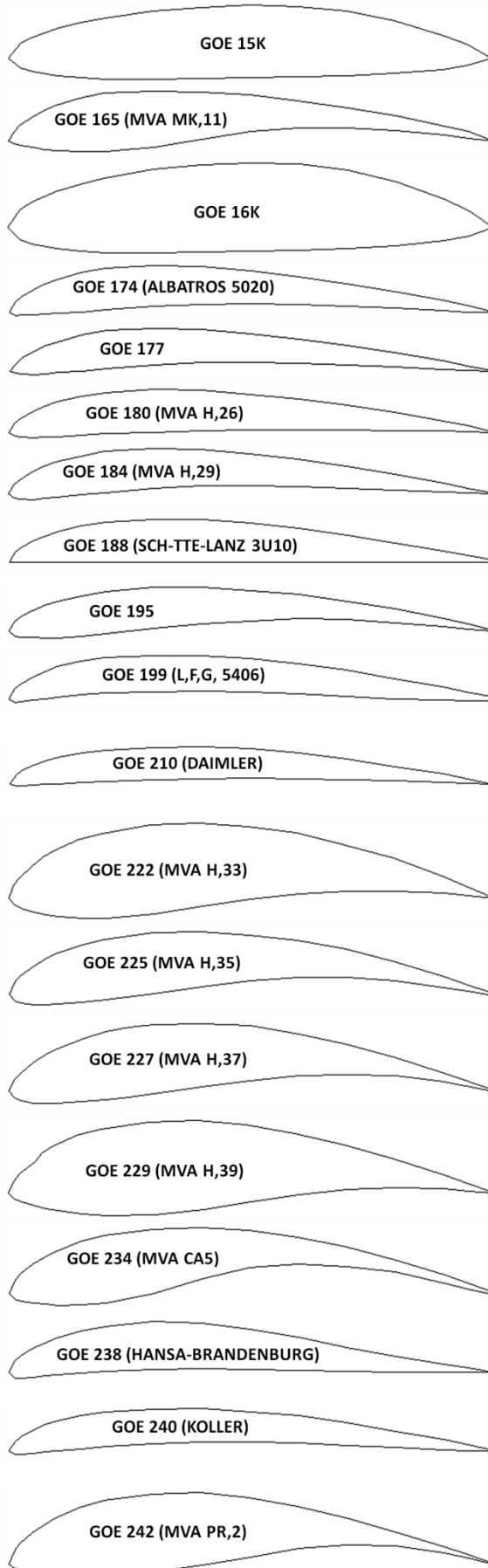


**Impact Factor:**

**ISRA (India) = 6.317**  
**ISI (Dubai, UAE) = 1.582**  
**GIF (Australia) = 0.564**  
**JIF = 1.500**

**SIS (USA) = 0.912**  
**ПИИЦ (Russia) = 3.939**  
**ESJI (KZ) = 9.035**  
**SJIF (Morocco) = 7.184**

**ICV (Poland) = 6.630**  
**PIF (India) = 1.940**  
**IBI (India) = 4.260**  
**OAJI (USA) = 0.350**

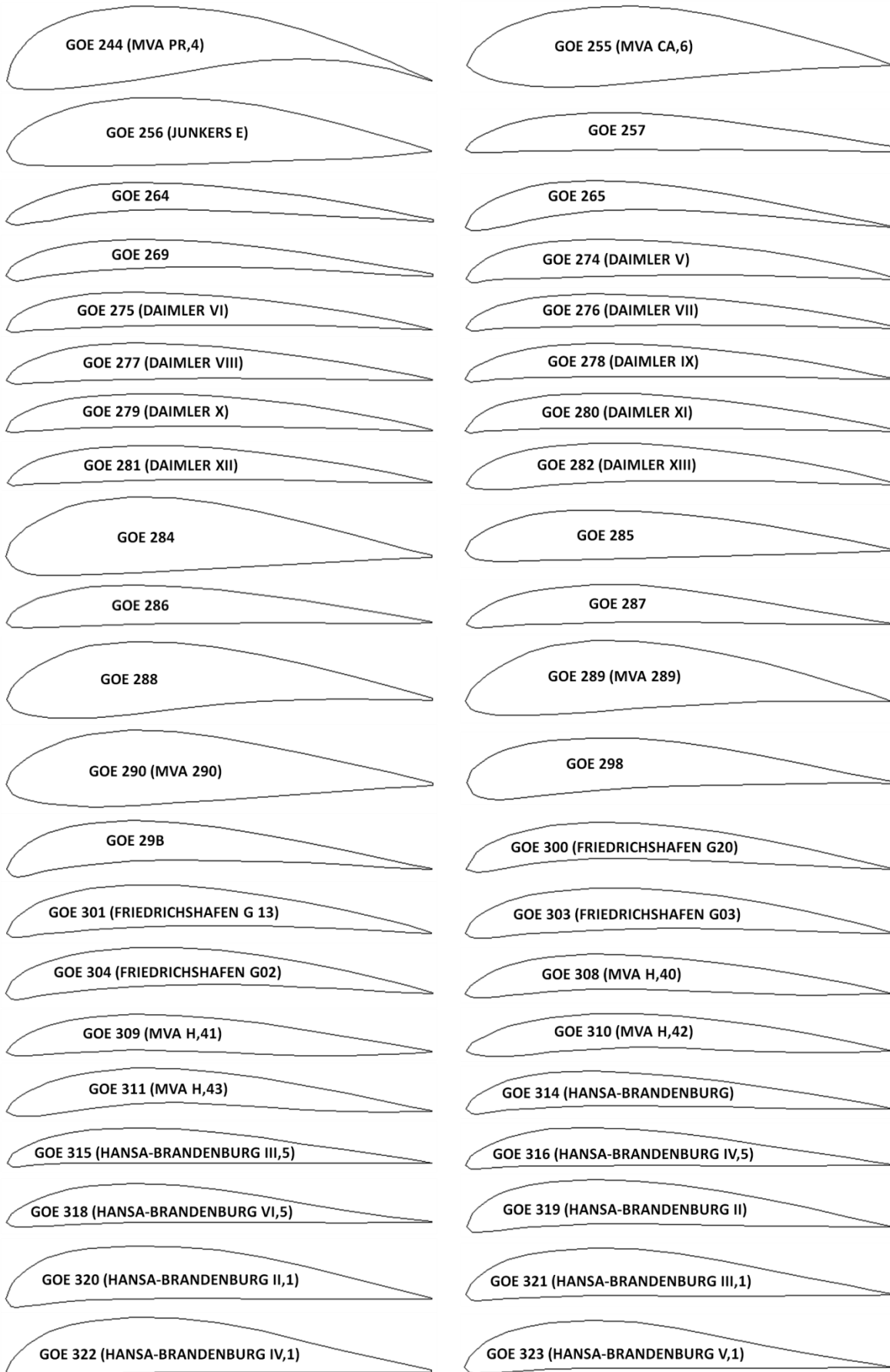


**Impact Factor:**

**ISRA (India) = 6.317**  
**ISI (Dubai, UAE) = 1.582**  
**GIF (Australia) = 0.564**  
**JIF = 1.500**

**SIS (USA) = 0.912**  
**ПИИЦ (Russia) = 3.939**  
**ESJI (KZ) = 9.035**  
**SJIF (Morocco) = 7.184**

**ICV (Poland) = 6.630**  
**PIF (India) = 1.940**  
**IBI (India) = 4.260**  
**OAJI (USA) = 0.350**

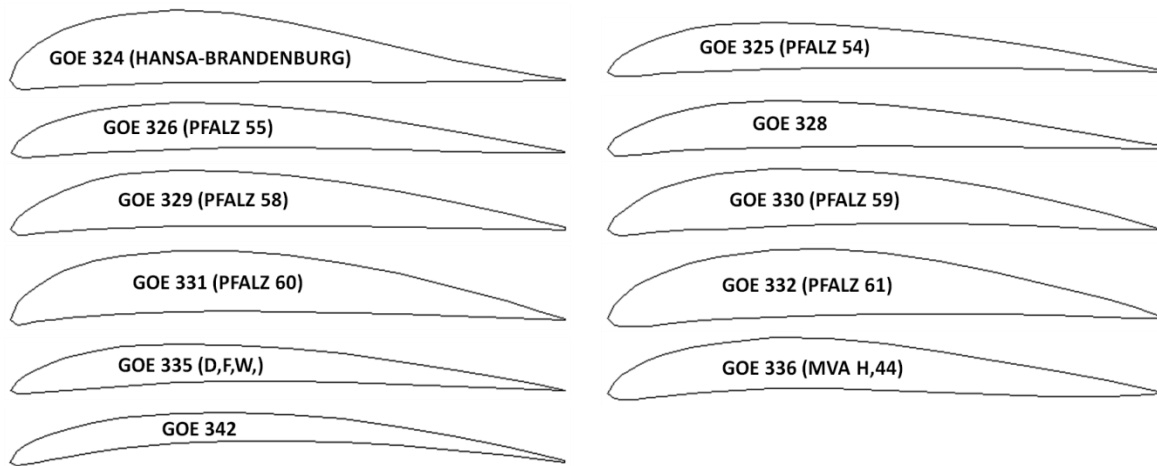


## Impact Factor:

ISRA (India) = 6.317  
ISI (Dubai, UAE) = 1.582  
GIF (Australia) = 0.564  
JIF = 1.500

SIS (USA) = 0.912  
ПИИИ (Russia) = 3.939  
ESJI (KZ) = 9.035  
SJIF (Morocco) = 7.184

ICV (Poland) = 6.630  
PIF (India) = 1.940  
IBI (India) = 4.260  
OAJI (USA) = 0.350



### Results and discussion

The calculated pressure contours on the surfaces of the airfoils at the different angles of attack are presented in the Figs. 1-149. The calculated values on the scale can be represented as the basic values when comparing the pressure drop under conditions of changing the angle of attack of the airfoils. 149 airfoils were studied in the work. The following asymmetric airfoils for the airplane wings have been considered among them:

#### 1. Subsonic airplane.

- convex-concave: GOE 222 (MVA H,33), GOE 217 (MVA MK,12), GOE 223 (MVA H,34), GOE 226 (MVA H,36) etc.;

- flat-convex: GOE 180 (MVA H,26), GOE 277 (DAIMLER VIII), GO-463B, GOE 178 etc.;

- biconvex asymmetric: GEMINI (smoothed), GIII BL369 etc.;

- S-shaped: G3, G4, G6.

#### 2. Transonic airplane.

- biconvex symmetric: GIII BL126, GIII BL145, GIII BL288 etc.

#### 3. Supersonic airplane.

- arc: GOE 10K.

For the airfoils selected above (from each type of the wing profile) used at the subsonic airplane flight speed, the calculated values of pressure changes at the leading edge (drag) were analyzed. The calculated values of positive and negative pressures arising at the different angles of attack of the airfoil are (at  $\alpha = 0/15/-15$  degrees):

GOE 222 (MVA H,33) – 6.72/-25.2/-52.5 kPa;

GOE 217 (MVA MK,12) – 6.64/-28.4/-48 kPa;

GOE 223 (MVA H,34) – 6.66/-29.2/-60.5 kPa;

GOE 226 (MVA H,36) – 6.65/-33.1/-33 kPa;

GOE 180 (MVA H,26) – 6.52/-63.6/-26.5 kPa;

GOE 277 (DAIMLER VIII) – 6.52/-68.7/-22.3

kPa;

GO-463B – 6.62/-61.5/-67.1 kPa;

GOE 178 – 6.54/-77.4/-26.7 kPa;

GEMINI (smoothed) – 6.62/-47.1/-56.1 kPa;

GIII BL369 – 6.5/-73.5/-14.5 kPa;

G3 – 6.51/-79.3/-43.5 kPa;

G4 – 6.48/-76.5/-32.4 kPa;

G6 – 6.48/-37.5/-70 kPa.

The GOE 226 (MVA H,36), GOE 277 (DAIMLER VIII), GIII BL369 and G4 have the best aerodynamic characteristics of the considered airfoils (since drag is the lowest at all angles of attack).

The similar analysis of the aerodynamic characteristics was performed for the airfoils of the wings used at the transonic airplane flight speed. The calculated values of pressures arising at the different angles of attack of the airfoil are (at  $\alpha = 0/15/-15$  degrees):

GIII BL126 – 6.54/-112/-42.5 kPa;

GIII BL145 – 6.55/-109/-36.3 kPa;

GIII BL288 – 6.52/-87.1/-25.3 kPa.

Thus, it can be concluded that for the GIII BL288 airfoil during horizontal flight of the airplane and maneuvers, drag is 0.7 times less than for other airfoils.

The GOE 10K airfoil at the zero, positive and negative angles of attack has low lift and drag, which is due to the need to develop maximum flight speed. The aerodynamic characteristics are improved in conditions of the airplane descent with the given wing airfoil.

The GO-624B airfoil is the inverted version of the GO series airfoils. This airfoil of the wing during horizontal flight of the airplane causes the shift of maximum drag downward relative to the leading edge. When the airplane climbs, there is observed the action of positive pressure on the convex lower surface of the wing airfoil and a twofold decrease in pressure compared to other airfoils of this series.

**Impact Factor:**

ISRA (India) = 6.317	SIS (USA) = 0.912	ICV (Poland) = 6.630
ISI (Dubai, UAE) = 1.582	ПИИЦ (Russia) = 3.939	PIF (India) = 1.940
GIF (Australia) = 0.564	ESJI (KZ) = 9.035	IBI (India) = 4.260
JIF = 1.500	SJIF (Morocco) = 7.184	OAJI (USA) = 0.350

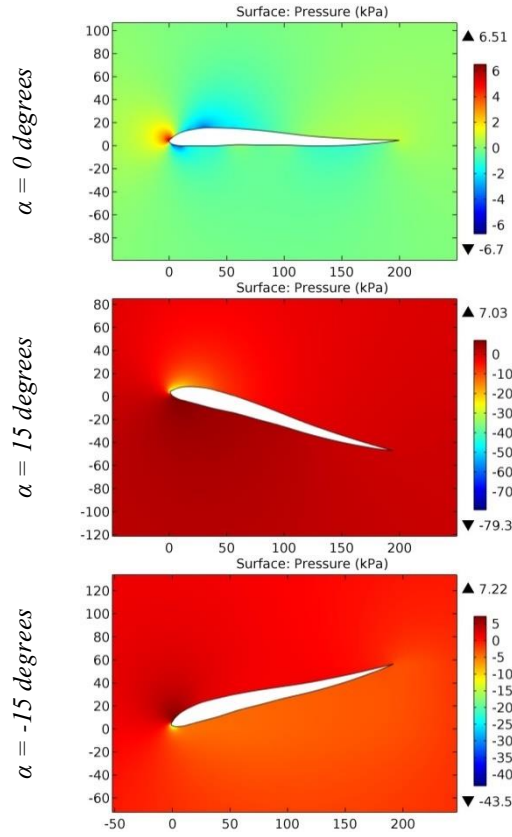


Figure 1. The pressure contours on the surfaces of the G 3 airfoil.

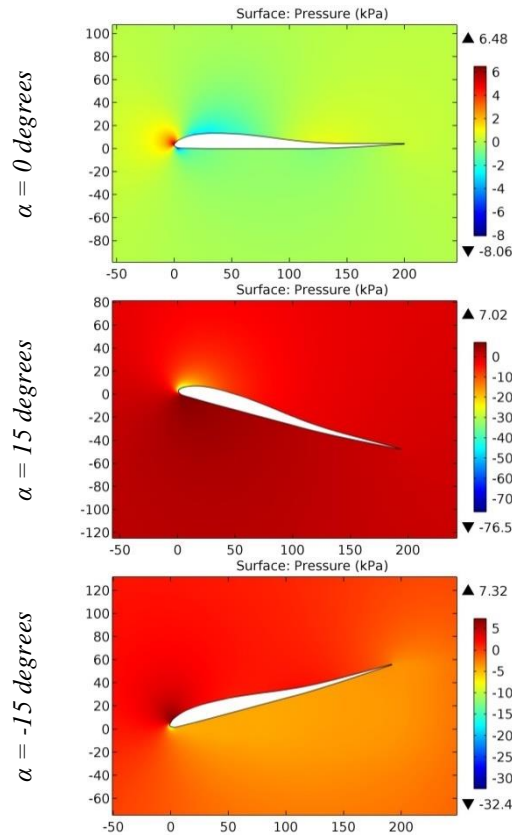
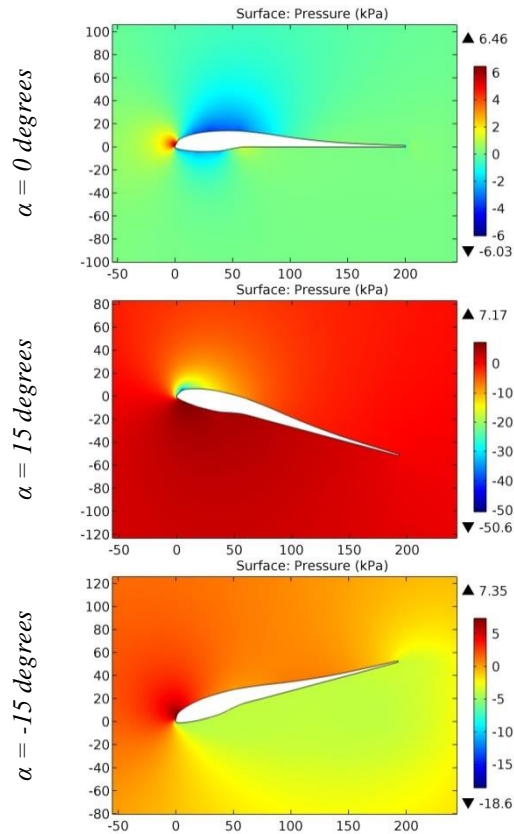


Figure 2. The pressure contours on the surfaces of the G 4 airfoil.



**Impact Factor:**

<b>SISRA</b> (India) = <b>6.317</b>	<b>SIS</b> (USA) = <b>0.912</b>	<b>ICV</b> (Poland) = <b>6.630</b>
<b>ISI</b> (Dubai, UAE) = <b>1.582</b>	<b>ПИИЦ</b> (Russia) = <b>3.939</b>	<b>PIF</b> (India) = <b>1.940</b>
<b>GIF</b> (Australia) = <b>0.564</b>	<b>ESJI</b> (KZ) = <b>9.035</b>	<b>IBI</b> (India) = <b>4.260</b>
<b>JIF</b> = <b>1.500</b>	<b>SJIF</b> (Morocco) = <b>7.184</b>	<b>OAJI</b> (USA) = <b>0.350</b>



**Figure 3.** The pressure contours on the surfaces of the G 5 airfoil.

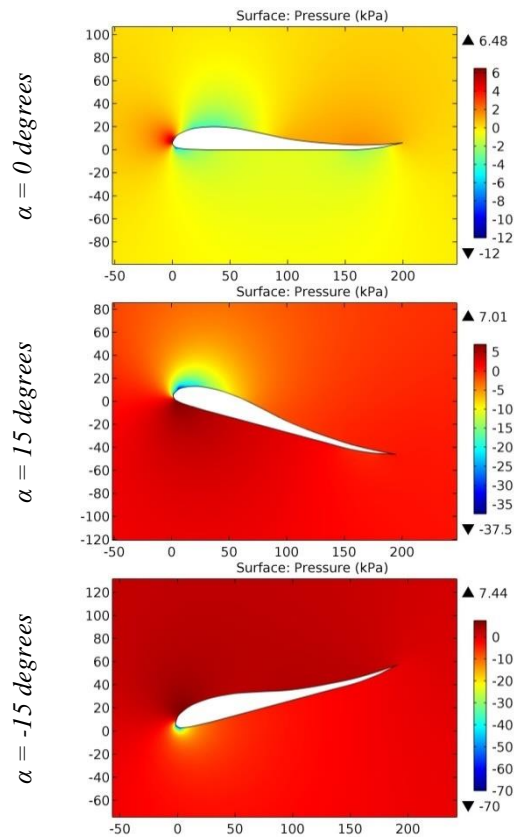


**Figure 4.** The pressure contours on the surfaces of the G 6 airfoil.

**Impact Factor:**

ISRA (India) = 6.317	SIS (USA) = 0.912	ICV (Poland) = 6.630
ISI (Dubai, UAE) = 1.582	ПИИЦ (Russia) = 3.939	PIF (India) = 1.940
GIF (Australia) = 0.564	ESJI (KZ) = 9.035	IBI (India) = 4.260
JIF = 1.500	SJIF (Morocco) = 7.184	OAJI (USA) = 0.350

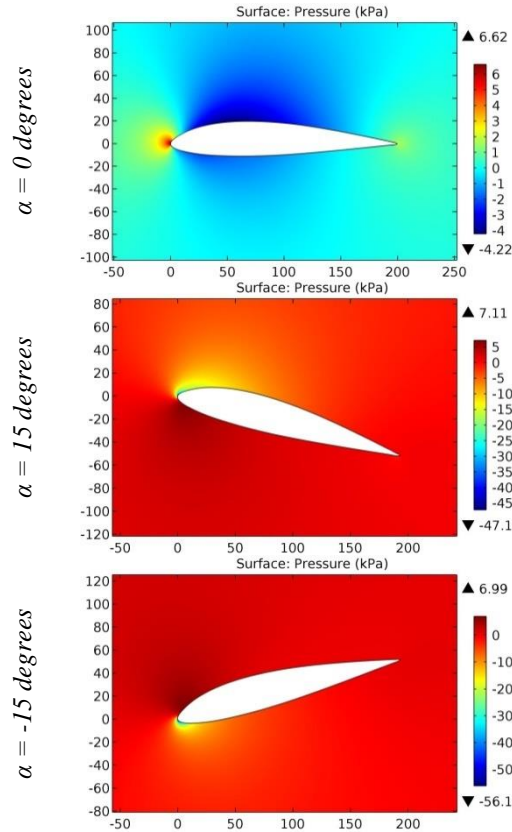


Figure 5. The pressure contours on the surfaces of the GEMINI (smoothed) airfoil.

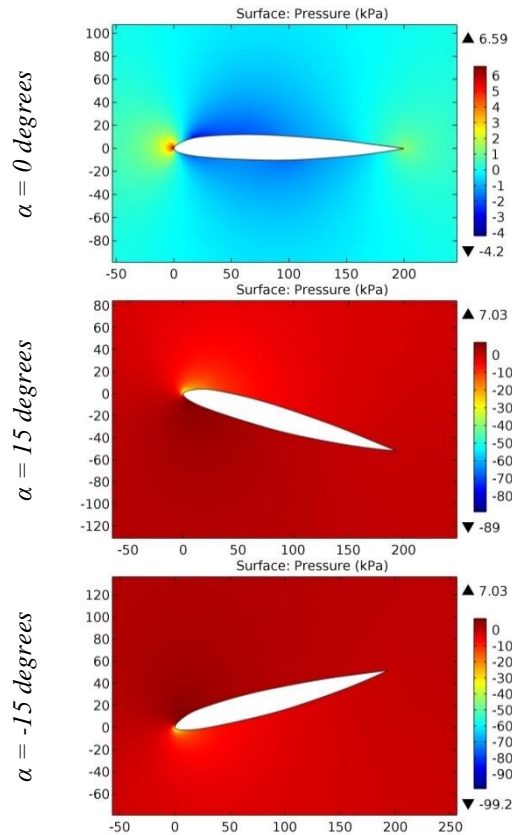


Figure 6. The pressure contours on the surfaces of the GIII BL0 airfoil.

**Impact Factor:**

ISRA (India) = 6.317	SIS (USA) = 0.912	ICV (Poland) = 6.630
ISI (Dubai, UAE) = 1.582	ПИИЦ (Russia) = 3.939	PIF (India) = 1.940
GIF (Australia) = 0.564	ESJI (KZ) = 9.035	IBI (India) = 4.260
JIF = 1.500	SJIF (Morocco) = 7.184	OAJI (USA) = 0.350

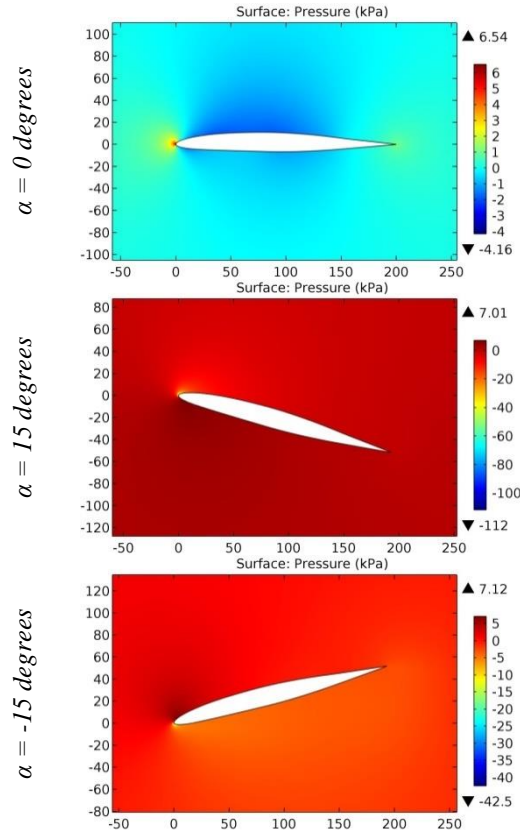


Figure 7. The pressure contours on the surfaces of the GIII BL126 airfoil.

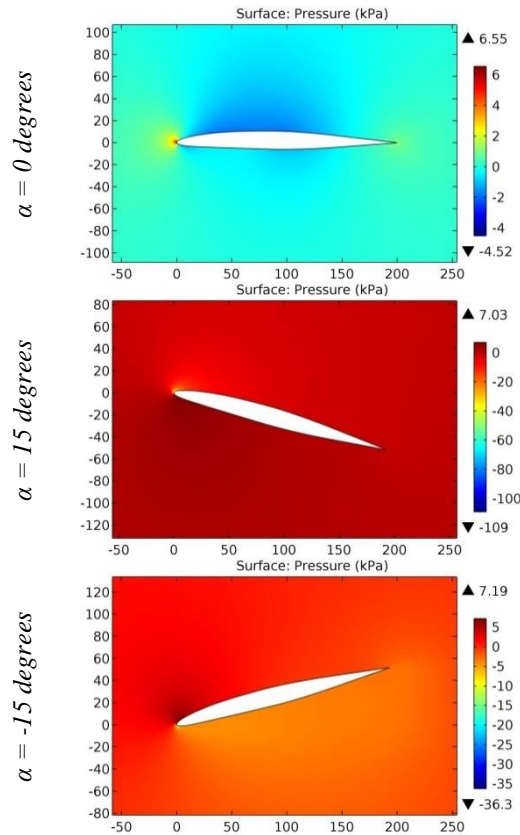


Figure 8. The pressure contours on the surfaces of the GIII BL145 airfoil.

**Impact Factor:**

ISRA (India) = 6.317	SIS (USA) = 0.912	ICV (Poland) = 6.630
ISI (Dubai, UAE) = 1.582	ПИИИ (Russia) = 3.939	PIF (India) = 1.940
GIF (Australia) = 0.564	ESJI (KZ) = 9.035	IBI (India) = 4.260
JIF = 1.500	SJIF (Morocco) = 7.184	OAJI (USA) = 0.350

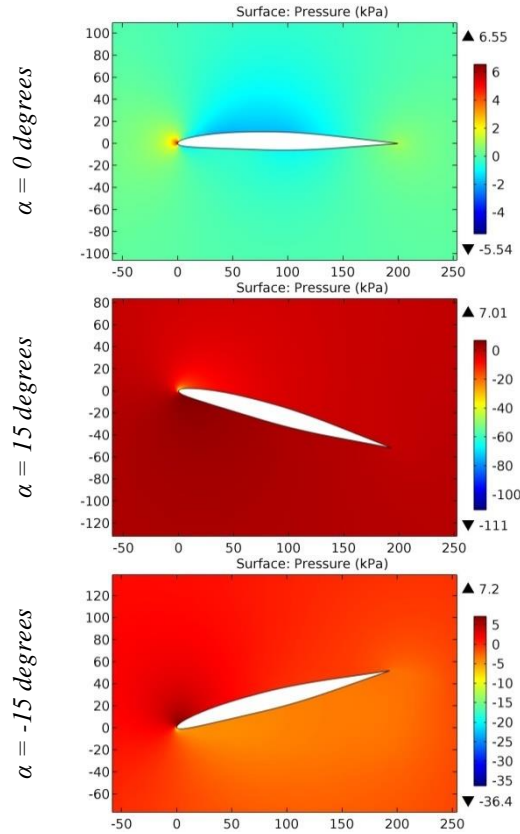


Figure 9. The pressure contours on the surfaces of the GIII BL167 airfoil.

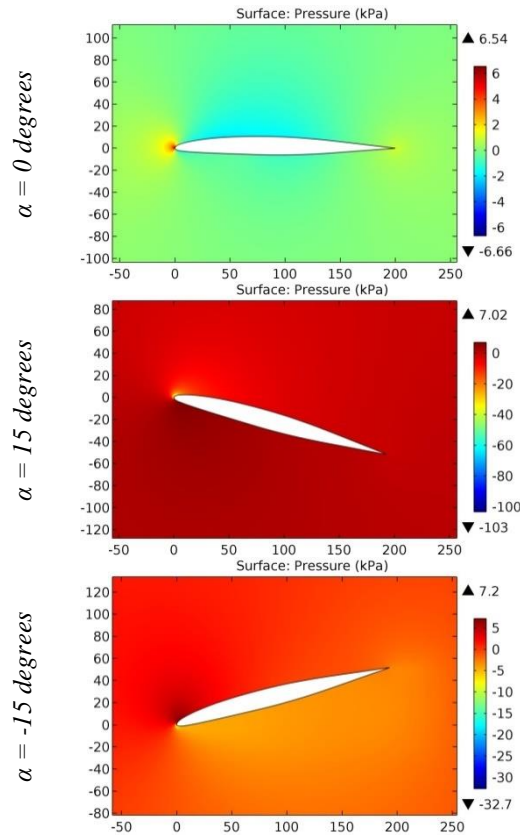


Figure 10. The pressure contours on the surfaces of the GIII BL207 airfoil.

**Impact Factor:**

ISRA (India) = 6.317	SIS (USA) = 0.912	ICV (Poland) = 6.630
ISI (Dubai, UAE) = 1.582	ПИИЦ (Russia) = 3.939	PIF (India) = 1.940
GIF (Australia) = 0.564	ESJI (KZ) = 9.035	IBI (India) = 4.260
JIF = 1.500	SJIF (Morocco) = 7.184	OAJI (USA) = 0.350

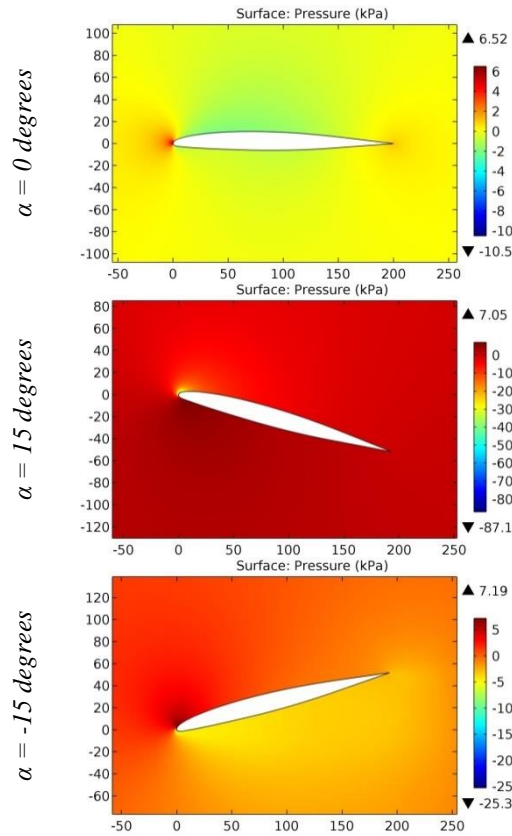


Figure 11. The pressure contours on the surfaces of the GIII BL288 airfoil.

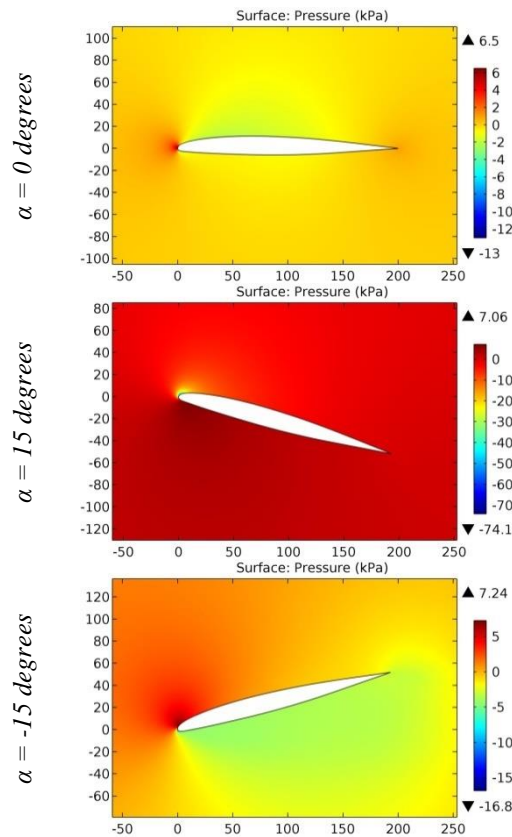


Figure 12. The pressure contours on the surfaces of the GIII BL332 airfoil.



**Impact Factor:**

ISRA (India) = 6.317	SIS (USA) = 0.912	ICV (Poland) = 6.630
ISI (Dubai, UAE) = 1.582	ПИИЦ (Russia) = 3.939	PIF (India) = 1.940
GIF (Australia) = 0.564	ESJI (KZ) = 9.035	IBI (India) = 4.260
JIF = 1.500	SJIF (Morocco) = 7.184	OAJI (USA) = 0.350

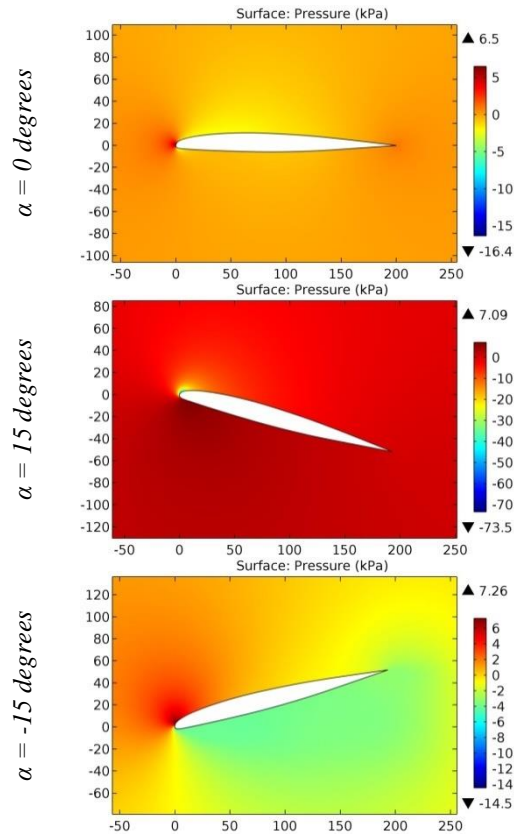


Figure 13. The pressure contours on the surfaces of the GIII BL369 airfoil.

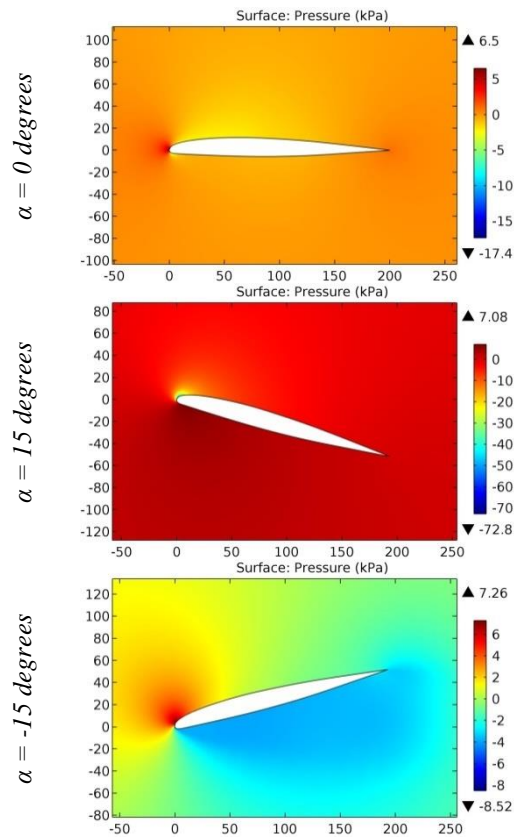


Figure 14. The pressure contours on the surfaces of the GIII BL387 airfoil.

**Impact Factor:**

ISRA (India) = 6.317	SIS (USA) = 0.912	ICV (Poland) = 6.630
ISI (Dubai, UAE) = 1.582	ПИИЦ (Russia) = 3.939	PIF (India) = 1.940
GIF (Australia) = 0.564	ESJI (KZ) = 9.035	IBI (India) = 4.260
JIF = 1.500	SJIF (Morocco) = 7.184	OAJI (USA) = 0.350

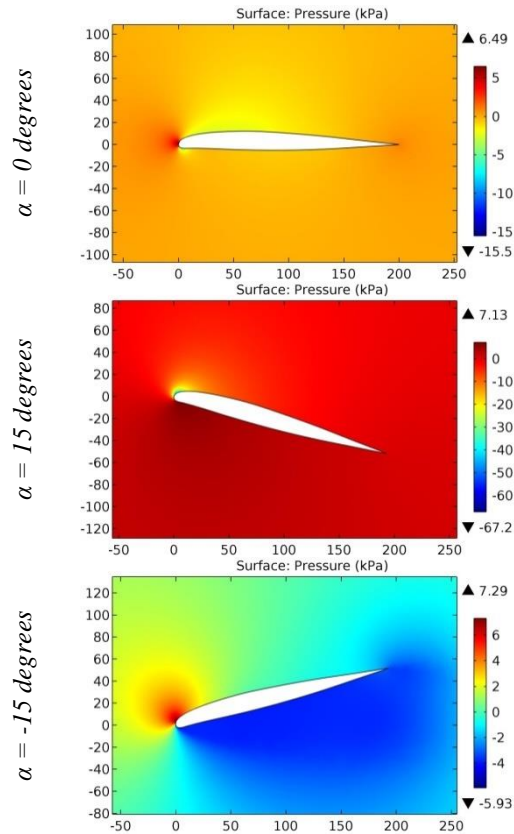


Figure 15. The pressure contours on the surfaces of the GIII BL430 airfoil.

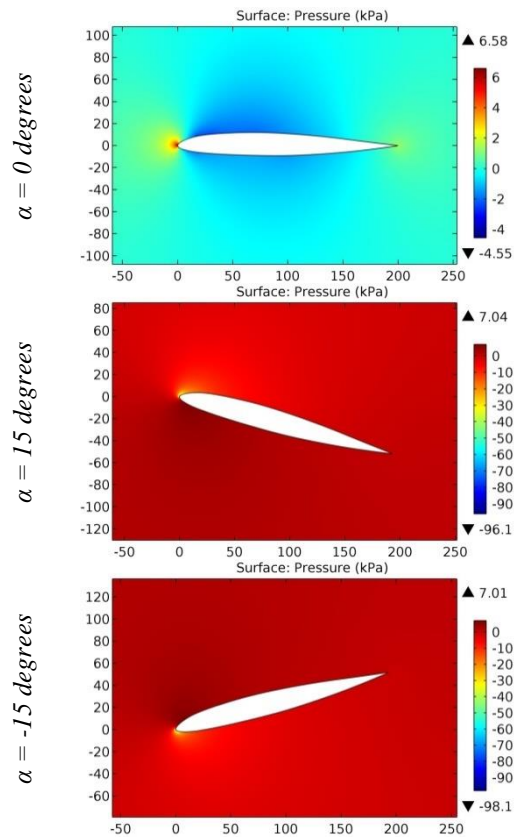


Figure 16. The pressure contours on the surfaces of the GIII BL45 airfoil.

**Impact Factor:**

ISRA (India) = 6.317	SIS (USA) = 0.912	ICV (Poland) = 6.630
ISI (Dubai, UAE) = 1.582	ПИИЦ (Russia) = 3.939	PIF (India) = 1.940
GIF (Australia) = 0.564	ESJI (KZ) = 9.035	IBI (India) = 4.260
JIF = 1.500	SJIF (Morocco) = 7.184	OAJI (USA) = 0.350

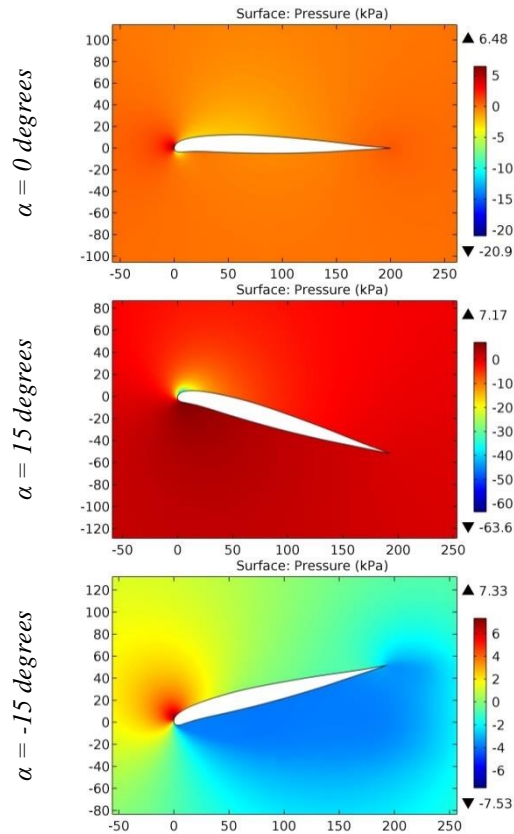


Figure 17. The pressure contours on the surfaces of the GIII BL450 airfoil.

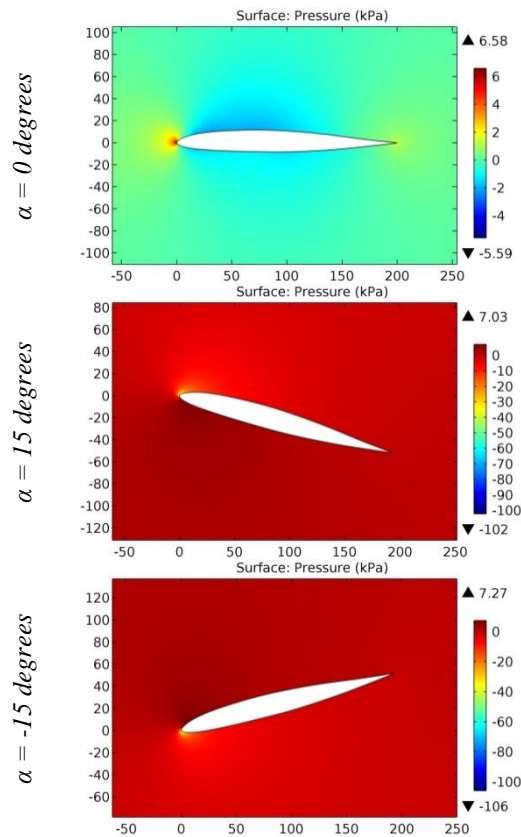


Figure 18. The pressure contours on the surfaces of the GIII BL75 airfoil.

**Impact Factor:**

ISRA (India) = 6.317	SIS (USA) = 0.912	ICV (Poland) = 6.630
ISI (Dubai, UAE) = 1.582	ПИИЦ (Russia) = 3.939	PIF (India) = 1.940
GIF (Australia) = 0.564	ESJI (KZ) = 9.035	IBI (India) = 4.260
JIF = 1.500	SJIF (Morocco) = 7.184	OAJI (USA) = 0.350

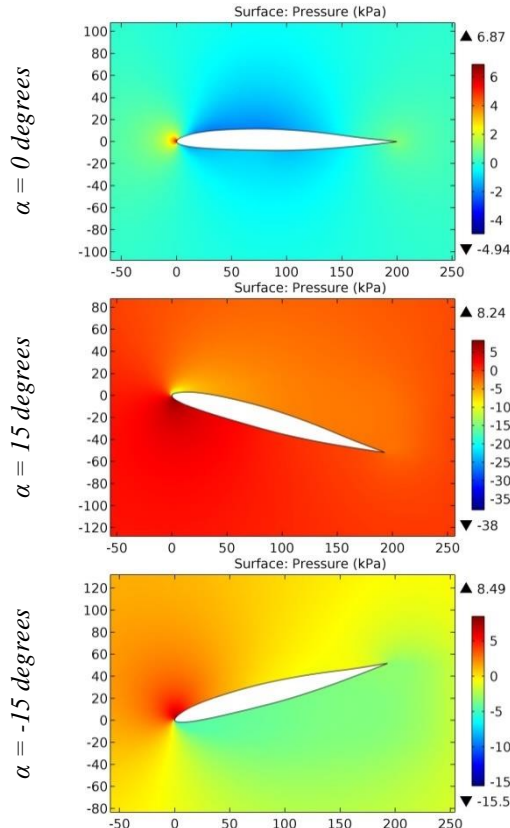


Figure 19. The pressure contours on the surfaces of the GIII BL86 airfoil.

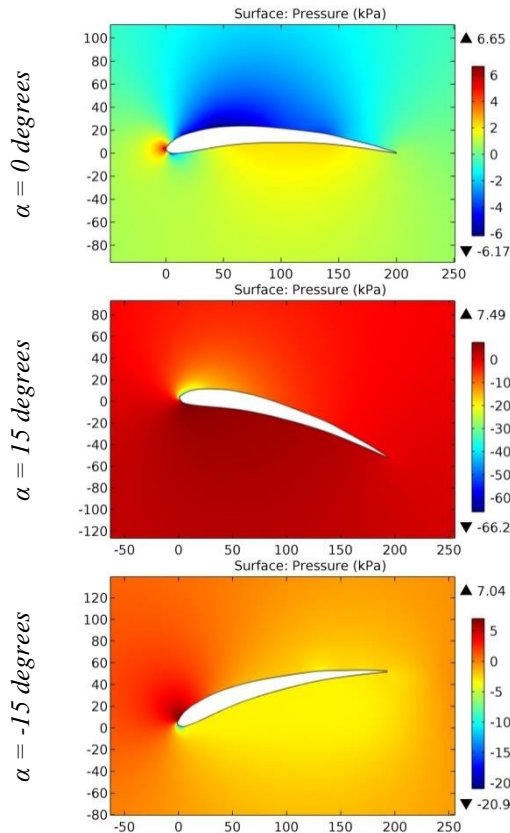


Figure 20. The pressure contours on the surfaces of the Gilroy airfoil.

**Impact Factor:**

ISRA (India) = 6.317	SIS (USA) = 0.912	ICV (Poland) = 6.630
ISI (Dubai, UAE) = 1.582	ПИИЦ (Russia) = 3.939	PIF (India) = 1.940
GIF (Australia) = 0.564	ESJI (KZ) = 9.035	IBI (India) = 4.260
JIF = 1.500	SJFI (Morocco) = 7.184	OAJI (USA) = 0.350

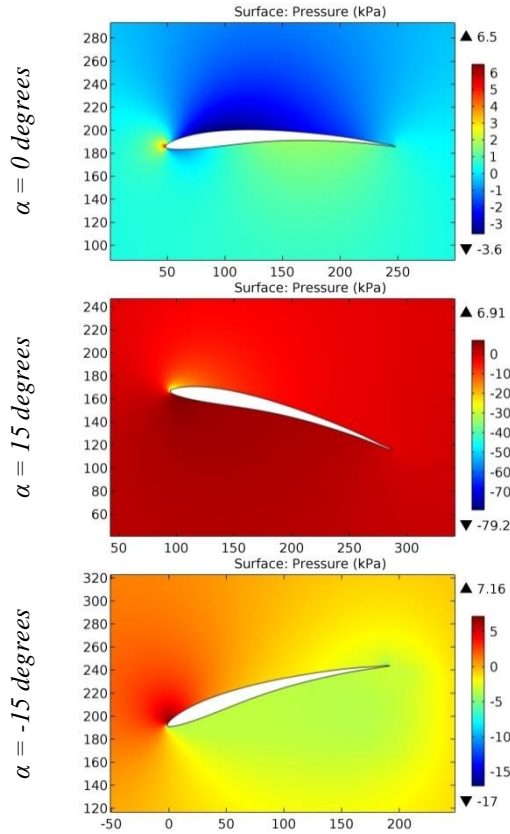


Figure 21. The pressure contours on the surfaces of the GM15 airfoil.

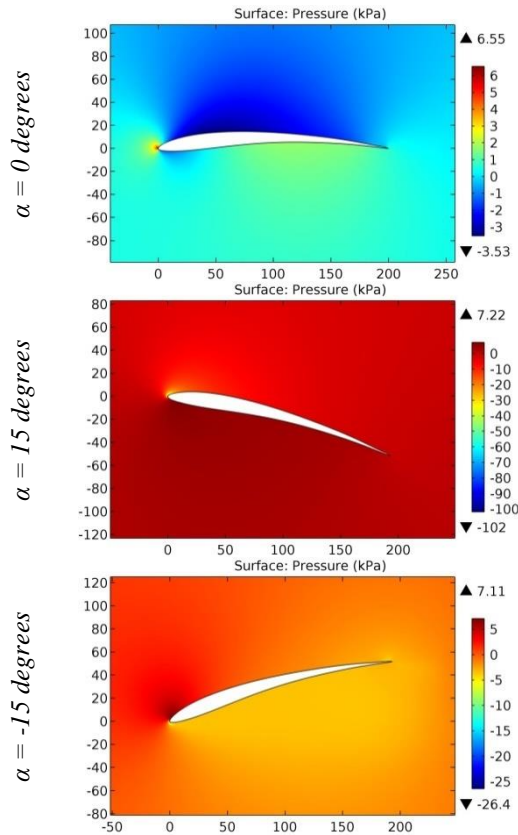


Figure 22. The pressure contours on the surfaces of the GM15 (smoothed) airfoil.



**Impact Factor:**

ISRA (India) = 6.317	SIS (USA) = 0.912	ICV (Poland) = 6.630
ISI (Dubai, UAE) = 1.582	ПИИЦ (Russia) = 3.939	PIF (India) = 1.940
GIF (Australia) = 0.564	ESJI (KZ) = 9.035	IBI (India) = 4.260
JIF = 1.500	SJIF (Morocco) = 7.184	OAJI (USA) = 0.350

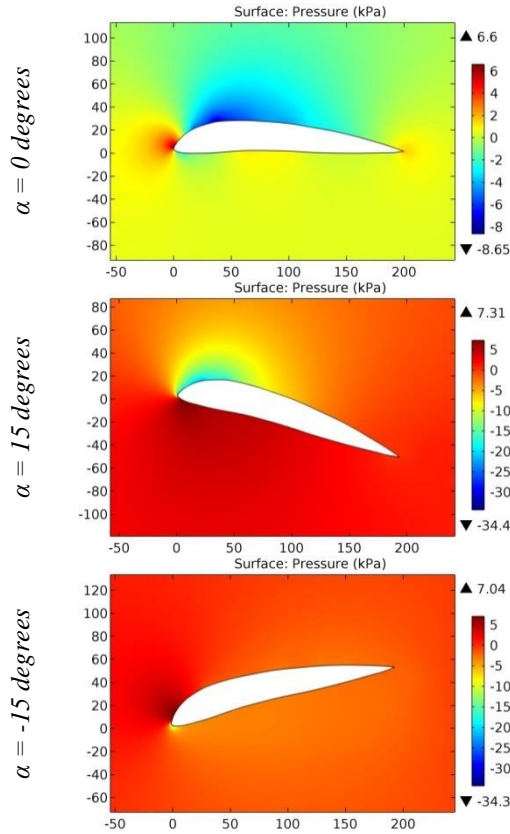


Figure 23. The pressure contours on the surfaces of the GMARTIN2 airfoil.

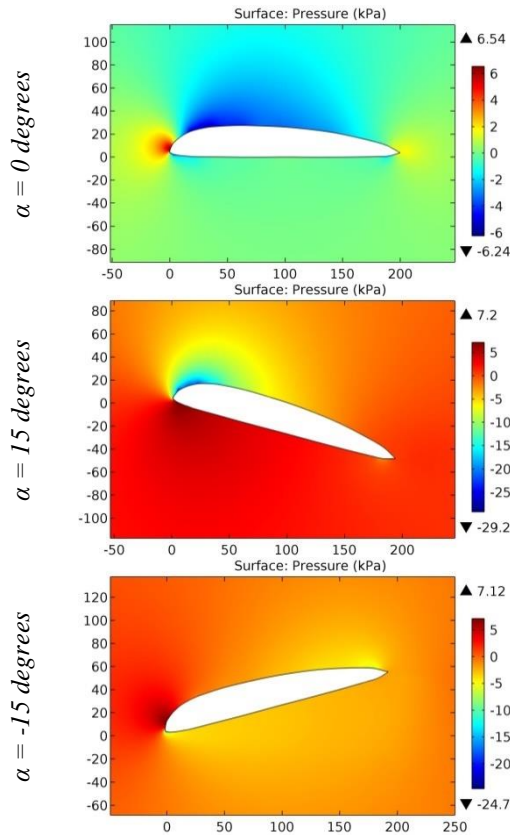


Figure 24. The pressure contours on the surfaces of the GMARTIN3 airfoil.

**Impact Factor:**

<b>ISRA (India)</b> = <b>6.317</b>	<b>SIS (USA)</b> = <b>0.912</b>	<b>ICV (Poland)</b> = <b>6.630</b>
<b>ISI (Dubai, UAE)</b> = <b>1.582</b>	<b>ПИИЦ (Russia)</b> = <b>3.939</b>	<b>PIF (India)</b> = <b>1.940</b>
<b>GIF (Australia)</b> = <b>0.564</b>	<b>ESJI (KZ)</b> = <b>9.035</b>	<b>IBI (India)</b> = <b>4.260</b>
<b>JIF</b> = <b>1.500</b>	<b>SJIF (Morocco)</b> = <b>7.184</b>	<b>OAJI (USA)</b> = <b>0.350</b>

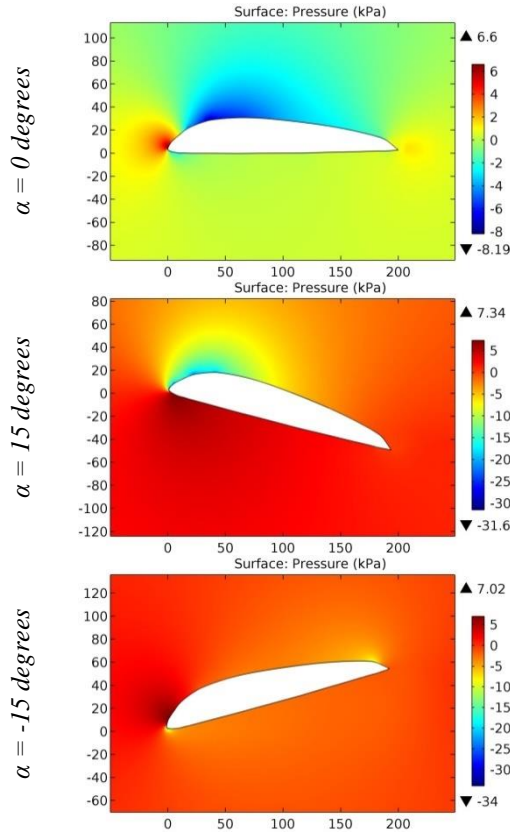


Figure 25. The pressure contours on the surfaces of the GMARTIN4 airfoil.

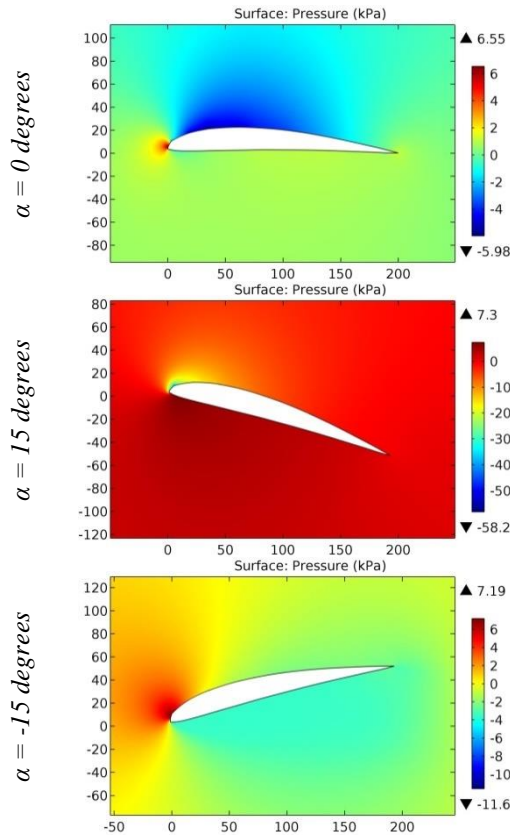


Figure 26. The pressure contours on the surfaces of the GO-398B airfoil.

**Impact Factor:**

ISRA (India) = 6.317	SIS (USA) = 0.912	ICV (Poland) = 6.630
ISI (Dubai, UAE) = 1.582	ПИИЦ (Russia) = 3.939	PIF (India) = 1.940
GIF (Australia) = 0.564	ESJI (KZ) = 9.035	IBI (India) = 4.260
JIF = 1.500	SJIF (Morocco) = 7.184	OAJI (USA) = 0.350

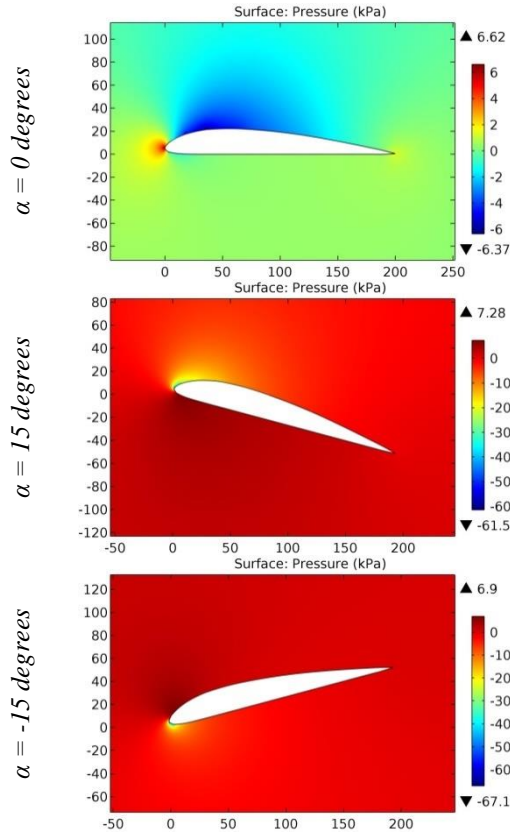


Figure 27. The pressure contours on the surfaces of the GO-436B airfoil.

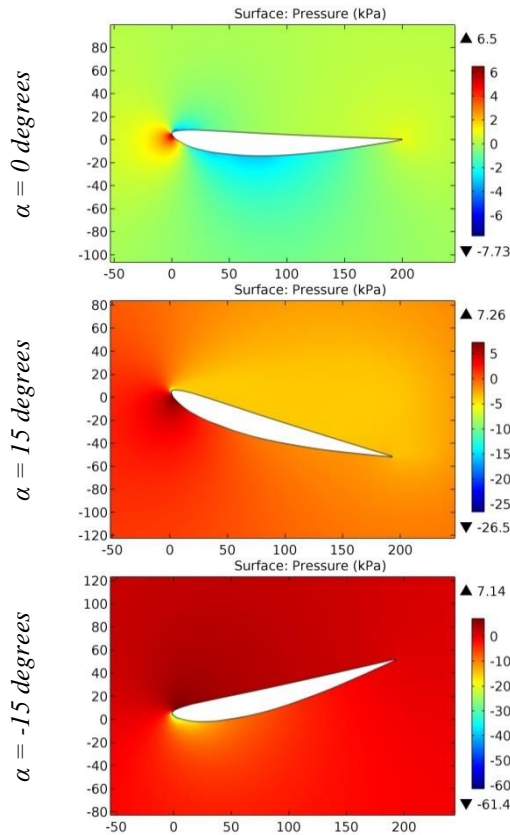


Figure 28. The pressure contours on the surfaces of the GO-624B airfoil.

**Impact Factor:**

ISRA (India) = 6.317	SIS (USA) = 0.912	ICV (Poland) = 6.630
ISI (Dubai, UAE) = 1.582	ПИИЦ (Russia) = 3.939	PIF (India) = 1.940
GIF (Australia) = 0.564	ESJI (KZ) = 9.035	IBI (India) = 4.260
JIF = 1.500	SJIF (Morocco) = 7.184	OAJI (USA) = 0.350

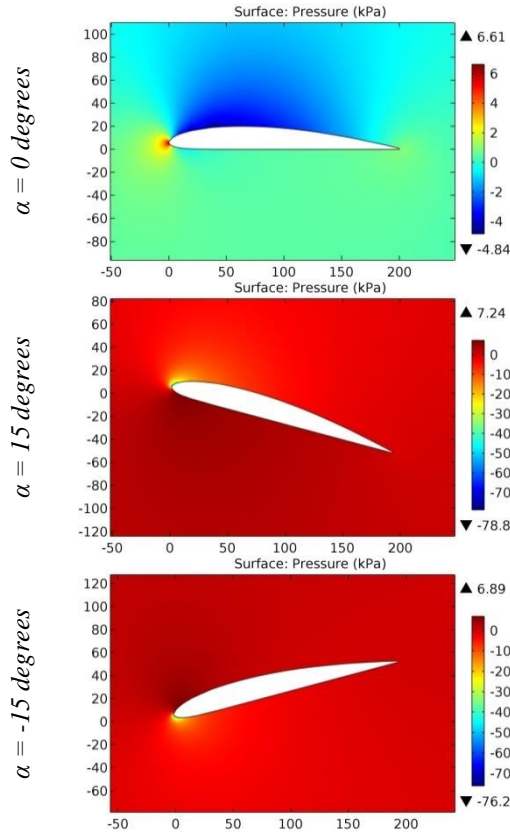


Figure 29. The pressure contours on the surfaces of the GO-7955 airfoil.

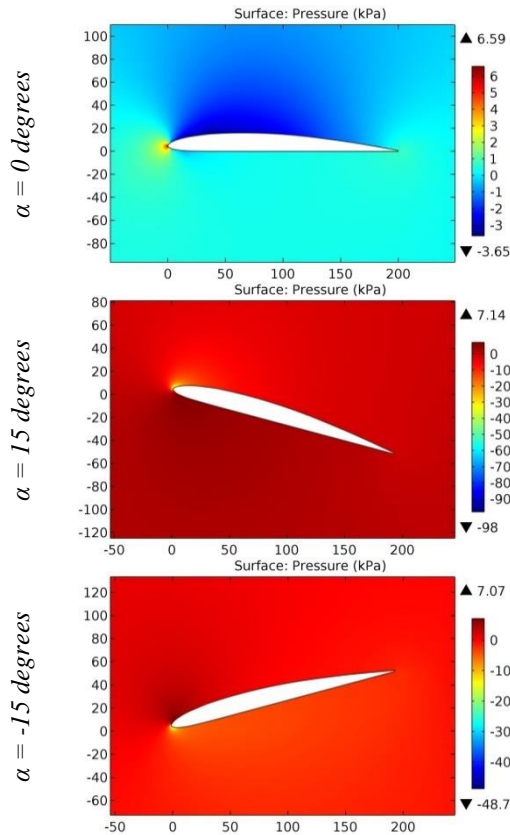


Figure 30. The pressure contours on the surfaces of the GO-795B airfoil.

**Impact Factor:**

ISRA (India) = 6.317	SIS (USA) = 0.912	ICV (Poland) = 6.630
ISI (Dubai, UAE) = 1.582	ПИИЦ (Russia) = 3.939	PIF (India) = 1.940
GIF (Australia) = 0.564	ESJI (KZ) = 9.035	IBI (India) = 4.260
JIF = 1.500	SJIF (Morocco) = 7.184	OAJI (USA) = 0.350

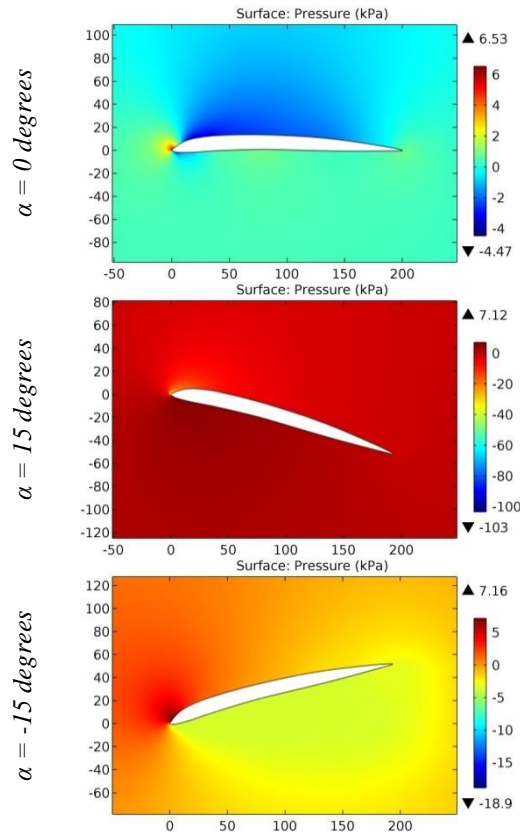


Figure 31. The pressure contours on the surfaces of the GOE 100 (SOPWITH) airfoil.

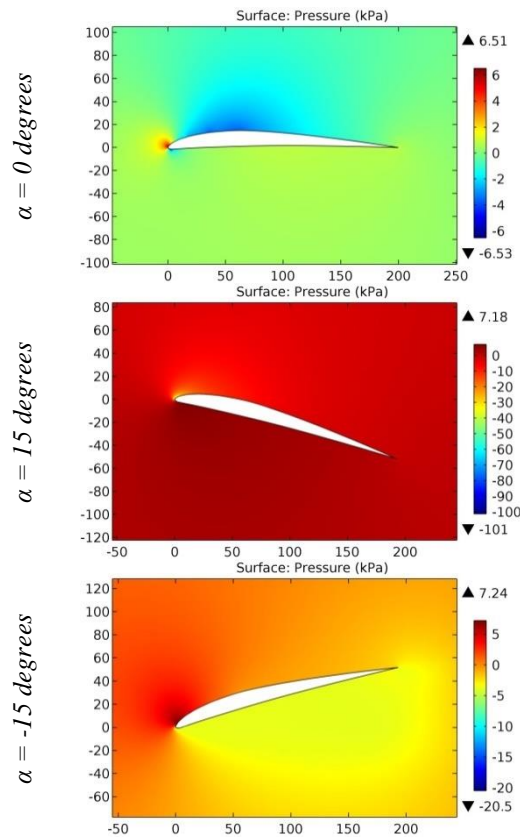


Figure 32. The pressure contours on the surfaces of the GOE 101 airfoil.



**Impact Factor:**

ISRA (India) = 6.317	SIS (USA) = 0.912	ICV (Poland) = 6.630
ISI (Dubai, UAE) = 1.582	ПИИЦ (Russia) = 3.939	PIF (India) = 1.940
GIF (Australia) = 0.564	ESJI (KZ) = 9.035	IBI (India) = 4.260
JIF = 1.500	SJIF (Morocco) = 7.184	OAJI (USA) = 0.350

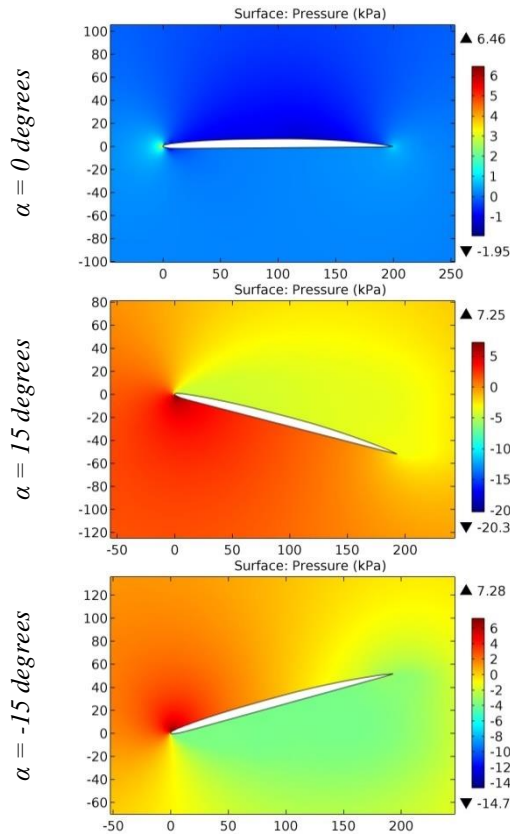


Figure 33. The pressure contours on the surfaces of the GOE 10K airfoil.

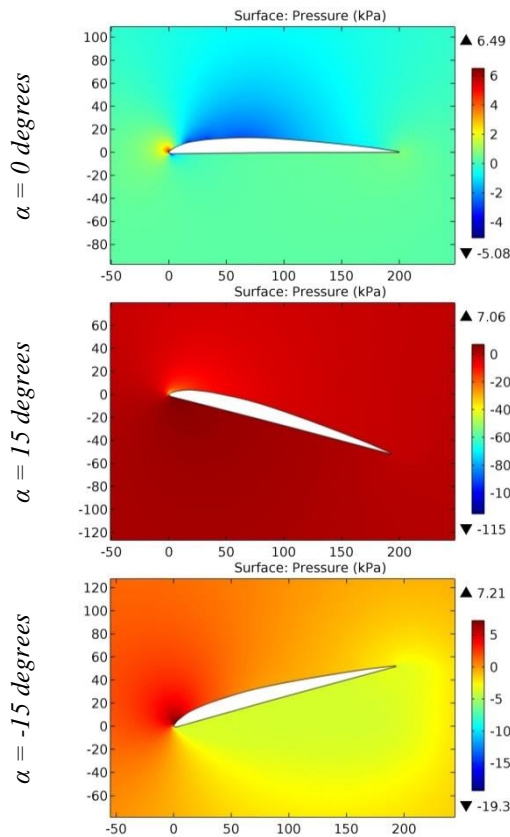


Figure 34. The pressure contours on the surfaces of the GOE 113 airfoil.

**Impact Factor:**

<b>SISRA</b> (India) = <b>6.317</b>	<b>SIS</b> (USA) = <b>0.912</b>	<b>ICV</b> (Poland) = <b>6.630</b>
<b>ISI</b> (Dubai, UAE) = <b>1.582</b>	<b>ПИИЦ</b> (Russia) = <b>3.939</b>	<b>PIF</b> (India) = <b>1.940</b>
<b>GIF</b> (Australia) = <b>0.564</b>	<b>ESJI</b> (KZ) = <b>9.035</b>	<b>IBI</b> (India) = <b>4.260</b>
<b>JIF</b> = <b>1.500</b>	<b>SJIF</b> (Morocco) = <b>7.184</b>	<b>OAJI</b> (USA) = <b>0.350</b>

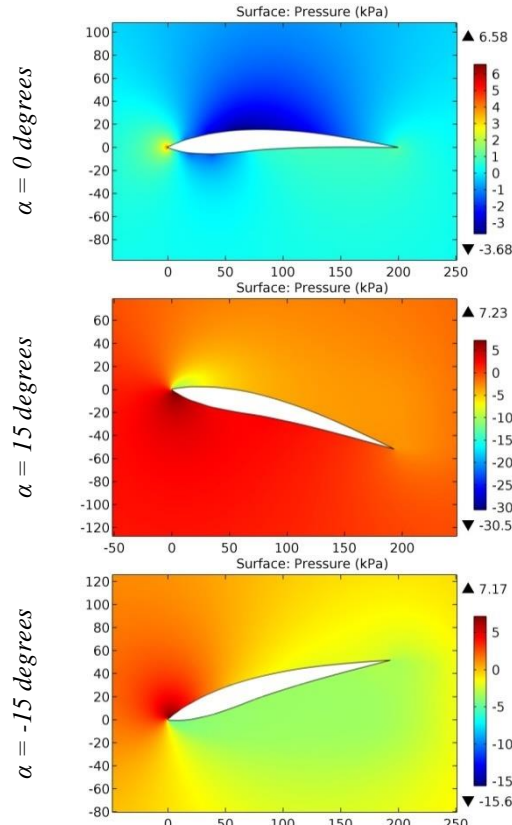


Figure 35. The pressure contours on the surfaces of the GOE 114 (MVA MK,1) airfoil.

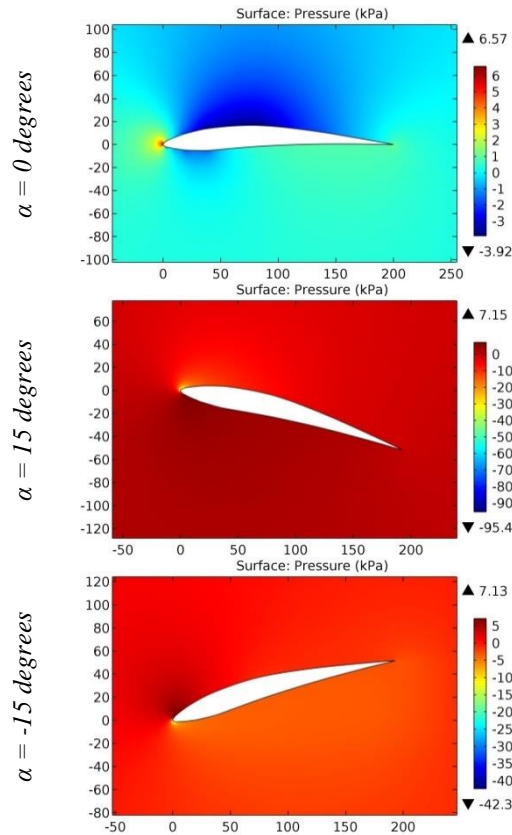


Figure 36. The pressure contours on the surfaces of the GOE 115 (MVA MK,2) airfoil.

**Impact Factor:**

<b>SISRA</b> (India) = <b>6.317</b>	<b>SIS</b> (USA) = <b>0.912</b>	<b>ICV</b> (Poland) = <b>6.630</b>
<b>ISI</b> (Dubai, UAE) = <b>1.582</b>	<b>ПИИЦ</b> (Russia) = <b>3.939</b>	<b>PIF</b> (India) = <b>1.940</b>
<b>GIF</b> (Australia) = <b>0.564</b>	<b>ESJI</b> (KZ) = <b>9.035</b>	<b>IBI</b> (India) = <b>4.260</b>
<b>JIF</b> = <b>1.500</b>	<b>SJIF</b> (Morocco) = <b>7.184</b>	<b>OAJI</b> (USA) = <b>0.350</b>

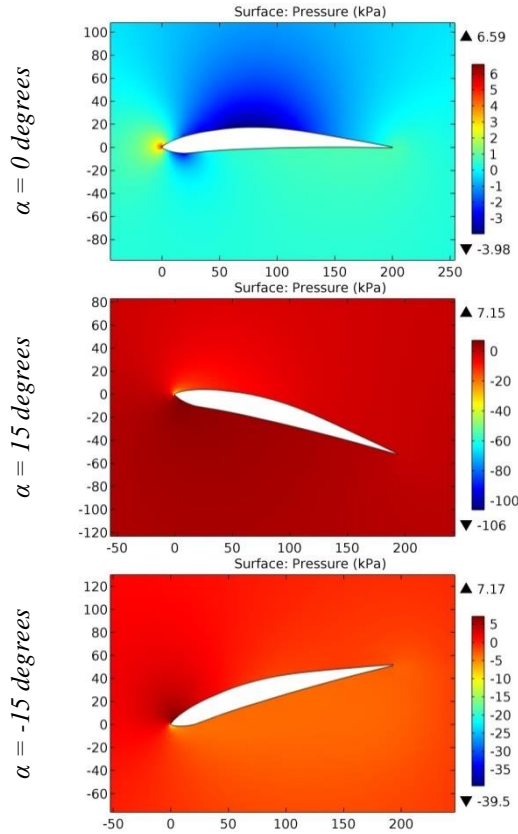


Figure 37. The pressure contours on the surfaces of the GOE 116 (MVA MK,3) airfoil.

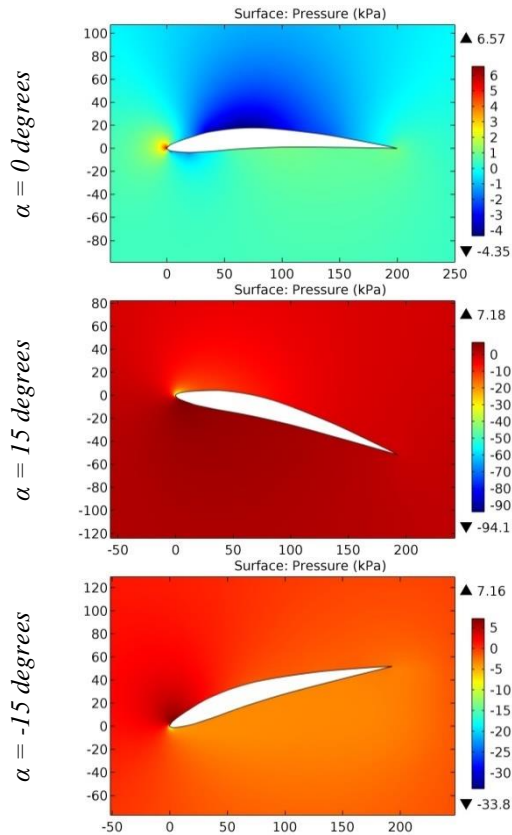


Figure 38. The pressure contours on the surfaces of the GOE 117 (MVA MK,4) airfoil.

**Impact Factor:**

<b>SISRA</b> (India) = <b>6.317</b>	<b>SIS</b> (USA) = <b>0.912</b>	<b>ICV</b> (Poland) = <b>6.630</b>
<b>ISI</b> (Dubai, UAE) = <b>1.582</b>	<b>ПИИЦ</b> (Russia) = <b>3.939</b>	<b>PIF</b> (India) = <b>1.940</b>
<b>GIF</b> (Australia) = <b>0.564</b>	<b>ESJI</b> (KZ) = <b>9.035</b>	<b>IBI</b> (India) = <b>4.260</b>
<b>JIF</b> = <b>1.500</b>	<b>SJIF</b> (Morocco) = <b>7.184</b>	<b>OAJI</b> (USA) = <b>0.350</b>

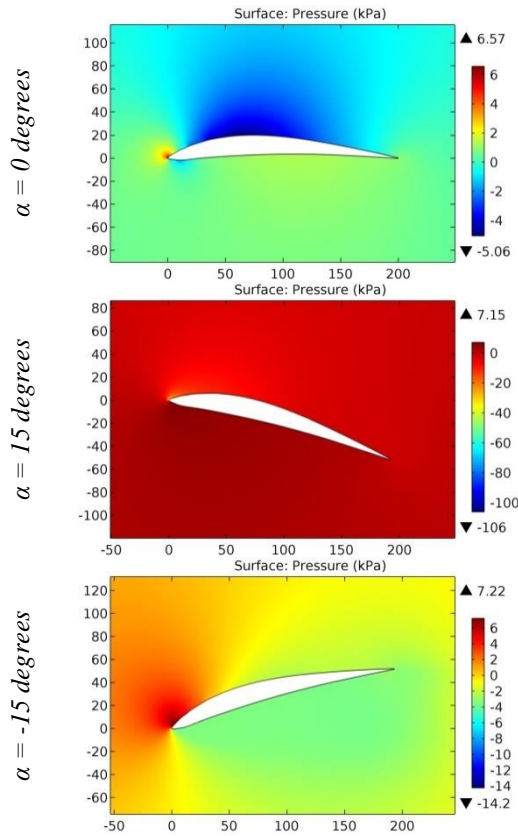


Figure 39. The pressure contours on the surfaces of the GOE 118 (MVA MK,7) airfoil.

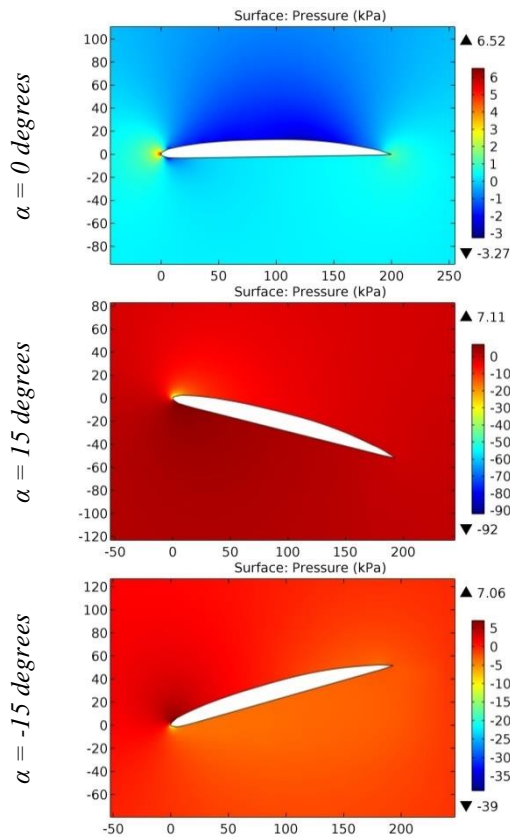


Figure 40. The pressure contours on the surfaces of the GOE 11K airfoil.

**Impact Factor:**

ISRA (India) = 6.317	SIS (USA) = 0.912	ICV (Poland) = 6.630
ISI (Dubai, UAE) = 1.582	ПИИЦ (Russia) = 3.939	PIF (India) = 1.940
GIF (Australia) = 0.564	ESJI (KZ) = 9.035	IBI (India) = 4.260
JIF = 1.500	SJIF (Morocco) = 7.184	OAJI (USA) = 0.350

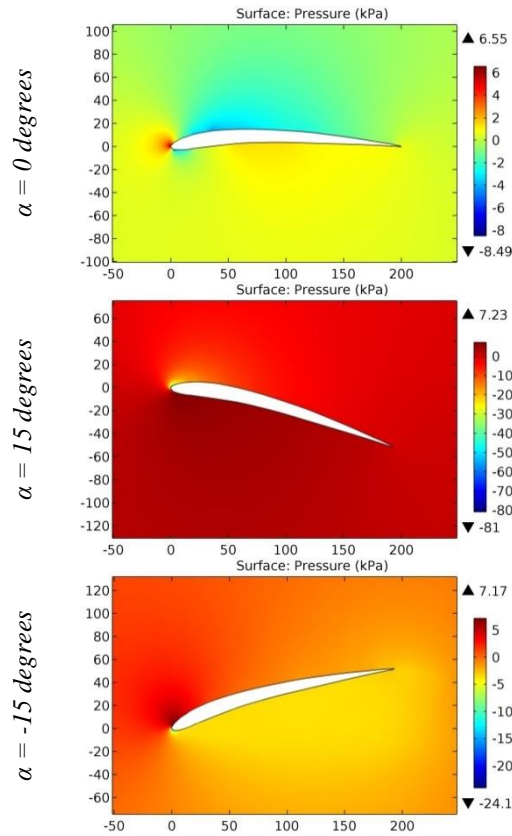


Figure 41. The pressure contours on the surfaces of the GOE 121 (MVA H,1) airfoil.

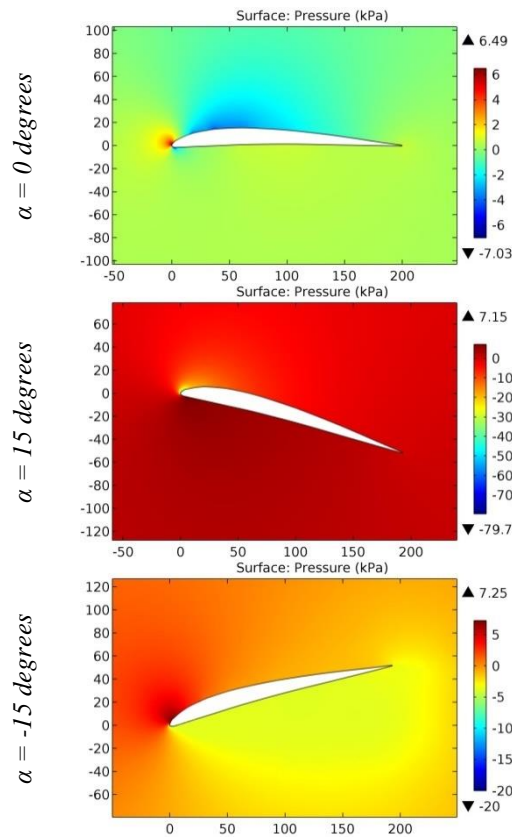


Figure 42. The pressure contours on the surfaces of the GOE 122 (MVA H,2) airfoil.



**Impact Factor:**

<b>ISRA (India)</b> = <b>6.317</b>	<b>SIS (USA)</b> = <b>0.912</b>	<b>ICV (Poland)</b> = <b>6.630</b>
<b>ISI (Dubai, UAE)</b> = <b>1.582</b>	<b>ПИИЦ (Russia)</b> = <b>3.939</b>	<b>PIF (India)</b> = <b>1.940</b>
<b>GIF (Australia)</b> = <b>0.564</b>	<b>ESJI (KZ)</b> = <b>9.035</b>	<b>IBI (India)</b> = <b>4.260</b>
<b>JIF</b> = <b>1.500</b>	<b>SJIF (Morocco)</b> = <b>7.184</b>	<b>OAJI (USA)</b> = <b>0.350</b>

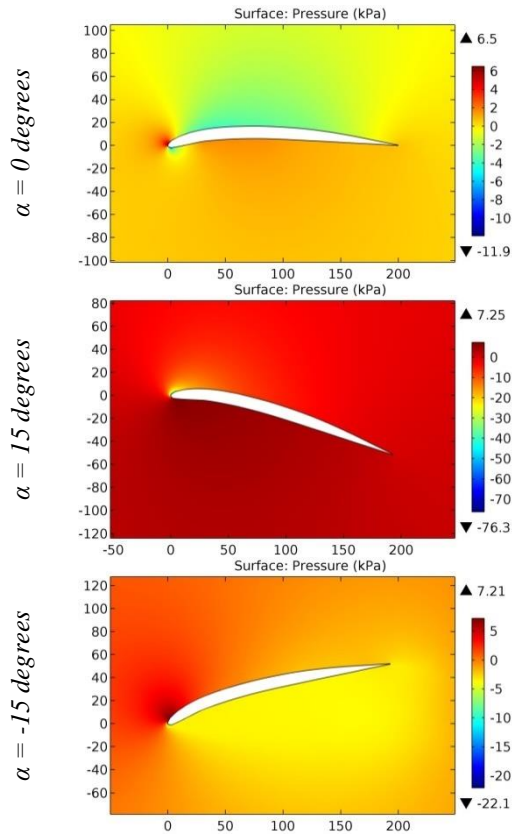


Figure 43. The pressure contours on the surfaces of the GOE 123 airfoil.

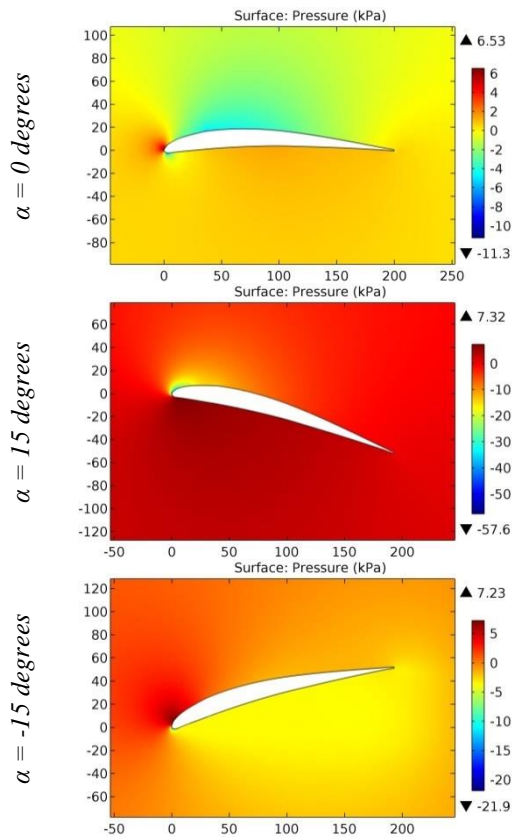


Figure 44. The pressure contours on the surfaces of the GOE 124 (MVA H,4) airfoil.

**Impact Factor:**

ISRA (India) = 6.317	SIS (USA) = 0.912	ICV (Poland) = 6.630
ISI (Dubai, UAE) = 1.582	ПИИЦ (Russia) = 3.939	PIF (India) = 1.940
GIF (Australia) = 0.564	ESJI (KZ) = 9.035	IBI (India) = 4.260
JIF = 1.500	SJIF (Morocco) = 7.184	OAJI (USA) = 0.350

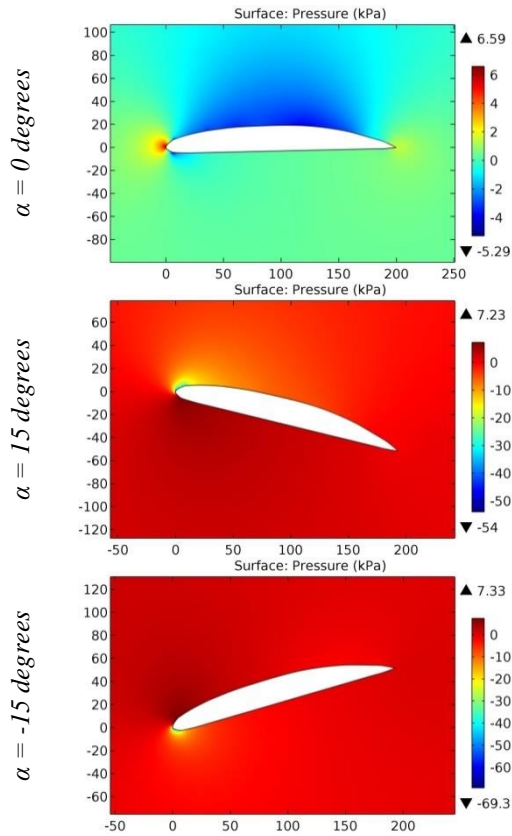


Figure 45. The pressure contours on the surfaces of the GOE 12K airfoil.

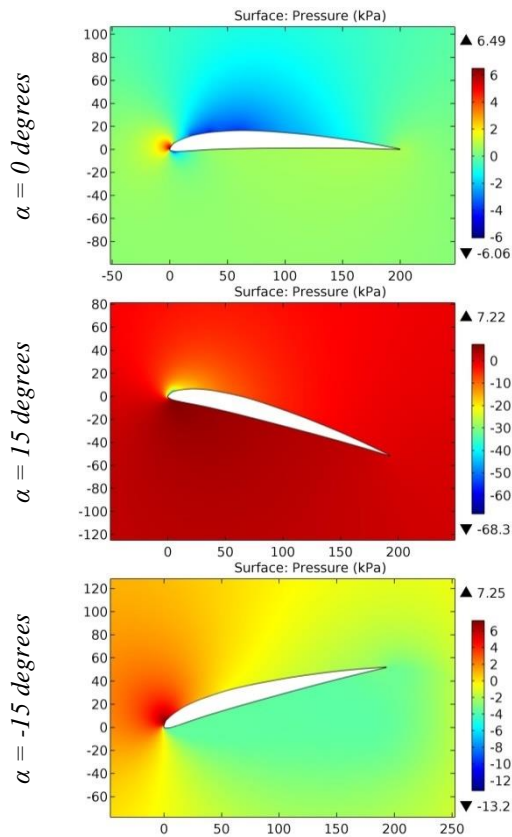


Figure 46. The pressure contours on the surfaces of the GOE 133 (MVA H,11) airfoil.

**Impact Factor:**

ISRA (India) = 6.317	SIS (USA) = 0.912	ICV (Poland) = 6.630
ISI (Dubai, UAE) = 1.582	ПИИЦ (Russia) = 3.939	PIF (India) = 1.940
GIF (Australia) = 0.564	ESJI (KZ) = 9.035	IBI (India) = 4.260
JIF = 1.500	SJIF (Morocco) = 7.184	OAJI (USA) = 0.350

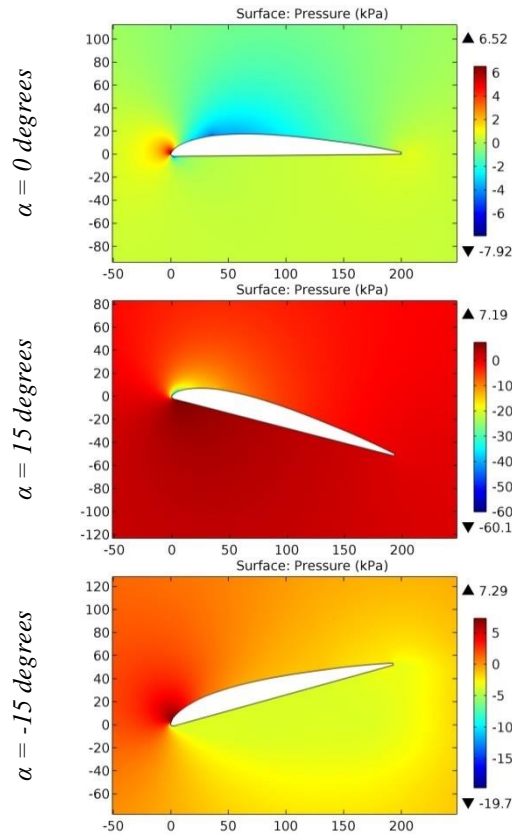


Figure 47. The pressure contours on the surfaces of the GOE 134 (MVA H,12) airfoil.

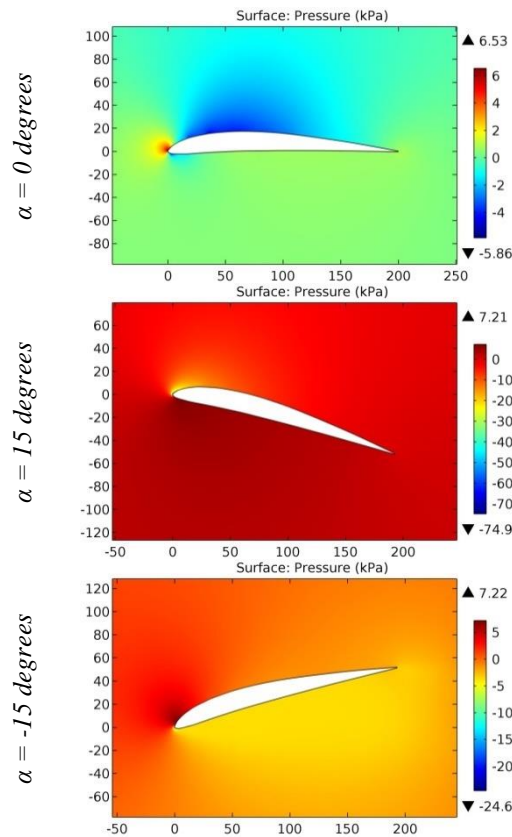


Figure 48. The pressure contours on the surfaces of the GOE 137 (MVA H,15) airfoil.

**Impact Factor:**

ISRA (India) = 6.317	SIS (USA) = 0.912	ICV (Poland) = 6.630
ISI (Dubai, UAE) = 1.582	ПИИЦ (Russia) = 3.939	PIF (India) = 1.940
GIF (Australia) = 0.564	ESJI (KZ) = 9.035	IBI (India) = 4.260
JIF = 1.500	SJIF (Morocco) = 7.184	OAJI (USA) = 0.350

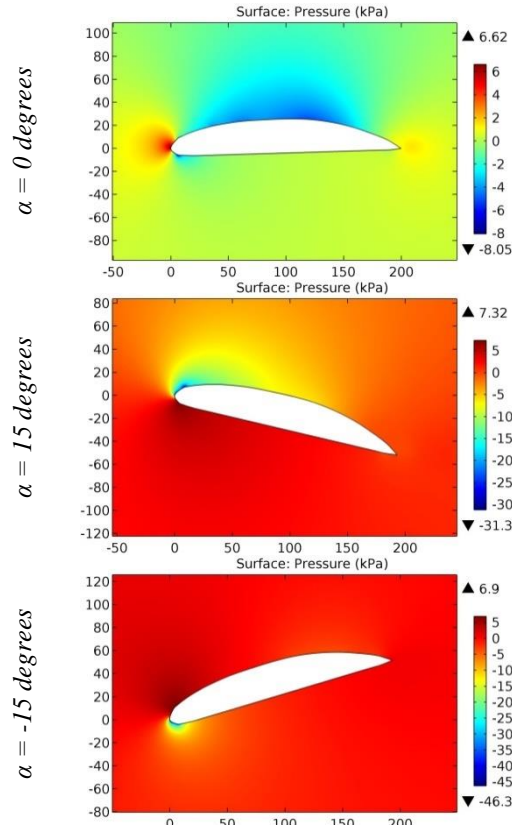


Figure 49. The pressure contours on the surfaces of the GOE 13K airfoil.

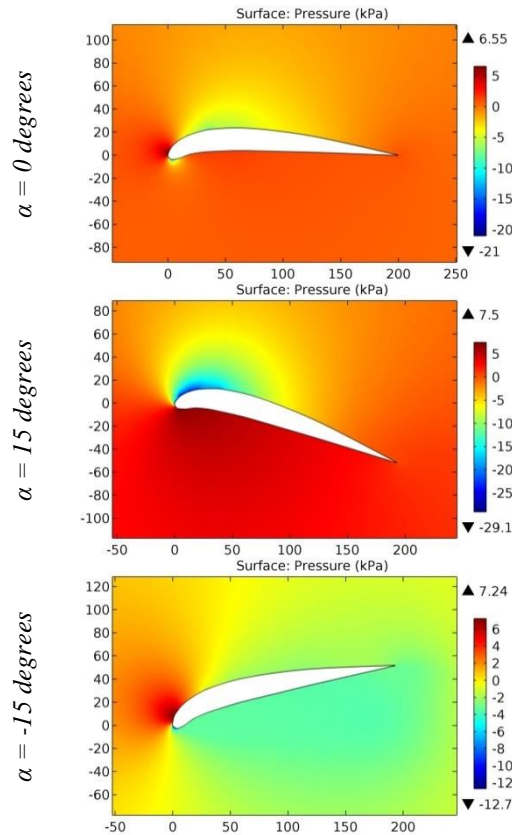


Figure 50. The pressure contours on the surfaces of the GOE 14 airfoil.

**Impact Factor:**

ISRA (India) = 6.317	SIS (USA) = 0.912	ICV (Poland) = 6.630
ISI (Dubai, UAE) = 1.582	ПИИЦ (Russia) = 3.939	PIF (India) = 1.940
GIF (Australia) = 0.564	ESJI (KZ) = 9.035	IBI (India) = 4.260
JIF = 1.500	SJIF (Morocco) = 7.184	OAJI (USA) = 0.350

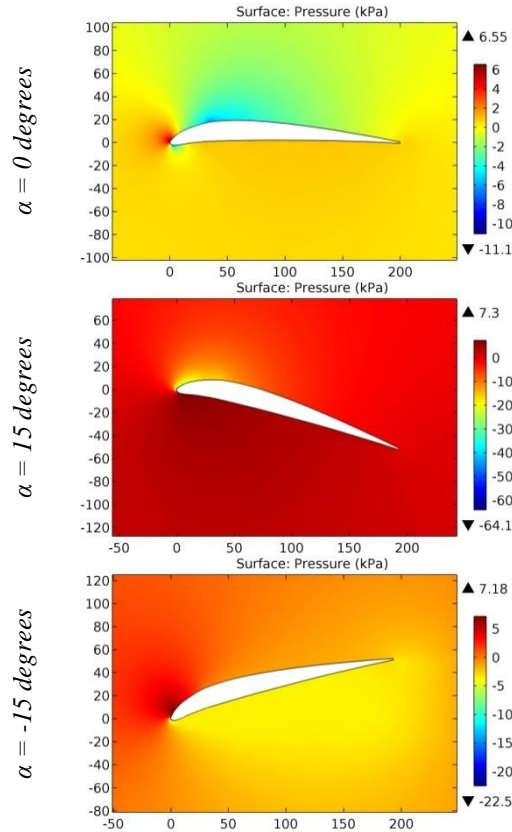


Figure 51. The pressure contours on the surfaces of the GOE 140 (MVA H,17) airfoil.

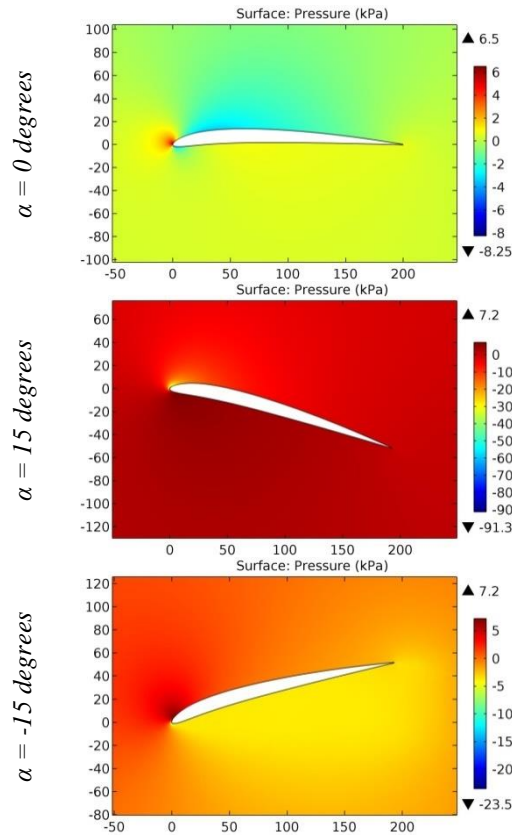


Figure 52. The pressure contours on the surfaces of the GOE 142 (MVA H,19) airfoil.



**Impact Factor:**

ISRA (India) = 6.317	SIS (USA) = 0.912	ICV (Poland) = 6.630
ISI (Dubai, UAE) = 1.582	ПИИЦ (Russia) = 3.939	PIF (India) = 1.940
GIF (Australia) = 0.564	ESJI (KZ) = 9.035	IBI (India) = 4.260
JIF = 1.500	SJIF (Morocco) = 7.184	OAJI (USA) = 0.350

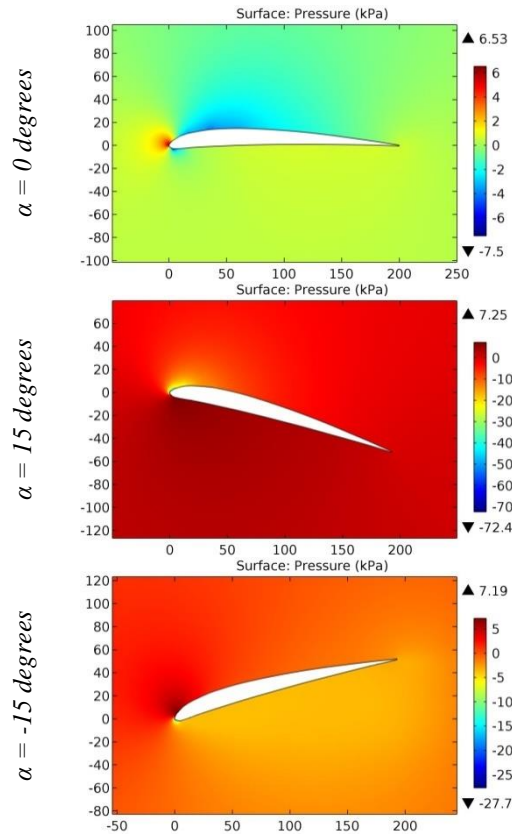


Figure 53. The pressure contours on the surfaces of the GOE 143 (MVA H,20) airfoil.

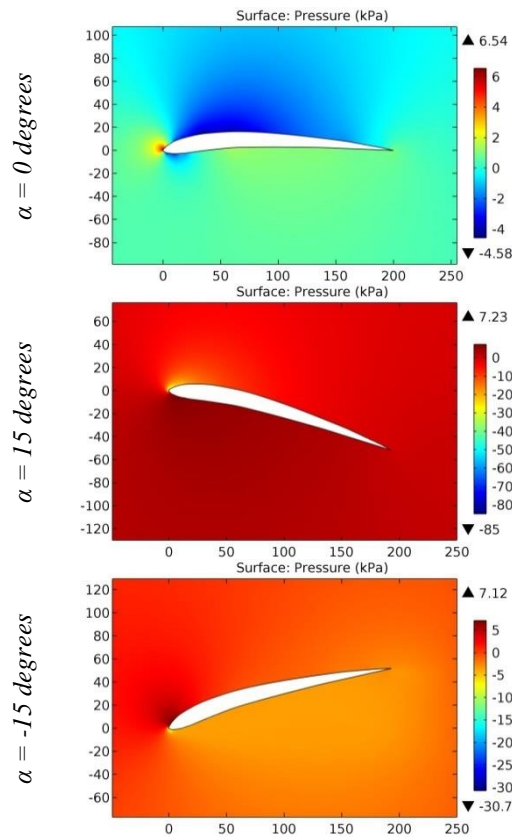


Figure 54. The pressure contours on the surfaces of the GOE 144 (MVA H,21) airfoil.

**Impact Factor:**

ISRA (India) = 6.317	SIS (USA) = 0.912	ICV (Poland) = 6.630
ISI (Dubai, UAE) = 1.582	ПИИЦ (Russia) = 3.939	PIF (India) = 1.940
GIF (Australia) = 0.564	ESJI (KZ) = 9.035	IBI (India) = 4.260
JIF = 1.500	SJIF (Morocco) = 7.184	OAJI (USA) = 0.350

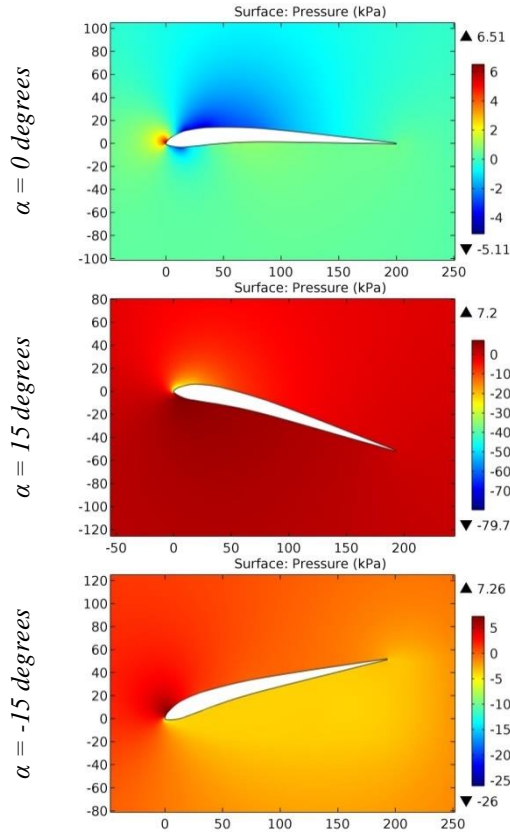


Figure 55. The pressure contours on the surfaces of the GOE 147 (MVA H,6) airfoil.

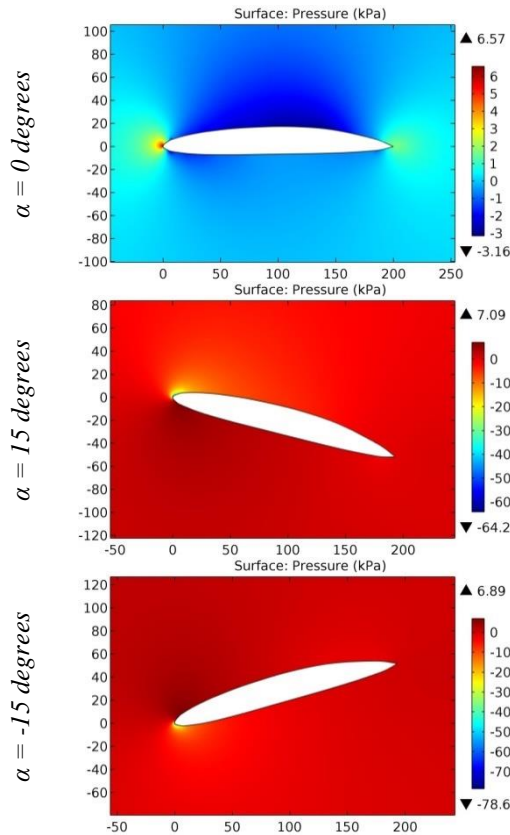


Figure 56. The pressure contours on the surfaces of the GOE 14K airfoil.

**Impact Factor:**

ISRA (India) = 6.317	SIS (USA) = 0.912	ICV (Poland) = 6.630
ISI (Dubai, UAE) = 1.582	ПИИЦ (Russia) = 3.939	PIF (India) = 1.940
GIF (Australia) = 0.564	ESJI (KZ) = 9.035	IBI (India) = 4.260
JIF = 1.500	SJIF (Morocco) = 7.184	OAJI (USA) = 0.350

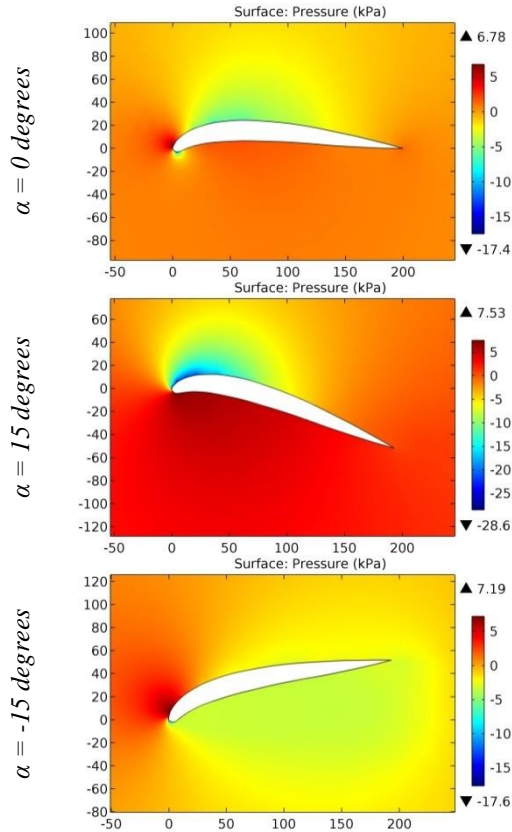


Figure 57. The pressure contours on the surfaces of the GOE 15 airfoil.

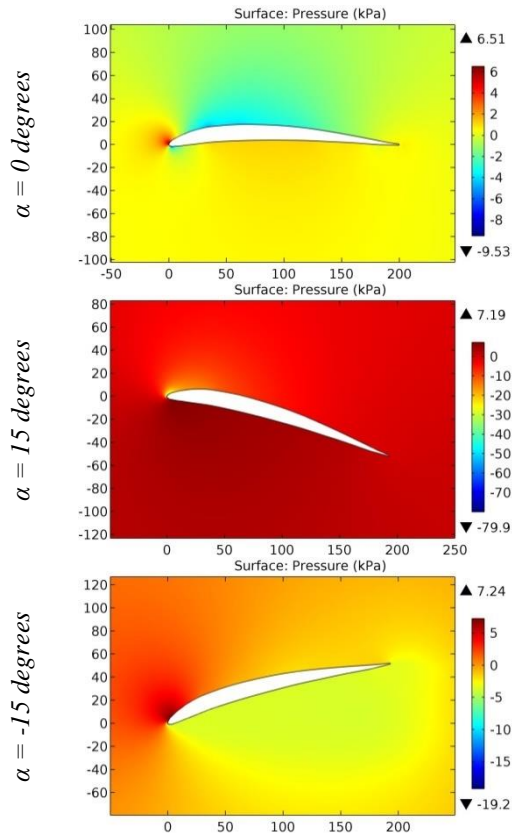


Figure 58. The pressure contours on the surfaces of the GOE 155 (SSW D,1) airfoil.

**Impact Factor:**

ISRA (India) = 6.317	SIS (USA) = 0.912	ICV (Poland) = 6.630
ISI (Dubai, UAE) = 1.582	ПИИЦ (Russia) = 3.939	PIF (India) = 1.940
GIF (Australia) = 0.564	ESJI (KZ) = 9.035	IBI (India) = 4.260
JIF = 1.500	SJIF (Morocco) = 7.184	OAJI (USA) = 0.350

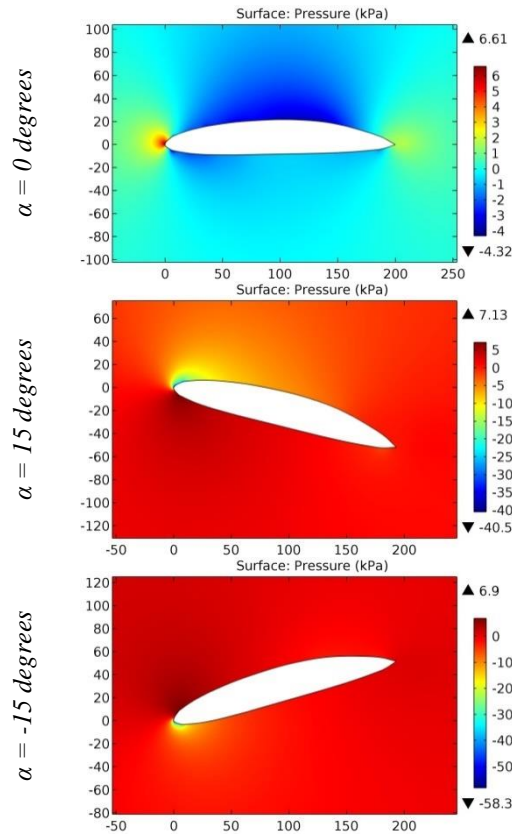


Figure 59. The pressure contours on the surfaces of the GOE 15K airfoil.

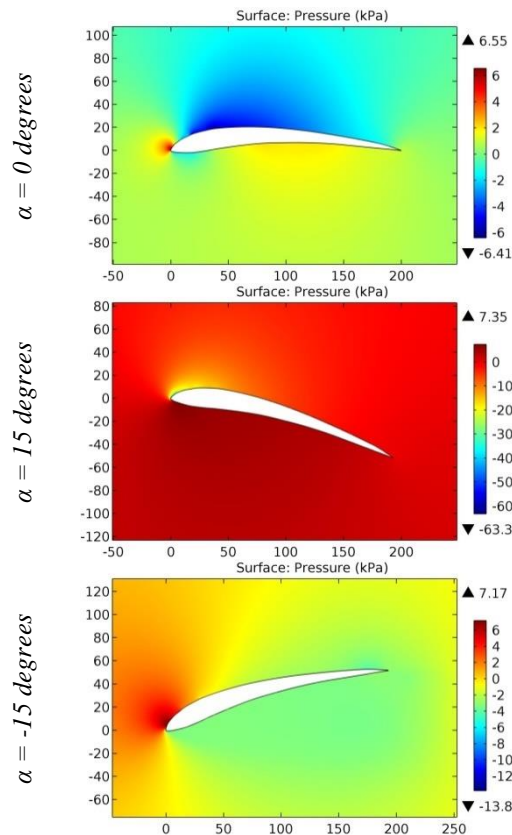


Figure 60. The pressure contours on the surfaces of the GOE 164 (MVA MK,10) airfoil.

**Impact Factor:**

ISRA (India) = 6.317	SIS (USA) = 0.912	ICV (Poland) = 6.630
ISI (Dubai, UAE) = 1.582	ПИИЦ (Russia) = 3.939	PIF (India) = 1.940
GIF (Australia) = 0.564	ESJI (KZ) = 9.035	IBI (India) = 4.260
JIF = 1.500	SJIF (Morocco) = 7.184	OAJI (USA) = 0.350

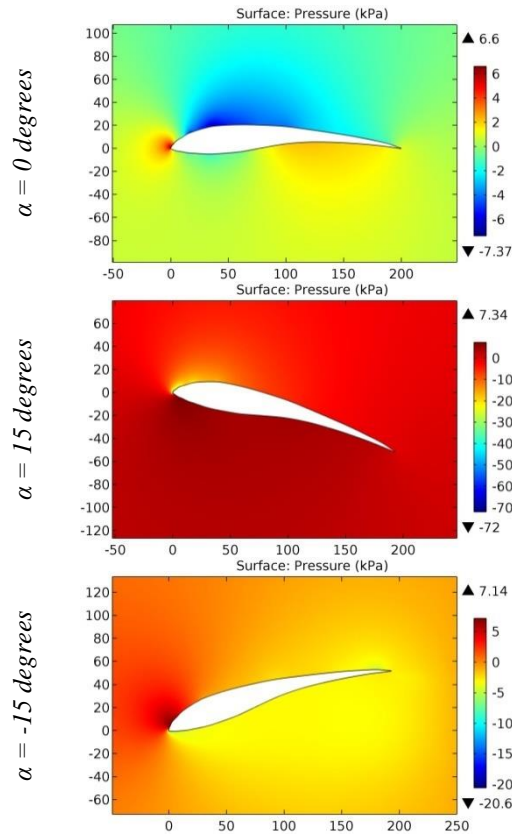


Figure 61. The pressure contours on the surfaces of the GOE 165 (MVA MK,11) airfoil.

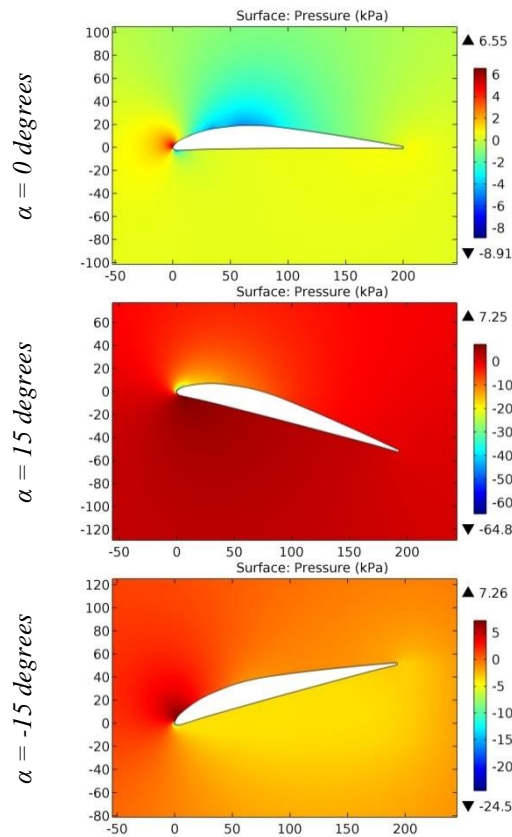


Figure 62. The pressure contours on the surfaces of the GOE 167 (V,KARMAN PROP,2) airfoil.



**Impact Factor:**

ISRA (India) = 6.317	SIS (USA) = 0.912	ICV (Poland) = 6.630
ISI (Dubai, UAE) = 1.582	ПИИЦ (Russia) = 3.939	PIF (India) = 1.940
GIF (Australia) = 0.564	ESJI (KZ) = 9.035	IBI (India) = 4.260
JIF = 1.500	SJIF (Morocco) = 7.184	OAJI (USA) = 0.350

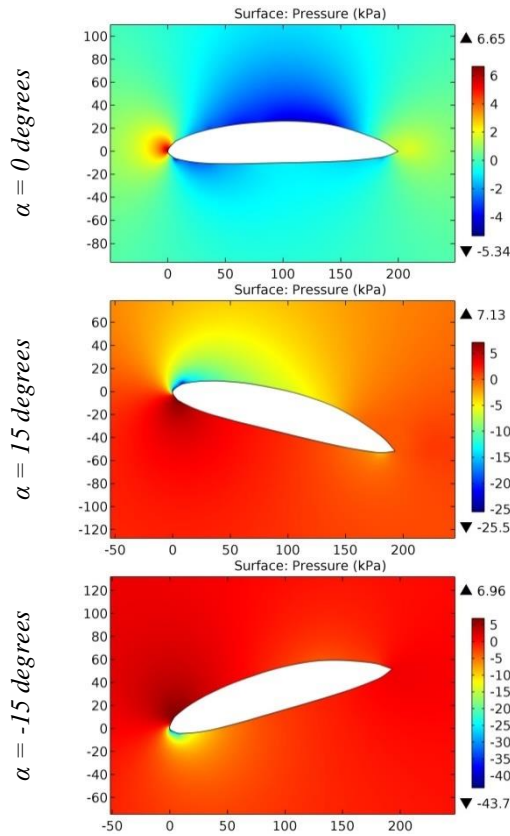


Figure 63. The pressure contours on the surfaces of the GOE 16K airfoil.

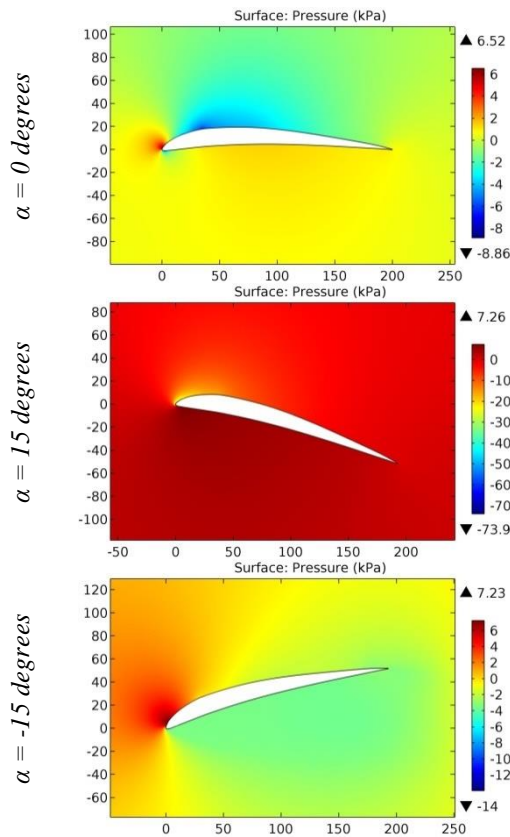


Figure 64. The pressure contours on the surfaces of the GOE 173 (ALBATROS 6020) airfoil.

**Impact Factor:**

ISRA (India) = 6.317	SIS (USA) = 0.912	ICV (Poland) = 6.630
ISI (Dubai, UAE) = 1.582	ПИИЦ (Russia) = 3.939	PIF (India) = 1.940
GIF (Australia) = 0.564	ESJI (KZ) = 9.035	IBI (India) = 4.260
JIF = 1.500	SJIF (Morocco) = 7.184	OAJI (USA) = 0.350

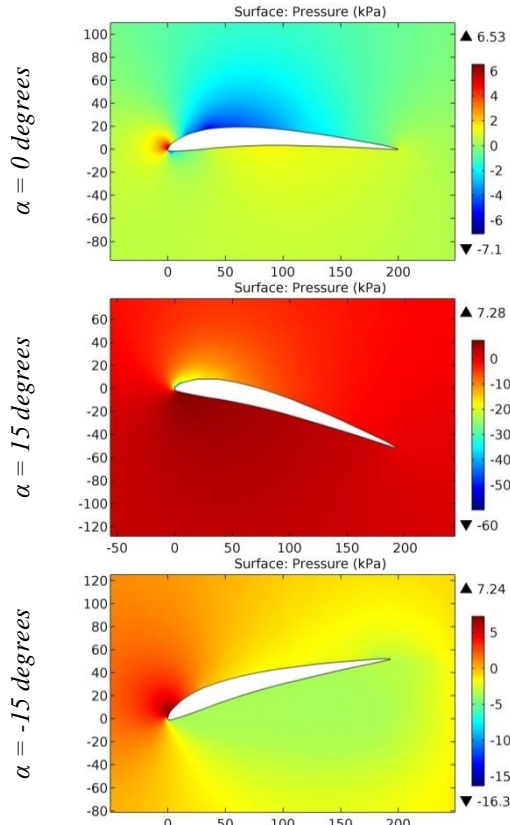


Figure 65. The pressure contours on the surfaces of the GOE 174 (ALBATROS 5020) airfoil.

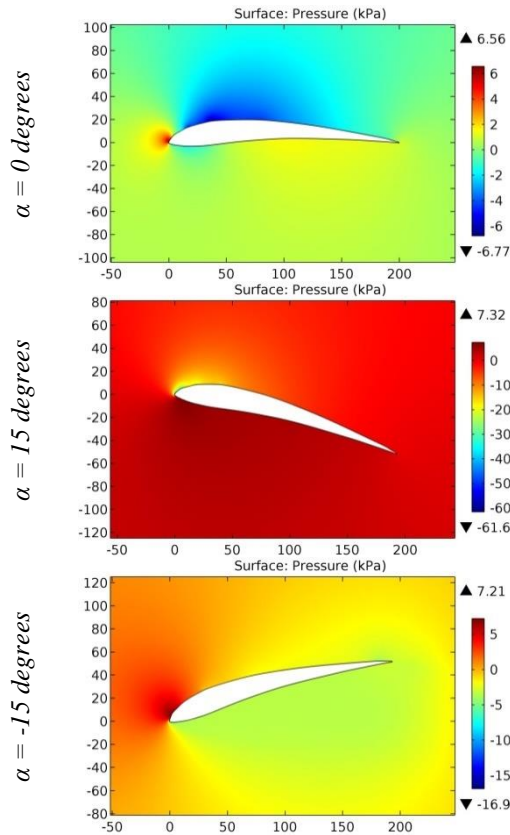


Figure 66. The pressure contours on the surfaces of the GOE 176 (ALBATROS 7020) airfoil.

**Impact Factor:**

<b>ISRA (India)</b> = <b>6.317</b>	<b>SIS (USA)</b> = <b>0.912</b>	<b>ICV (Poland)</b> = <b>6.630</b>
<b>ISI (Dubai, UAE)</b> = <b>1.582</b>	<b>ПИИЦ (Russia)</b> = <b>3.939</b>	<b>PIF (India)</b> = <b>1.940</b>
<b>GIF (Australia)</b> = <b>0.564</b>	<b>ESJI (KZ)</b> = <b>9.035</b>	<b>IBI (India)</b> = <b>4.260</b>
<b>JIF</b> = <b>1.500</b>	<b>SJIF (Morocco)</b> = <b>7.184</b>	<b>OAJI (USA)</b> = <b>0.350</b>

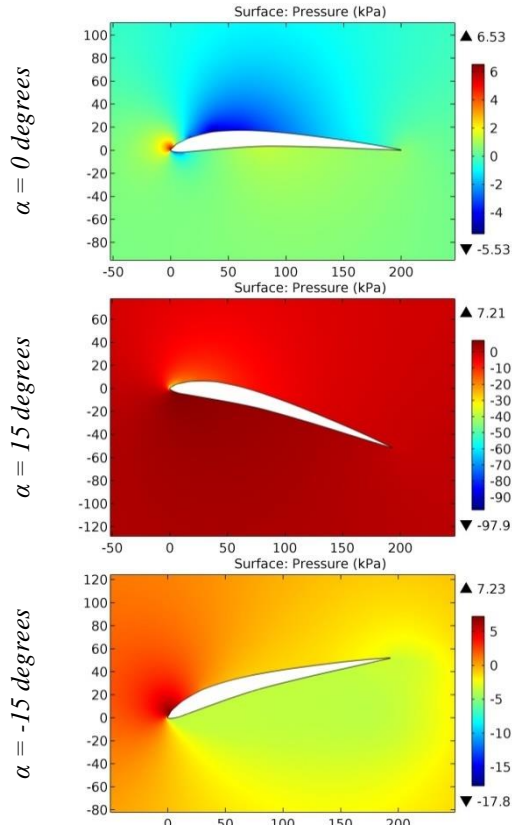


Figure 67. The pressure contours on the surfaces of the GOE 177 airfoil.

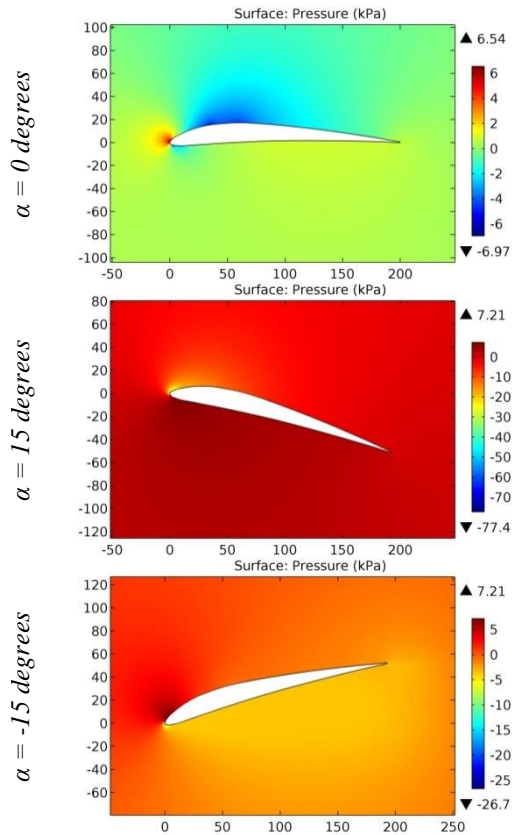


Figure 68. The pressure contours on the surfaces of the GOE 178 airfoil.

**Impact Factor:**

ISRA (India) = 6.317	SIS (USA) = 0.912	ICV (Poland) = 6.630
ISI (Dubai, UAE) = 1.582	ПИИЦ (Russia) = 3.939	PIF (India) = 1.940
GIF (Australia) = 0.564	ESJI (KZ) = 9.035	IBI (India) = 4.260
JIF = 1.500	SJIF (Morocco) = 7.184	OAJI (USA) = 0.350

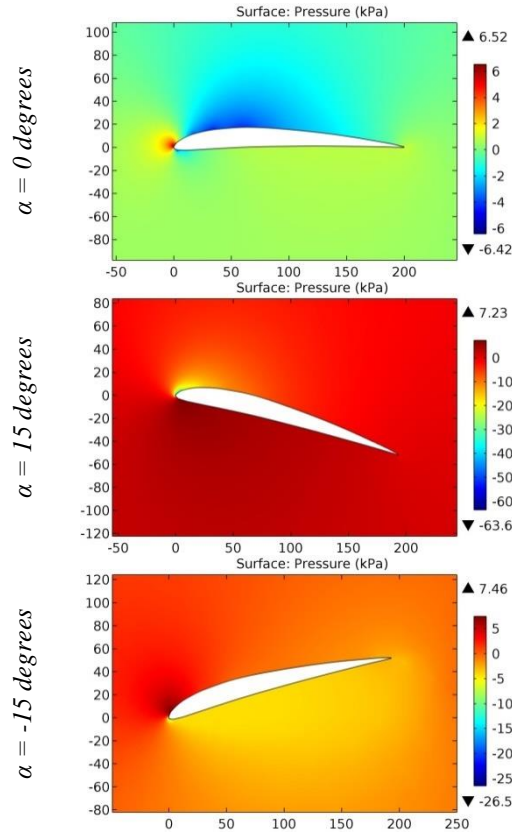


Figure 69. The pressure contours on the surfaces of the GOE 180 (MVA H,26) airfoil.

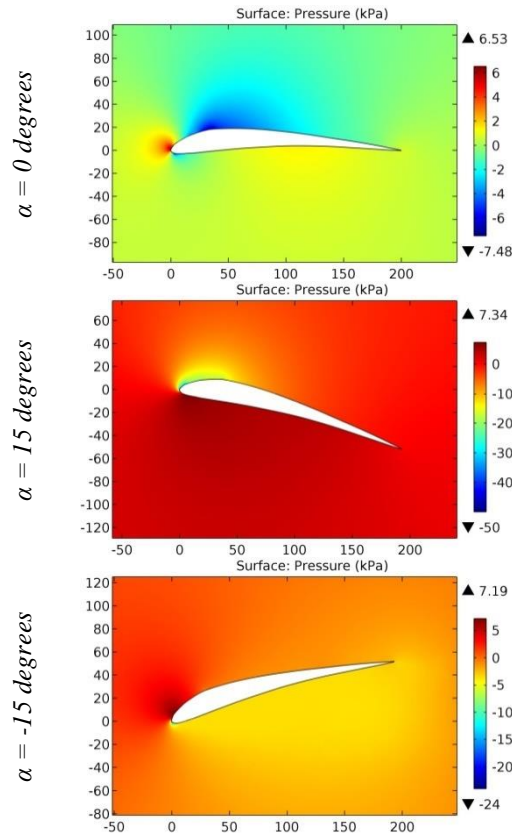


Figure 70. The pressure contours on the surfaces of the GOE 182 (MVA H,27) airfoil.

**Impact Factor:**

ISRA (India) = 6.317	SIS (USA) = 0.912	ICV (Poland) = 6.630
ISI (Dubai, UAE) = 1.582	ПИИЦ (Russia) = 3.939	PIF (India) = 1.940
GIF (Australia) = 0.564	ESJI (KZ) = 9.035	IBI (India) = 4.260
JIF = 1.500	SJIF (Morocco) = 7.184	OAJI (USA) = 0.350

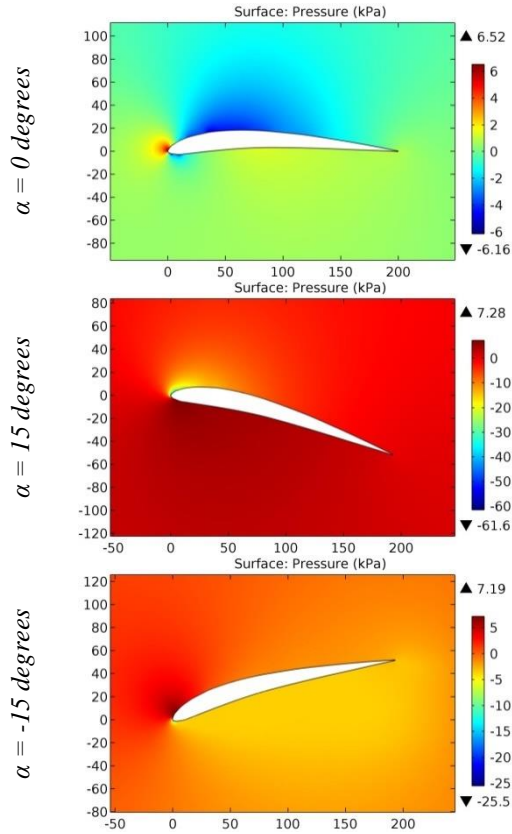


Figure 71. The pressure contours on the surfaces of the GOE 184 (MVA H,29) airfoil.

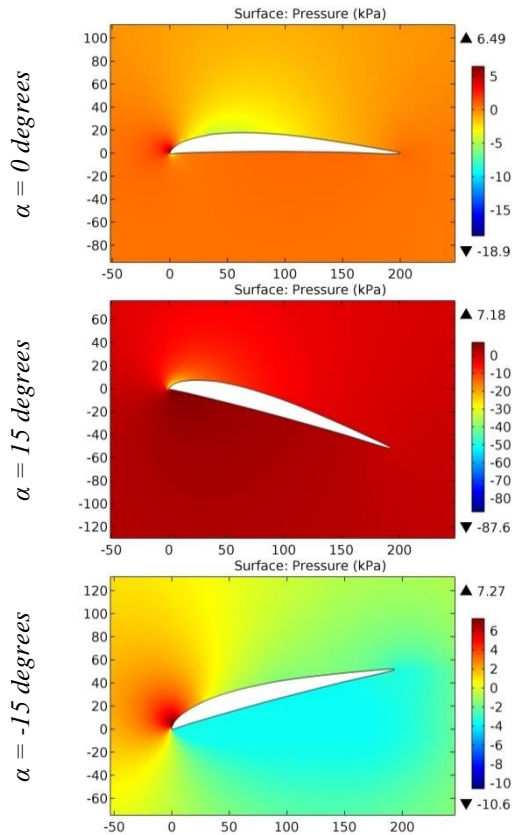


Figure 72. The pressure contours on the surfaces of the GOE 187 (SCH-TTE-LANZ 2U10) airfoil.



**Impact Factor:**

<b>SISRA</b> (India) = <b>6.317</b>	<b>SIS</b> (USA) = <b>0.912</b>	<b>ICV</b> (Poland) = <b>6.630</b>
<b>ISI</b> (Dubai, UAE) = <b>1.582</b>	<b>ПИИЦ</b> (Russia) = <b>3.939</b>	<b>PIF</b> (India) = <b>1.940</b>
<b>GIF</b> (Australia) = <b>0.564</b>	<b>ESJI</b> (KZ) = <b>9.035</b>	<b>IBI</b> (India) = <b>4.260</b>
<b>JIF</b> = <b>1.500</b>	<b>SJIF</b> (Morocco) = <b>7.184</b>	<b>OAJI</b> (USA) = <b>0.350</b>

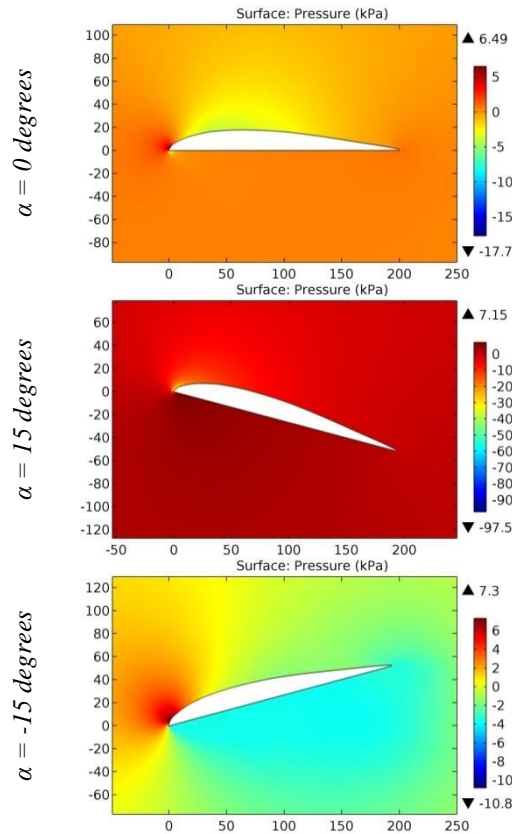


Figure 73. The pressure contours on the surfaces of the GOE 188 (SCH-TTE-LANZ 3U10) airfoil.

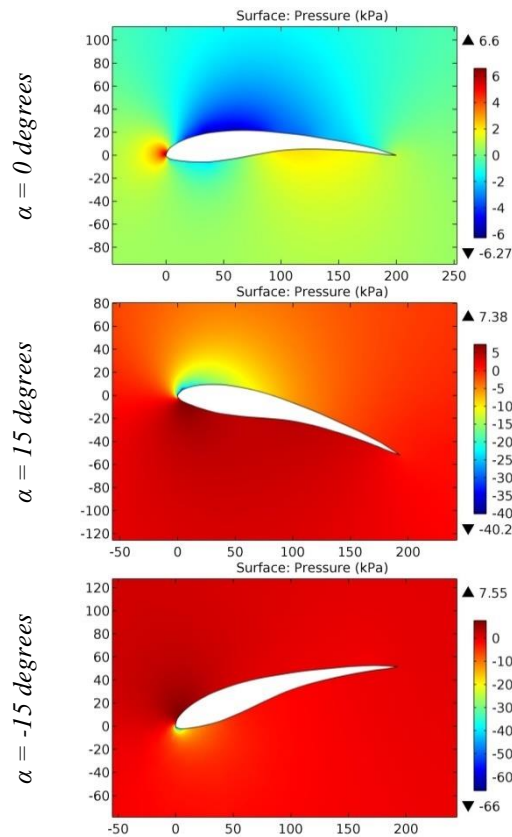


Figure 74. The pressure contours on the surfaces of the GOE 190 (MVA MK,18) airfoil.

**Impact Factor:**

ISRA (India) = 6.317	SIS (USA) = 0.912	ICV (Poland) = 6.630
ISI (Dubai, UAE) = 1.582	ПИИЦ (Russia) = 3.939	PIF (India) = 1.940
GIF (Australia) = 0.564	ESJI (KZ) = 9.035	IBI (India) = 4.260
JIF = 1.500	SJIF (Morocco) = 7.184	OAJI (USA) = 0.350

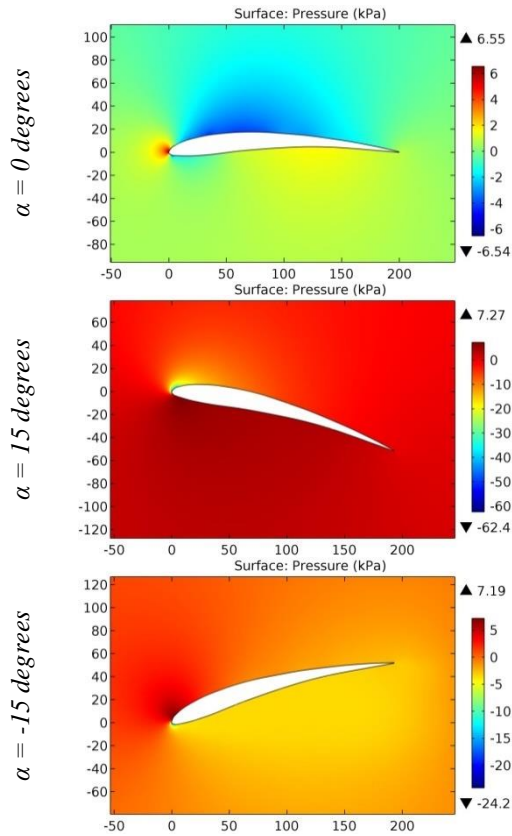


Figure 75. The pressure contours on the surfaces of the GOE 195 airfoil.

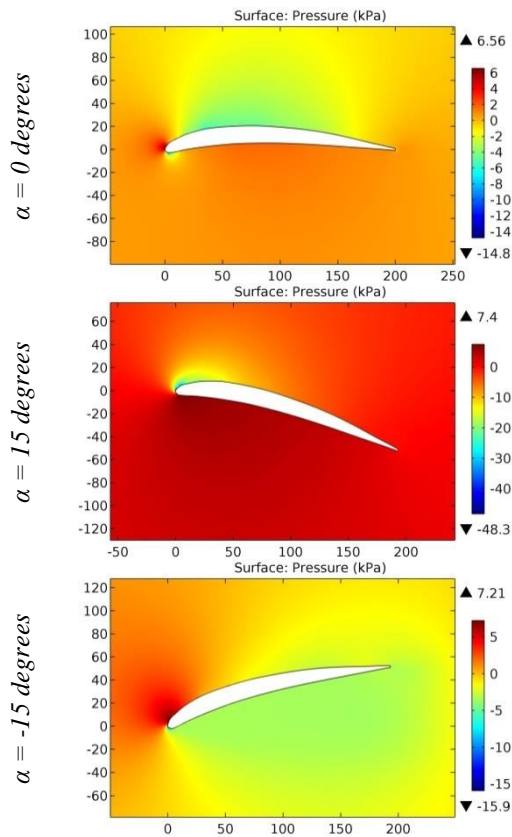


Figure 76. The pressure contours on the surfaces of the GOE 198 (L,F,G, 5294) airfoil.

**Impact Factor:**

ISRA (India) = 6.317	SIS (USA) = 0.912	ICV (Poland) = 6.630
ISI (Dubai, UAE) = 1.582	ПИИЦ (Russia) = 3.939	PIF (India) = 1.940
GIF (Australia) = 0.564	ESJI (KZ) = 9.035	IBI (India) = 4.260
JIF = 1.500	SJIF (Morocco) = 7.184	OAJI (USA) = 0.350

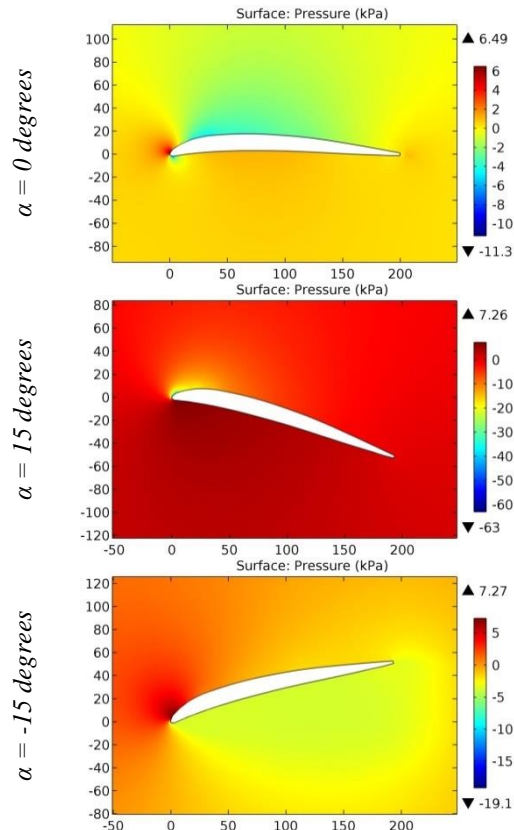


Figure 77. The pressure contours on the surfaces of the GOE 199 (L,F,G, 5406) airfoil.

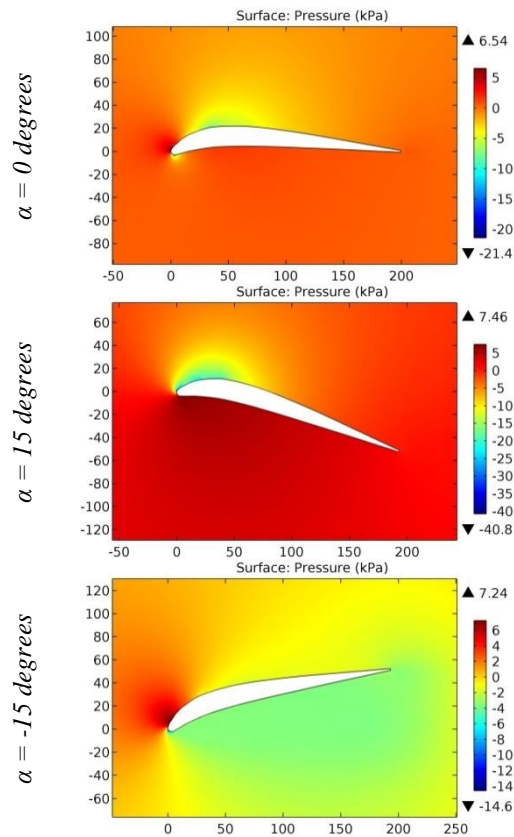


Figure 78. The pressure contours on the surfaces of the GOE 207 (AVIATIK V8) airfoil.

**Impact Factor:**

ISRA (India) = 6.317	SIS (USA) = 0.912	ICV (Poland) = 6.630
ISI (Dubai, UAE) = 1.582	ПИИЦ (Russia) = 3.939	PIF (India) = 1.940
GIF (Australia) = 0.564	ESJI (KZ) = 9.035	IBI (India) = 4.260
JIF = 1.500	SJIF (Morocco) = 7.184	OAJI (USA) = 0.350

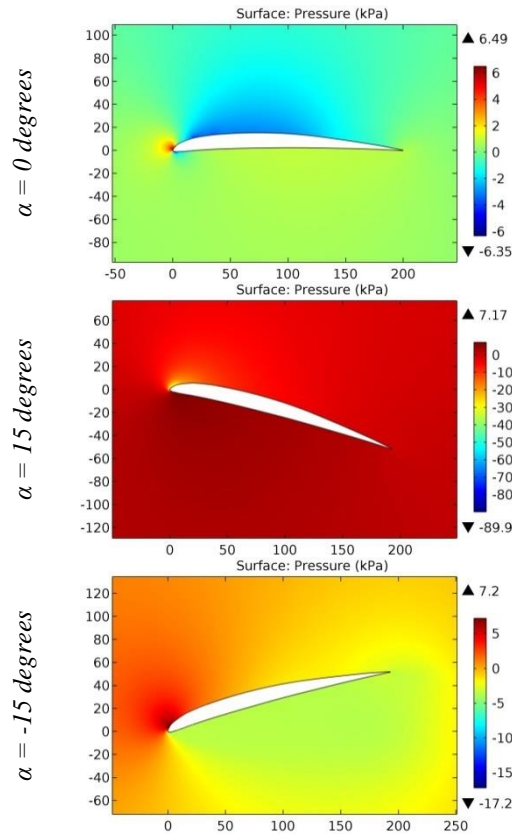


Figure 79. The pressure contours on the surfaces of the GOE 210 (DAIMLER) airfoil.

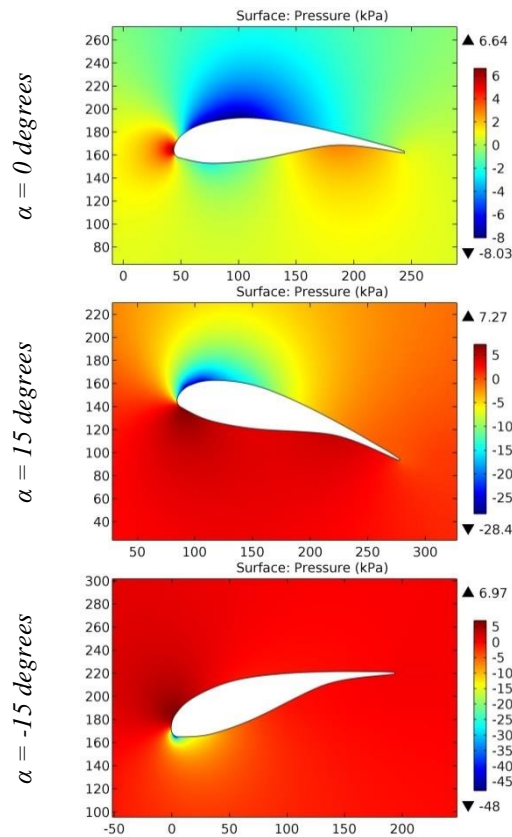


Figure 80. The pressure contours on the surfaces of the GOE 217 (MVA MK,12) airfoil.

**Impact Factor:**

<b>ISRA (India)</b> = <b>6.317</b>	<b>SIS (USA)</b> = <b>0.912</b>	<b>ICV (Poland)</b> = <b>6.630</b>
<b>ISI (Dubai, UAE)</b> = <b>1.582</b>	<b>ПИИЦ (Russia)</b> = <b>3.939</b>	<b>PIF (India)</b> = <b>1.940</b>
<b>GIF (Australia)</b> = <b>0.564</b>	<b>ESJI (KZ)</b> = <b>9.035</b>	<b>IBI (India)</b> = <b>4.260</b>
<b>JIF</b> = <b>1.500</b>	<b>SJIF (Morocco)</b> = <b>7.184</b>	<b>OAJI (USA)</b> = <b>0.350</b>

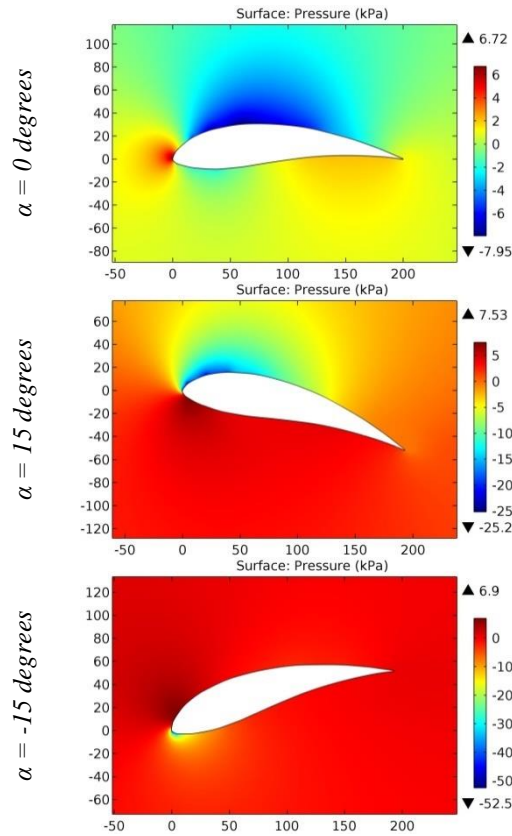


Figure 81. The pressure contours on the surfaces of the GOE 222 (MVA H,33) airfoil.

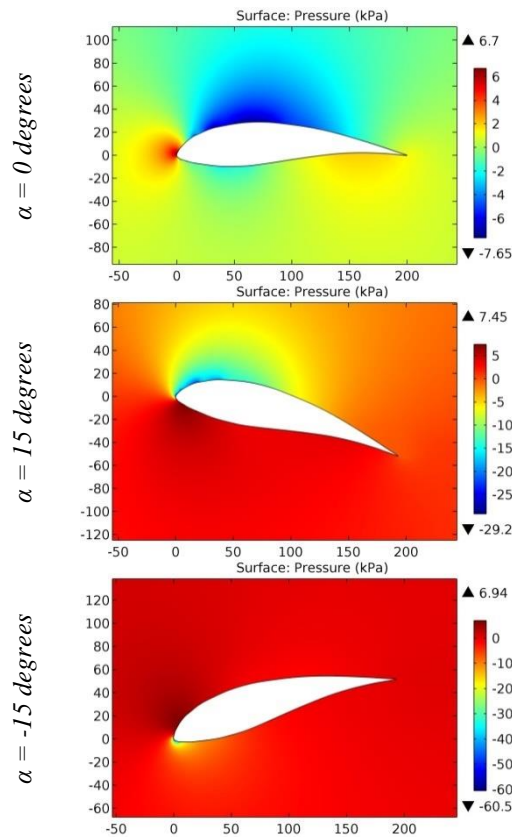


Figure 82. The pressure contours on the surfaces of the GOE 223 (MVA H,34) airfoil.



**Impact Factor:**

ISRA (India) = 6.317	SIS (USA) = 0.912	ICV (Poland) = 6.630
ISI (Dubai, UAE) = 1.582	ПИИЦ (Russia) = 3.939	PIF (India) = 1.940
GIF (Australia) = 0.564	ESJI (KZ) = 9.035	IBI (India) = 4.260
JIF = 1.500	SJIF (Morocco) = 7.184	OAJI (USA) = 0.350

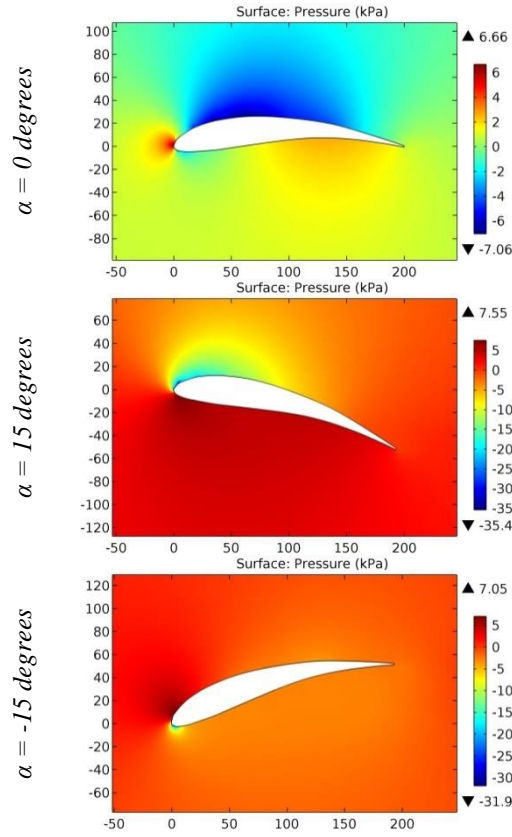


Figure 83. The pressure contours on the surfaces of the GOE 225 (MVA H,35) airfoil.

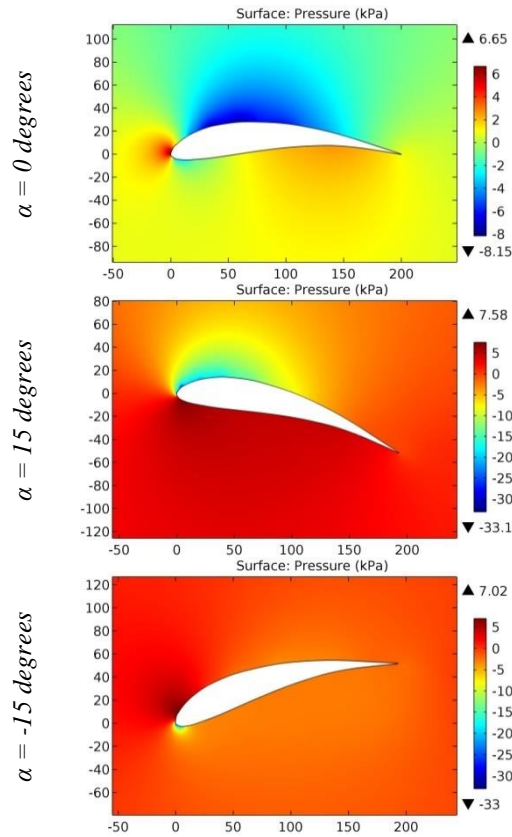


Figure 84. The pressure contours on the surfaces of the GOE 226 (MVA H,36) airfoil.

**Impact Factor:**

ISRA (India) = 6.317	SIS (USA) = 0.912	ICV (Poland) = 6.630
ISI (Dubai, UAE) = 1.582	ПИИЦ (Russia) = 3.939	PIF (India) = 1.940
GIF (Australia) = 0.564	ESJI (KZ) = 9.035	IBI (India) = 4.260
JIF = 1.500	SJIF (Morocco) = 7.184	OAJI (USA) = 0.350

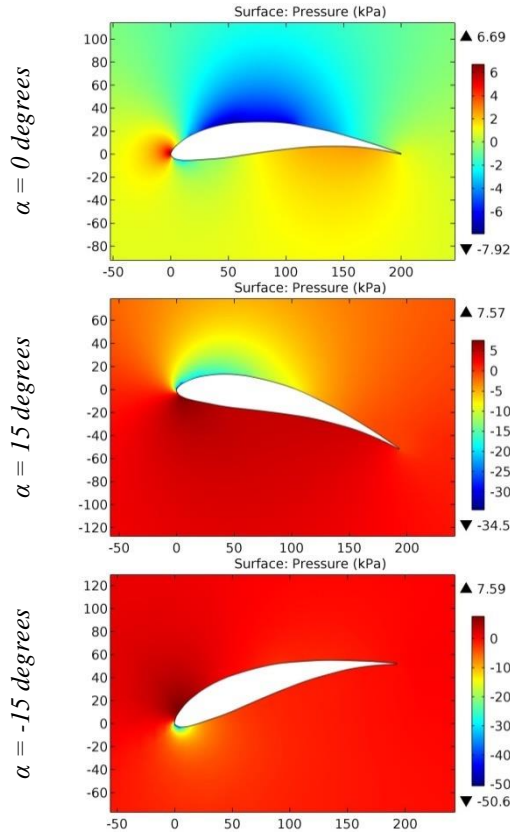


Figure 85. The pressure contours on the surfaces of the GOE 227 (MVA H,37) airfoil.

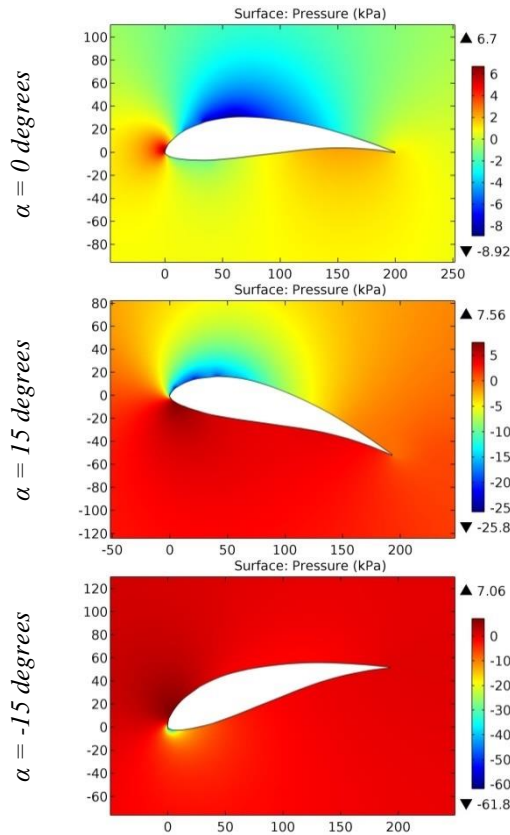


Figure 86. The pressure contours on the surfaces of the GOE 228 (MVA H,38) airfoil.

**Impact Factor:**

ISRA (India) = 6.317	SIS (USA) = 0.912	ICV (Poland) = 6.630
ISI (Dubai, UAE) = 1.582	ПИИЦ (Russia) = 3.939	PIF (India) = 1.940
GIF (Australia) = 0.564	ESJI (KZ) = 9.035	IBI (India) = 4.260
JIF = 1.500	SJIF (Morocco) = 7.184	OAJI (USA) = 0.350

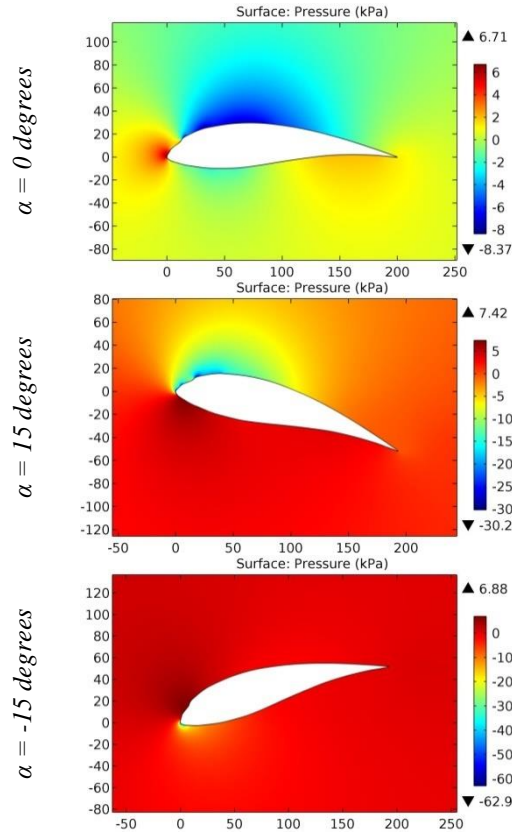


Figure 87. The pressure contours on the surfaces of the GOE 229 (MVA H,39) airfoil.

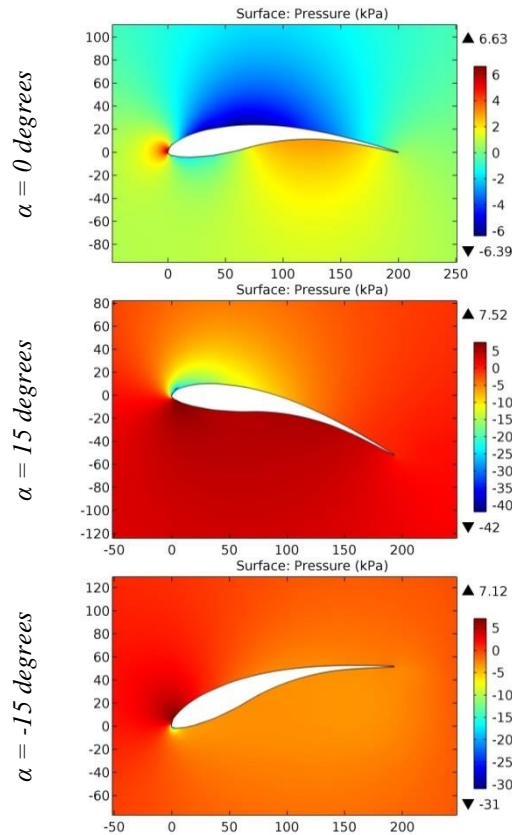


Figure 88. The pressure contours on the surfaces of the GOE 233 (MVA CA4) airfoil.

**Impact Factor:**

ISRA (India) = 6.317	SIS (USA) = 0.912	ICV (Poland) = 6.630
ISI (Dubai, UAE) = 1.582	ПИИЦ (Russia) = 3.939	PIF (India) = 1.940
GIF (Australia) = 0.564	ESJI (KZ) = 9.035	IBI (India) = 4.260
JIF = 1.500	SJIF (Morocco) = 7.184	OAJI (USA) = 0.350

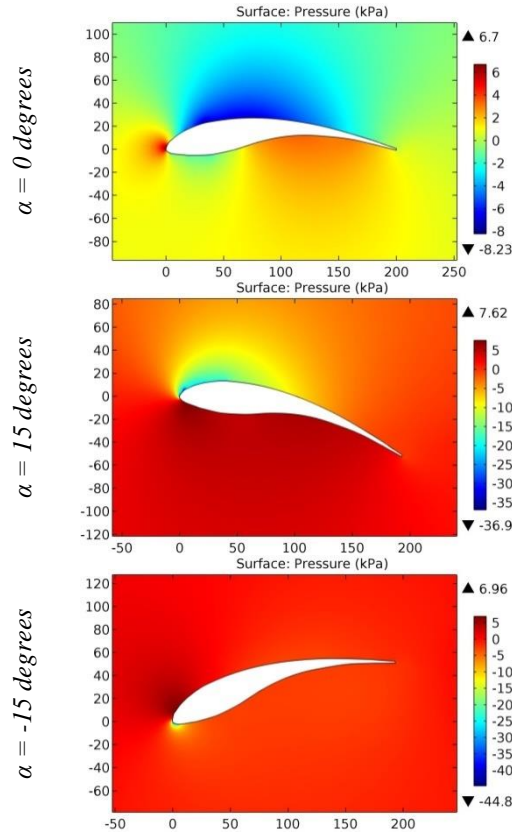


Figure 89. The pressure contours on the surfaces of the GOE 234 (MVA CA5) airfoil.

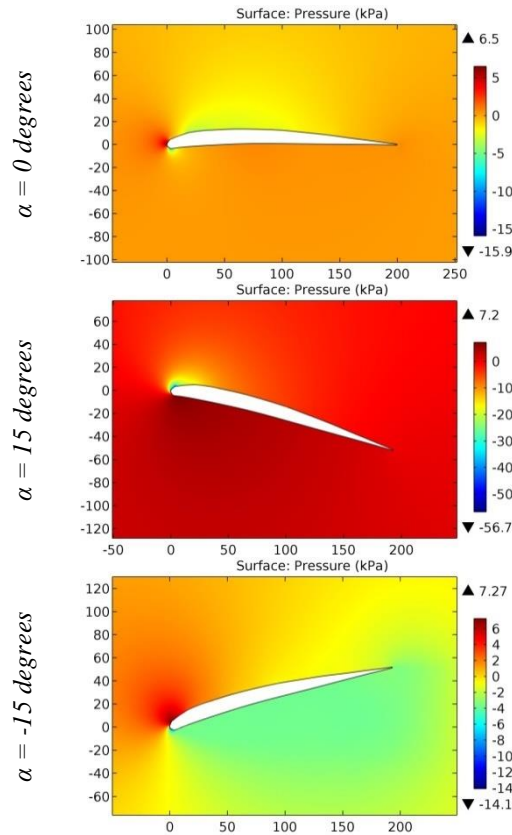


Figure 90. The pressure contours on the surfaces of the GOE 235 (SCH-TTE-LANZ) airfoil.

**Impact Factor:**

ISRA (India) = 6.317	SIS (USA) = 0.912	ICV (Poland) = 6.630
ISI (Dubai, UAE) = 1.582	ПИИЦ (Russia) = 3.939	PIF (India) = 1.940
GIF (Australia) = 0.564	ESJI (KZ) = 9.035	IBI (India) = 4.260
JIF = 1.500	SJIF (Morocco) = 7.184	OAJI (USA) = 0.350

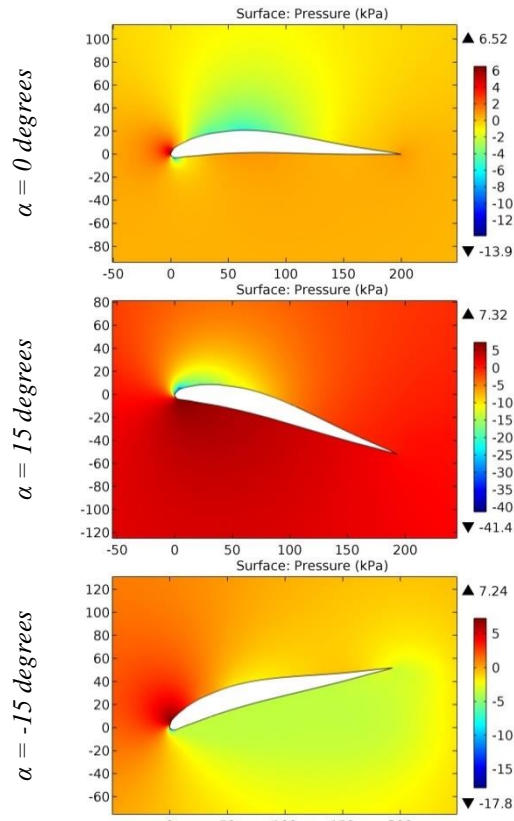


Figure 91. The pressure contours on the surfaces of the GOE 238 (HANSA-BRANDENBURG) airfoil.

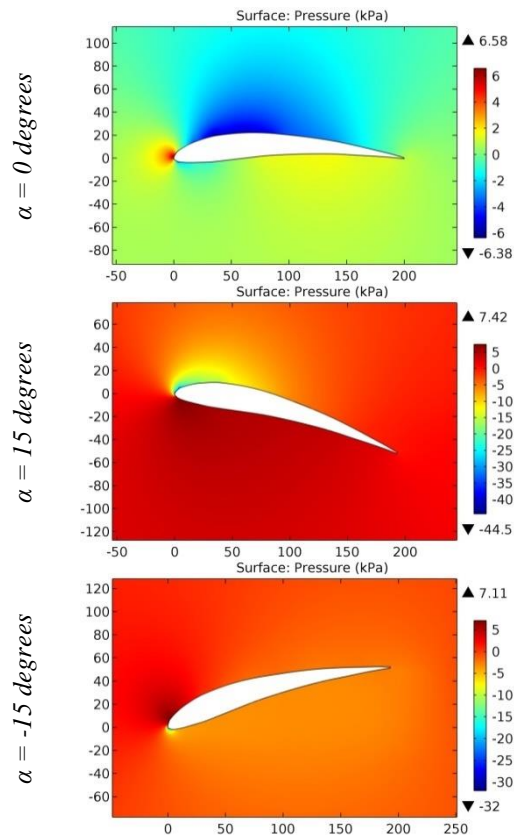


Figure 92. The pressure contours on the surfaces of the GOE 239 (MVA H,31) airfoil.



**Impact Factor:**

ISRA (India) = 6.317	SIS (USA) = 0.912	ICV (Poland) = 6.630
ISI (Dubai, UAE) = 1.582	ПИИЦ (Russia) = 3.939	PIF (India) = 1.940
GIF (Australia) = 0.564	ESJI (KZ) = 9.035	IBI (India) = 4.260
JIF = 1.500	SJIF (Morocco) = 7.184	OAJI (USA) = 0.350

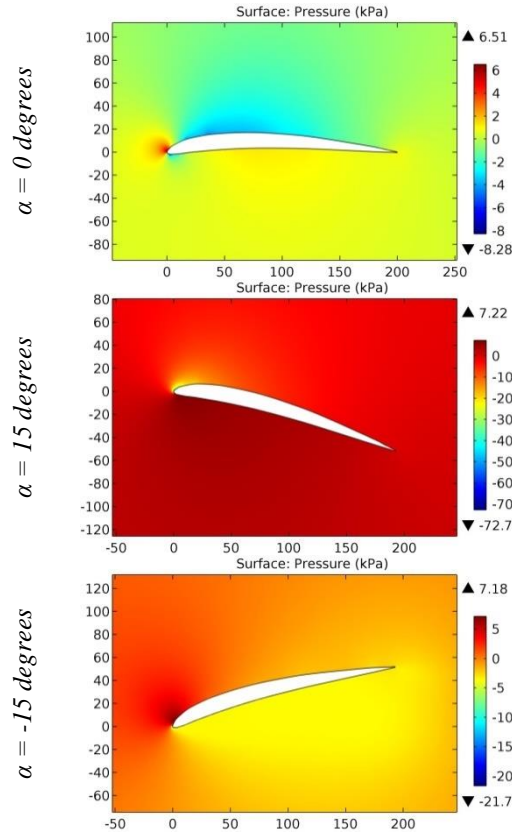


Figure 93. The pressure contours on the surfaces of the GOE 240 (KOLLER) airfoil.

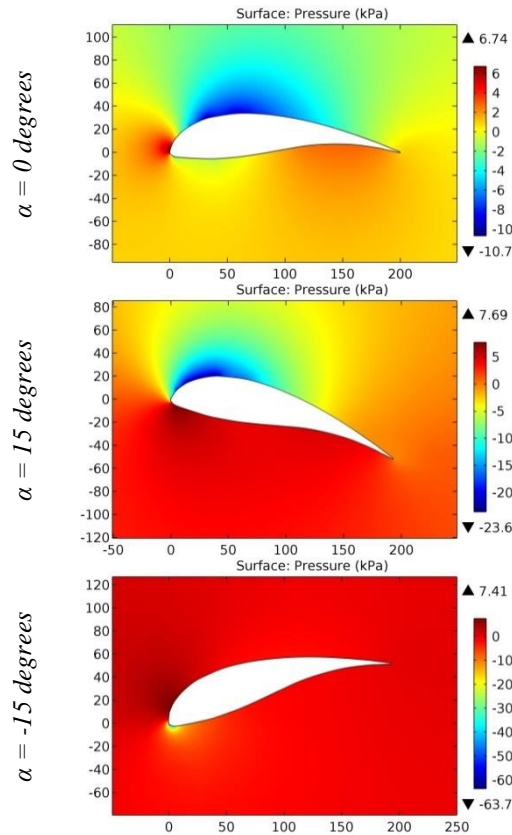


Figure 94. The pressure contours on the surfaces of the GOE 241 (MVA PR,1) airfoil.

**Impact Factor:**

ISRA (India) = 6.317	SIS (USA) = 0.912	ICV (Poland) = 6.630
ISI (Dubai, UAE) = 1.582	ПИИЦ (Russia) = 3.939	PIF (India) = 1.940
GIF (Australia) = 0.564	ESJI (KZ) = 9.035	IBI (India) = 4.260
JIF = 1.500	SJIF (Morocco) = 7.184	OAJI (USA) = 0.350

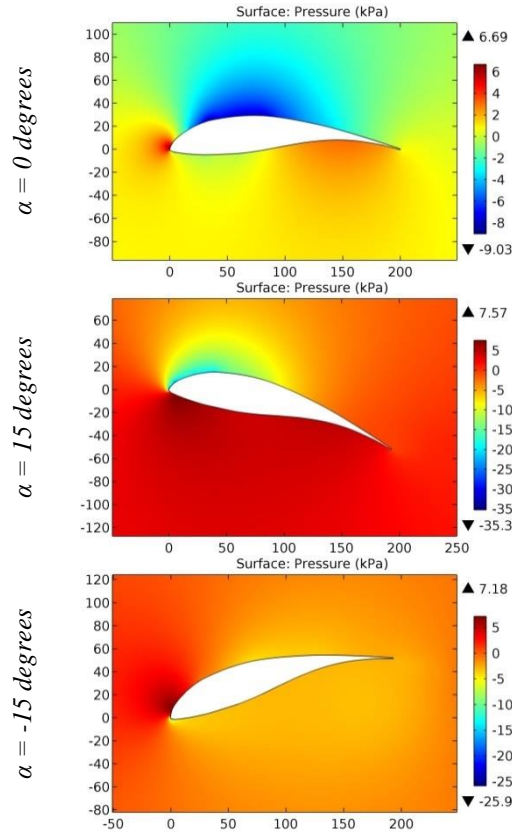


Figure 95. The pressure contours on the surfaces of the GOE 242 (MVA PR,2) airfoil.

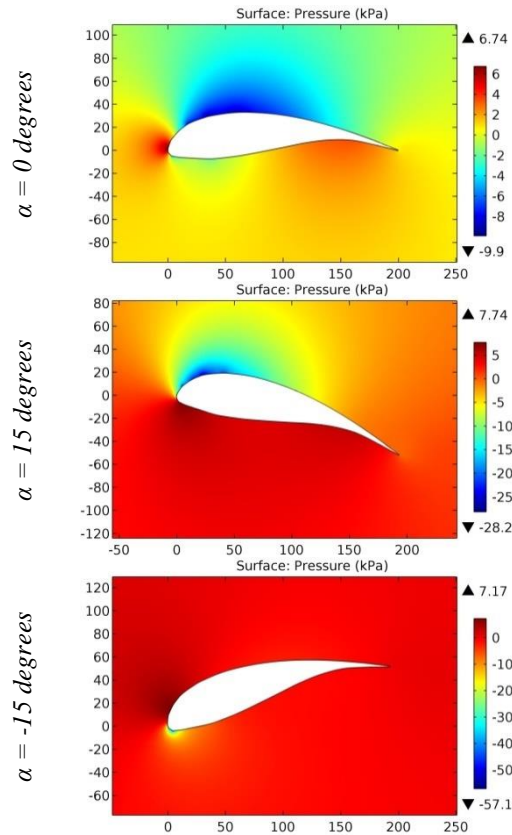


Figure 96. The pressure contours on the surfaces of the GOE 243 (MVA PR,3) airfoil.

**Impact Factor:**

<b>ISRA (India)</b> = <b>6.317</b>	<b>SIS (USA)</b> = <b>0.912</b>	<b>ICV (Poland)</b> = <b>6.630</b>
<b>ISI (Dubai, UAE)</b> = <b>1.582</b>	<b>ПИИЦ (Russia)</b> = <b>3.939</b>	<b>PIF (India)</b> = <b>1.940</b>
<b>GIF (Australia)</b> = <b>0.564</b>	<b>ESJI (KZ)</b> = <b>9.035</b>	<b>IBI (India)</b> = <b>4.260</b>
<b>JIF</b> = <b>1.500</b>	<b>SJIF (Morocco)</b> = <b>7.184</b>	<b>OAJI (USA)</b> = <b>0.350</b>

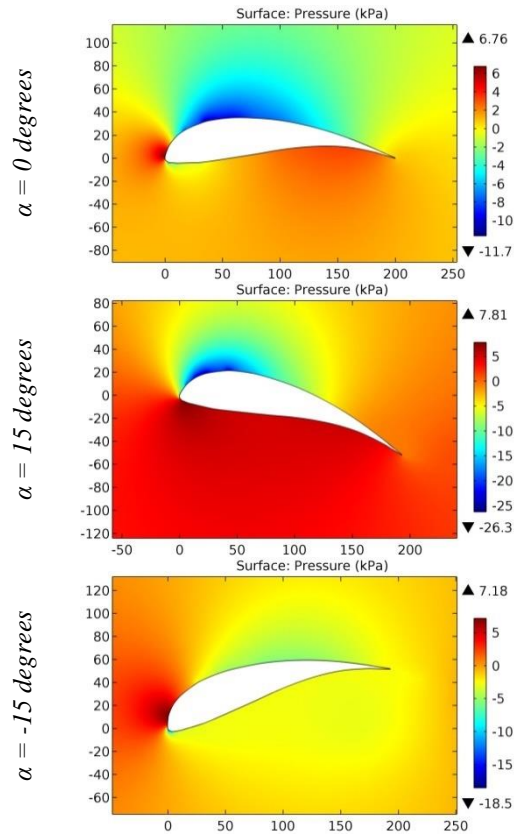


Figure 97. The pressure contours on the surfaces of the GOE 244 (MVA PR,4) airfoil.

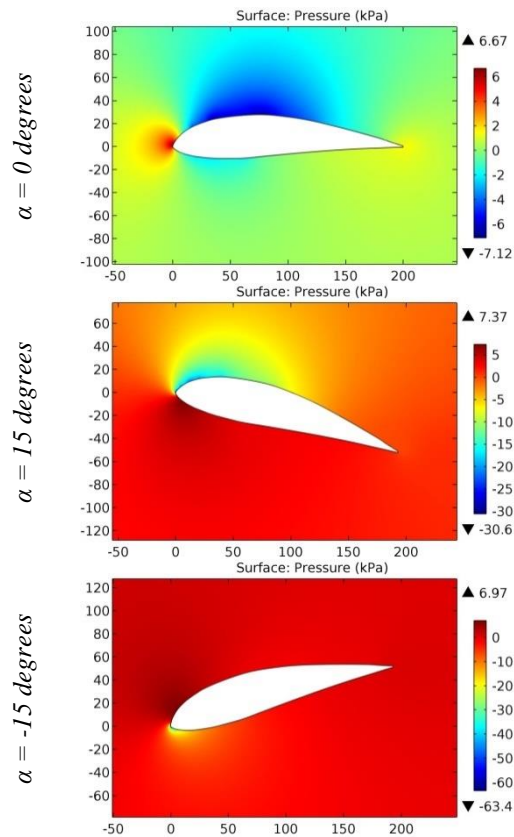


Figure 98. The pressure contours on the surfaces of the GOE 255 (MVA CA,6) airfoil.

**Impact Factor:**

ISRA (India) = 6.317	SIS (USA) = 0.912	ICV (Poland) = 6.630
ISI (Dubai, UAE) = 1.582	ПИИЦ (Russia) = 3.939	PIF (India) = 1.940
GIF (Australia) = 0.564	ESJI (KZ) = 9.035	IBI (India) = 4.260
JIF = 1.500	SJIF (Morocco) = 7.184	OAJI (USA) = 0.350

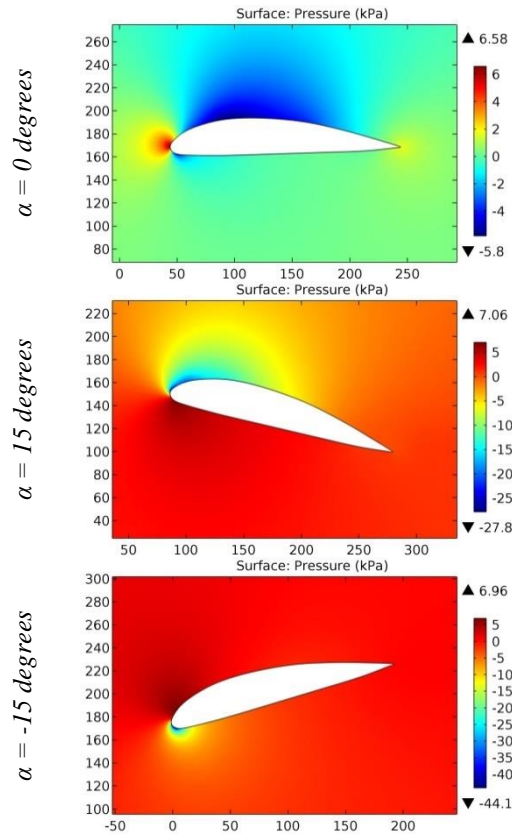


Figure 99. The pressure contours on the surfaces of the GOE 256 (JUNKERS E) airfoil.

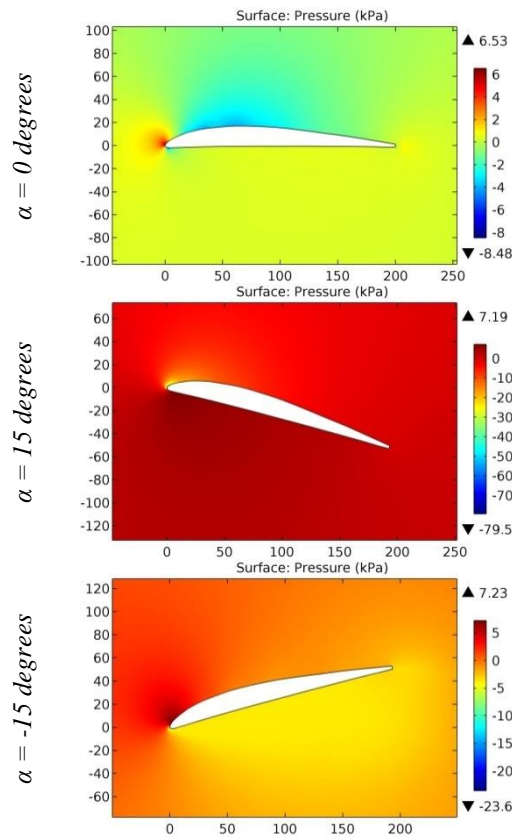


Figure 100. The pressure contours on the surfaces of the GOE 257 airfoil.

**Impact Factor:**

<b>ISRA (India)</b> = <b>6.317</b>	<b>SIS (USA)</b> = <b>0.912</b>	<b>ICV (Poland)</b> = <b>6.630</b>
<b>ISI (Dubai, UAE)</b> = <b>1.582</b>	<b>ПИИЦ (Russia)</b> = <b>3.939</b>	<b>PIF (India)</b> = <b>1.940</b>
<b>GIF (Australia)</b> = <b>0.564</b>	<b>ESJI (KZ)</b> = <b>9.035</b>	<b>IBI (India)</b> = <b>4.260</b>
<b>JIF</b> = <b>1.500</b>	<b>SJIF (Morocco)</b> = <b>7.184</b>	<b>OAJI (USA)</b> = <b>0.350</b>

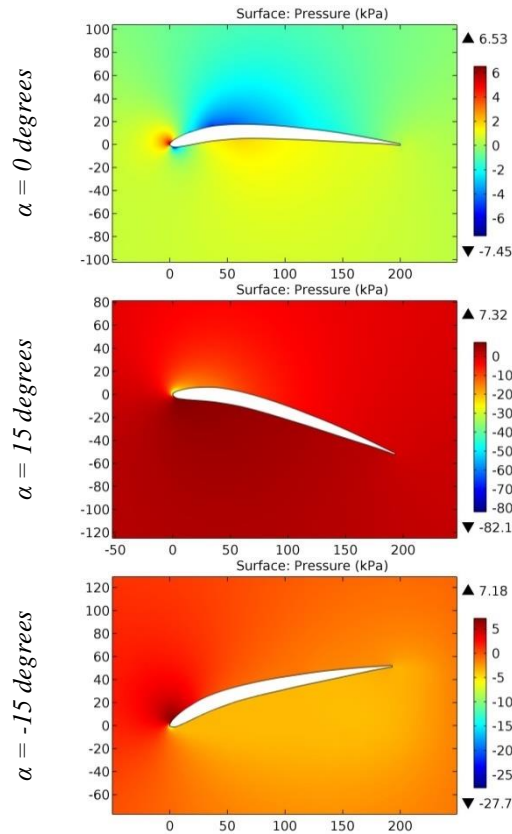


Figure 101. The pressure contours on the surfaces of the GOE 264 airfoil.

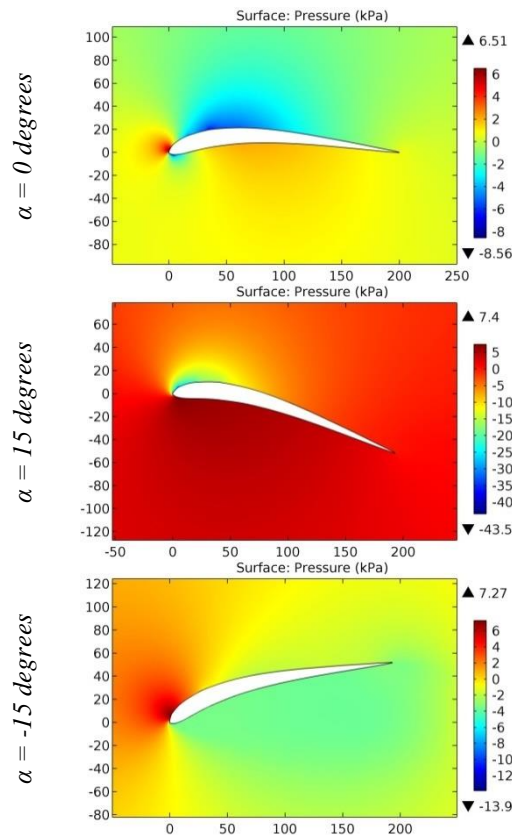
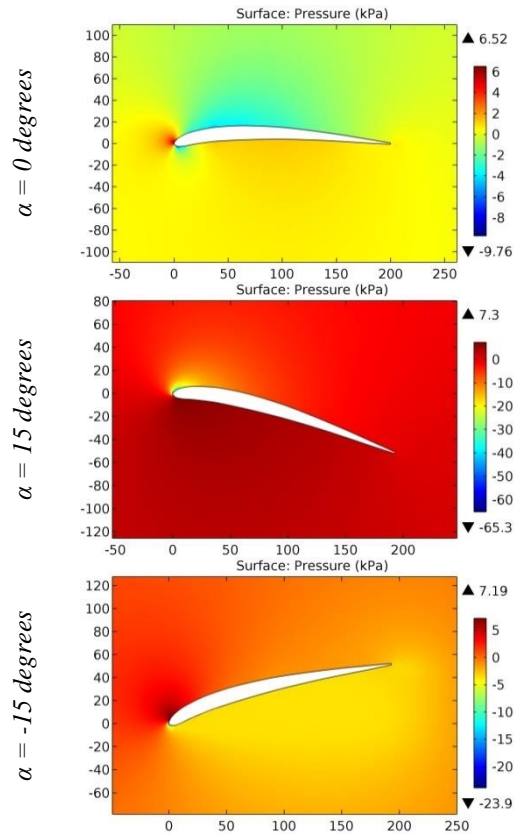


Figure 102. The pressure contours on the surfaces of the GOE 265 airfoil.



**Impact Factor:**

<b>SISRA</b> (India)	= <b>6.317</b>	<b>SIS</b> (USA)	= <b>0.912</b>	<b>ICV</b> (Poland)	= <b>6.630</b>
<b>ISI</b> (Dubai, UAE)	= <b>1.582</b>	<b>ПИИЦ</b> (Russia)	= <b>3.939</b>	<b>PIF</b> (India)	= <b>1.940</b>
<b>GIF</b> (Australia)	= <b>0.564</b>	<b>ESJI</b> (KZ)	= <b>9.035</b>	<b>IBI</b> (India)	= <b>4.260</b>
<b>JIF</b>	= <b>1.500</b>	<b>SJIF</b> (Morocco)	= <b>7.184</b>	<b>OAJI</b> (USA)	= <b>0.350</b>



**Figure 103.** The pressure contours on the surfaces of the GOE 269 airfoil.

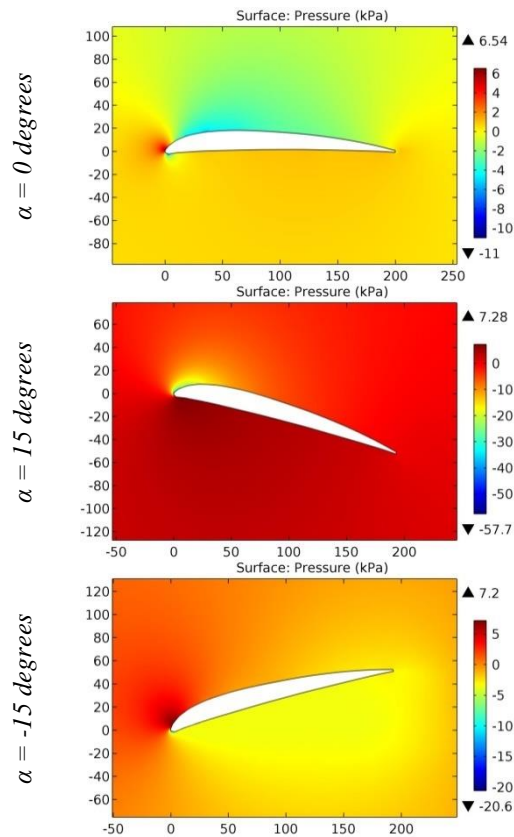


**Figure 104.** The pressure contours on the surfaces of the GOE 274 (DAIMLER V) airfoil.

**Impact Factor:**

ISRA (India) = 6.317	SIS (USA) = 0.912	ICV (Poland) = 6.630
ISI (Dubai, UAE) = 1.582	ПИИЦ (Russia) = 3.939	PIF (India) = 1.940
GIF (Australia) = 0.564	ESJI (KZ) = 9.035	IBI (India) = 4.260
JIF = 1.500	SJIF (Morocco) = 7.184	OAJI (USA) = 0.350

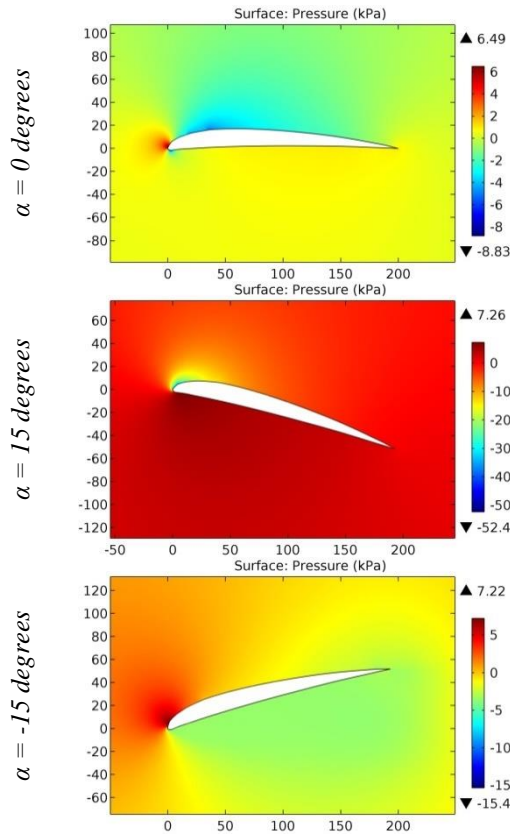


Figure 105. The pressure contours on the surfaces of the GOE 275 (DAIMLER VI) airfoil.

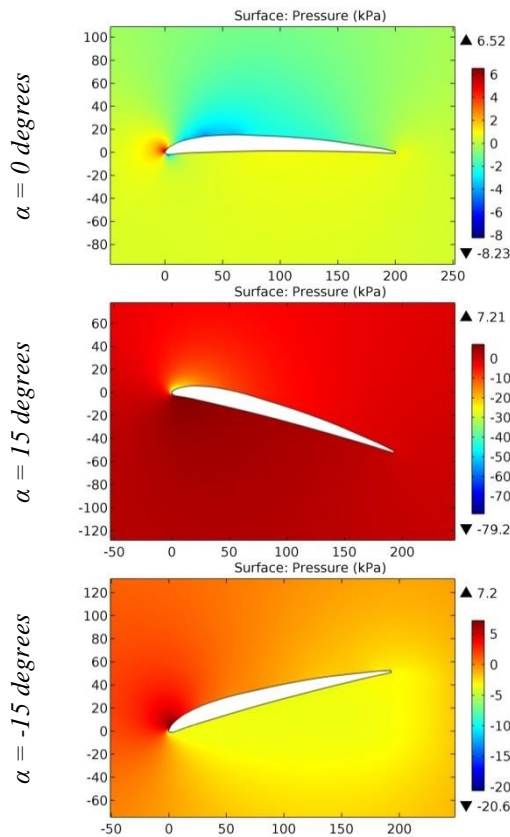
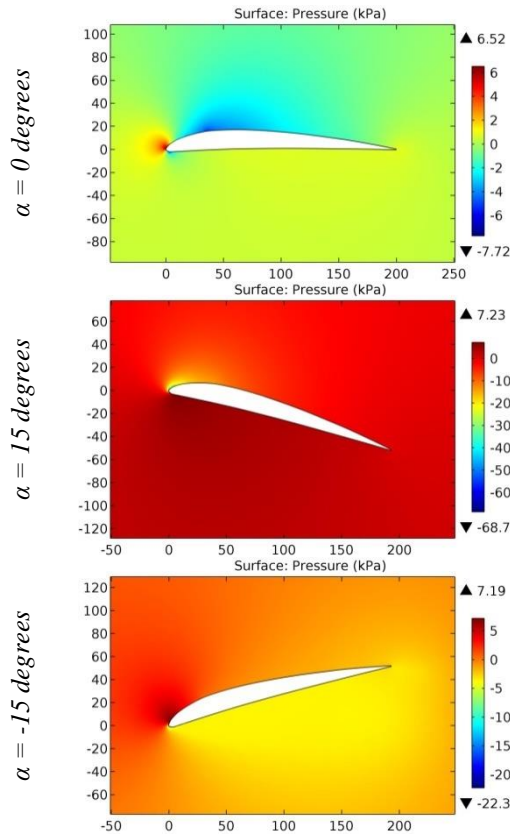


Figure 106. The pressure contours on the surfaces of the GOE 276 (DAIMLER VII) airfoil.

**Impact Factor:**

<b>ISRA (India)</b> = <b>6.317</b>	<b>SIS (USA)</b> = <b>0.912</b>	<b>ICV (Poland)</b> = <b>6.630</b>
<b>ISI (Dubai, UAE)</b> = <b>1.582</b>	<b>ПИИЦ (Russia)</b> = <b>3.939</b>	<b>PIF (India)</b> = <b>1.940</b>
<b>GIF (Australia)</b> = <b>0.564</b>	<b>ESJI (KZ)</b> = <b>9.035</b>	<b>IBI (India)</b> = <b>4.260</b>
<b>JIF</b> = <b>1.500</b>	<b>SJIF (Morocco)</b> = <b>7.184</b>	<b>OAJI (USA)</b> = <b>0.350</b>



**Figure 107. The pressure contours on the surfaces of the GOE 277 (DAIMLER VIII) airfoil.**

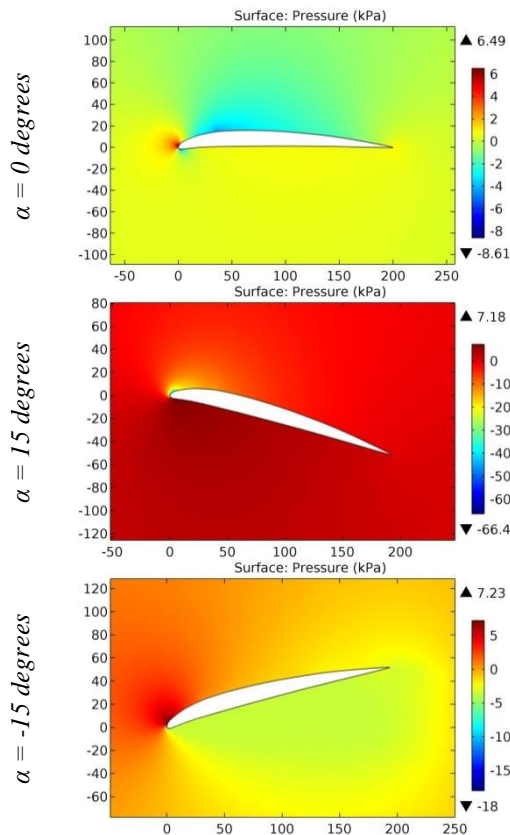


**Figure 108. The pressure contours on the surfaces of the GOE 278 (DAIMLER IX) airfoil.**

**Impact Factor:**

ISRA (India) = 6.317	SIS (USA) = 0.912	ICV (Poland) = 6.630
ISI (Dubai, UAE) = 1.582	ПИИЦ (Russia) = 3.939	PIF (India) = 1.940
GIF (Australia) = 0.564	ESJI (KZ) = 9.035	IBI (India) = 4.260
JIF = 1.500	SJIF (Morocco) = 7.184	OAJI (USA) = 0.350

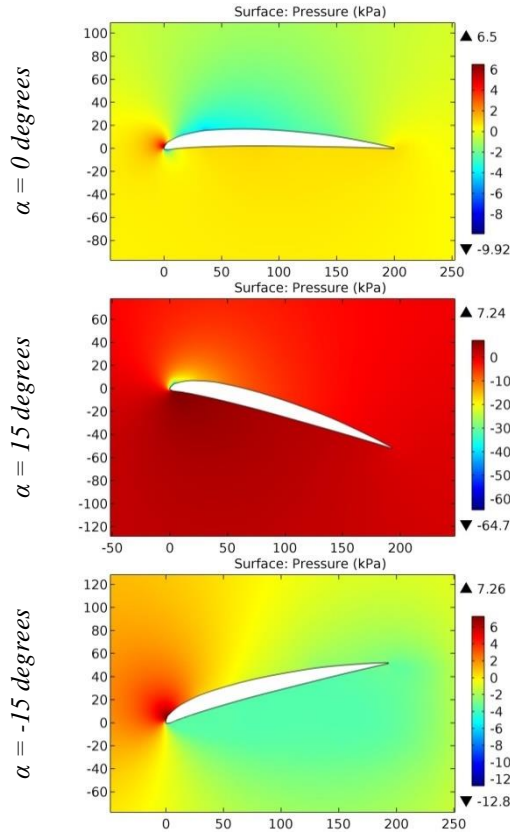


Figure 109. The pressure contours on the surfaces of the GOE 279 (DAIMLER X) airfoil.

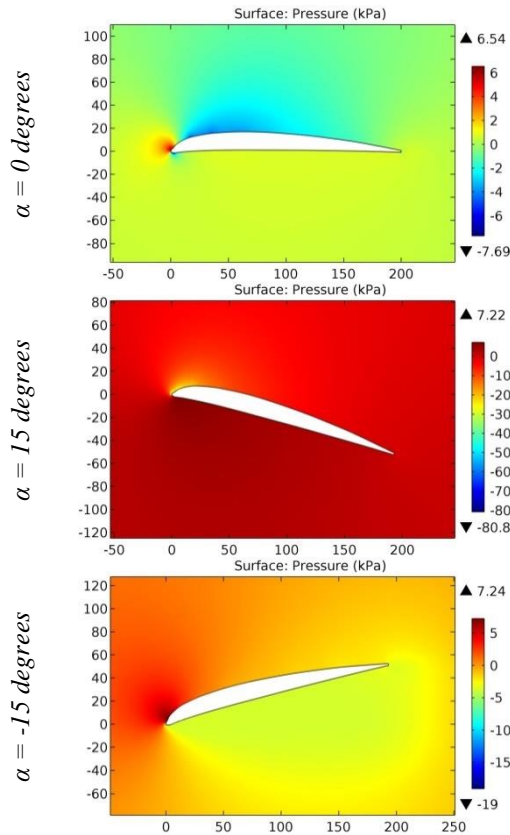


Figure 110. The pressure contours on the surfaces of the GOE 280 (DAIMLER XI) airfoil.

**Impact Factor:**

ISRA (India) = 6.317	SIS (USA) = 0.912	ICV (Poland) = 6.630
ISI (Dubai, UAE) = 1.582	ПИИЦ (Russia) = 3.939	PIF (India) = 1.940
GIF (Australia) = 0.564	ESJI (KZ) = 9.035	IBI (India) = 4.260
JIF = 1.500	SJIF (Morocco) = 7.184	OAJI (USA) = 0.350

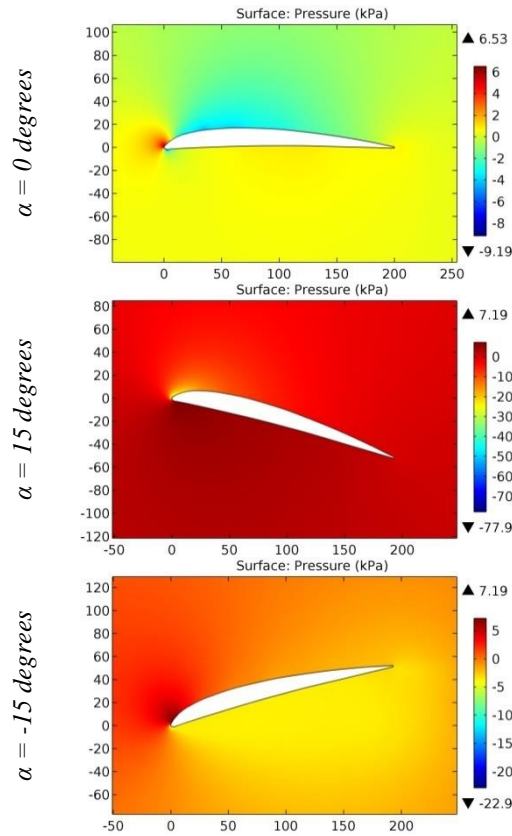


Figure 111. The pressure contours on the surfaces of the GOE 281 (DAIMLER XII) airfoil.

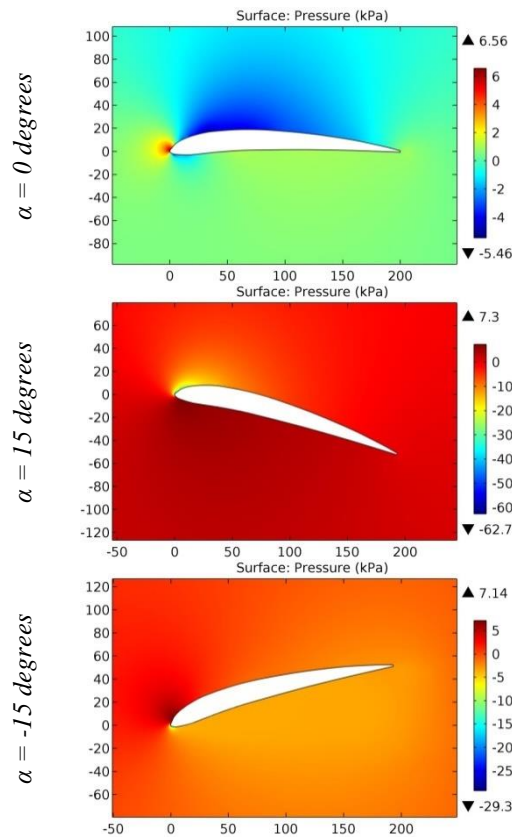


Figure 112. The pressure contours on the surfaces of the GOE 282 (DAIMLER XIII) airfoil.



**Impact Factor:**

<b>SISRA</b> (India)	= <b>6.317</b>	<b>SIS</b> (USA)	= <b>0.912</b>	<b>ICV</b> (Poland)	= <b>6.630</b>
<b>ISI</b> (Dubai, UAE)	= <b>1.582</b>	<b>ПИИЦ</b> (Russia)	= <b>3.939</b>	<b>PIF</b> (India)	= <b>1.940</b>
<b>GIF</b> (Australia)	= <b>0.564</b>	<b>ESJI</b> (KZ)	= <b>9.035</b>	<b>IBI</b> (India)	= <b>4.260</b>
<b>JIF</b>	= <b>1.500</b>	<b>SJIF</b> (Morocco)	= <b>7.184</b>	<b>OAJI</b> (USA)	= <b>0.350</b>

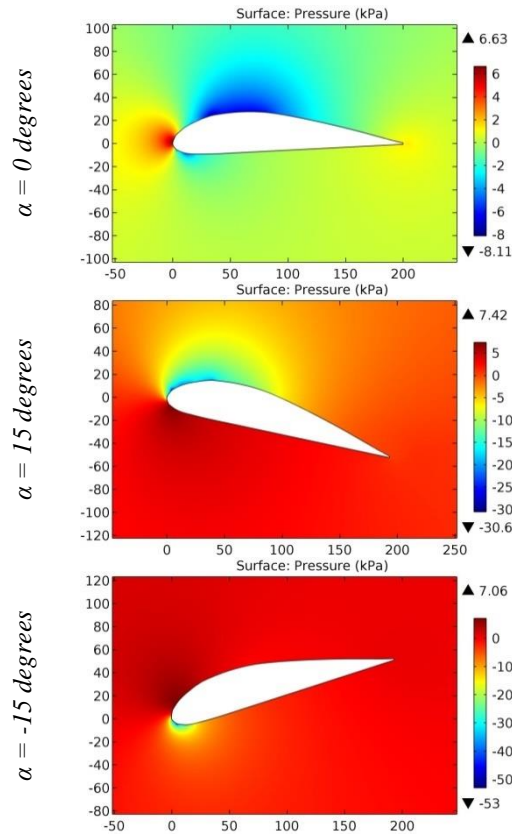


Figure 113. The pressure contours on the surfaces of the GOE 284 airfoil.

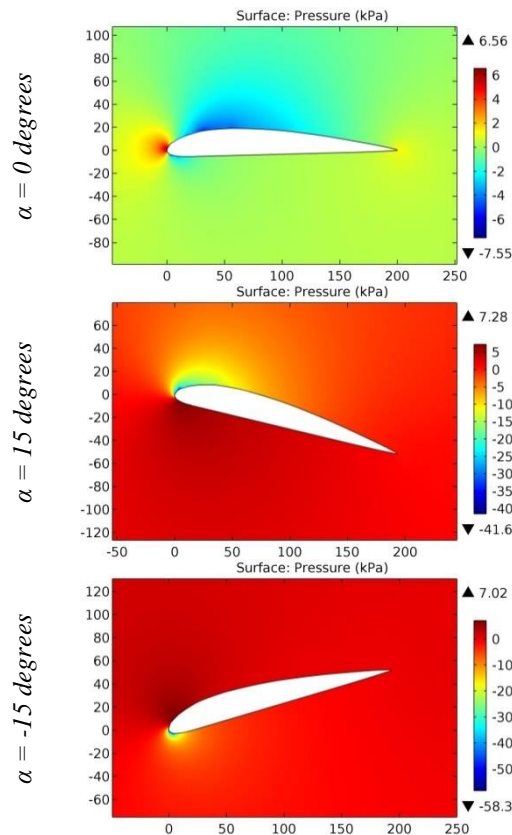


Figure 114. The pressure contours on the surfaces of the GOE 285 airfoil.

**Impact Factor:**

<b>ISRA (India)</b> = <b>6.317</b>	<b>SIS (USA)</b> = <b>0.912</b>	<b>ICV (Poland)</b> = <b>6.630</b>
<b>ISI (Dubai, UAE)</b> = <b>1.582</b>	<b>ПИИЦ (Russia)</b> = <b>3.939</b>	<b>PIF (India)</b> = <b>1.940</b>
<b>GIF (Australia)</b> = <b>0.564</b>	<b>ESJI (KZ)</b> = <b>9.035</b>	<b>IBI (India)</b> = <b>4.260</b>
<b>JIF</b> = <b>1.500</b>	<b>SJIF (Morocco)</b> = <b>7.184</b>	<b>OAJI (USA)</b> = <b>0.350</b>

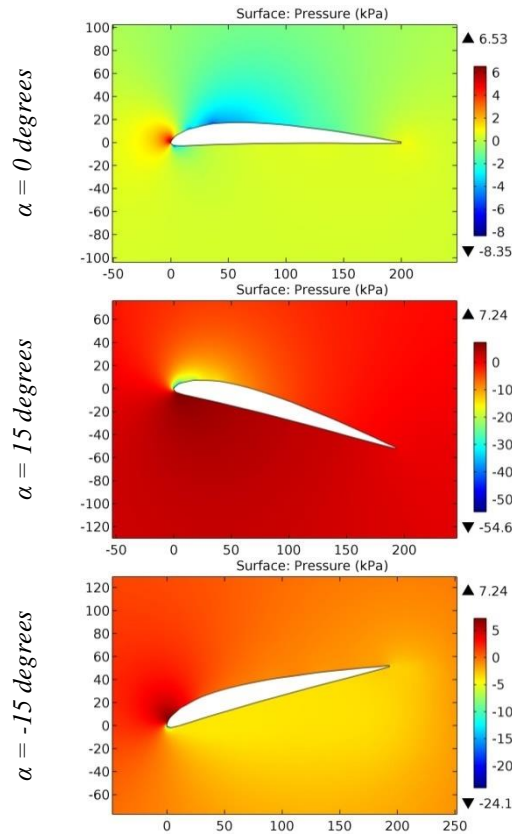


Figure 115. The pressure contours on the surfaces of the GOE 286 airfoil.

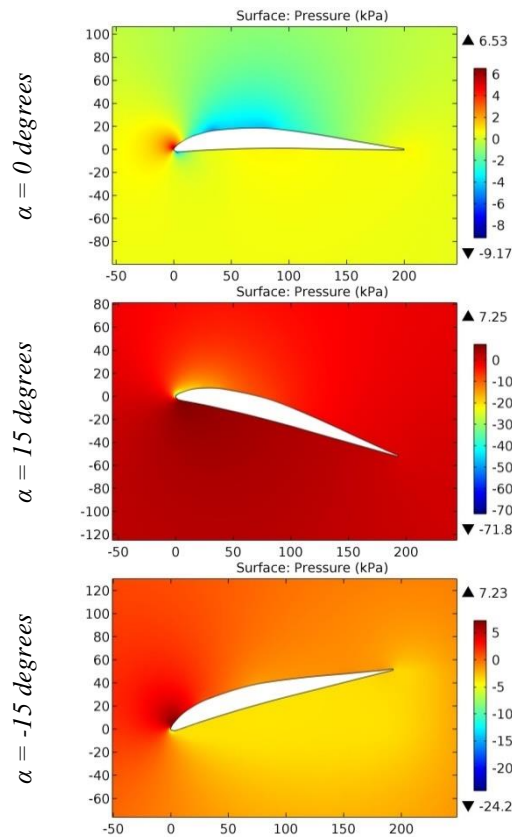


Figure 116. The pressure contours on the surfaces of the GOE 287 airfoil.

**Impact Factor:**

ISRA (India) = 6.317	SIS (USA) = 0.912	ICV (Poland) = 6.630
ISI (Dubai, UAE) = 1.582	ПИИЦ (Russia) = 3.939	PIF (India) = 1.940
GIF (Australia) = 0.564	ESJI (KZ) = 9.035	IBI (India) = 4.260
JIF = 1.500	SJIF (Morocco) = 7.184	OAJI (USA) = 0.350

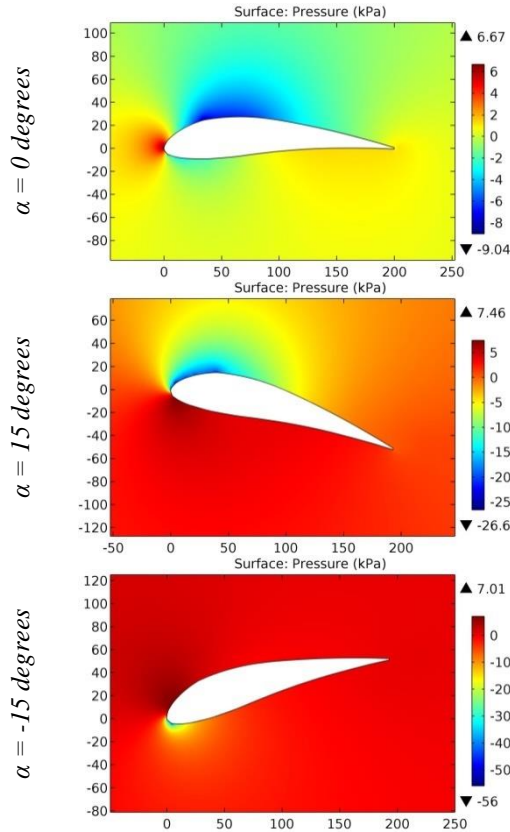


Figure 117. The pressure contours on the surfaces of the GOE 288 airfoil.

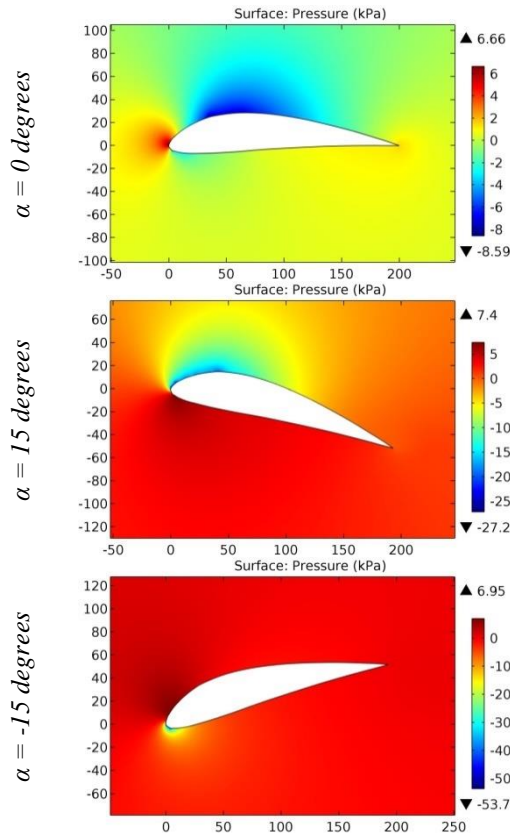


Figure 118. The pressure contours on the surfaces of the GOE 289 (MVA 289) airfoil.

**Impact Factor:**

<b>ISRA (India)</b>	<b>= 6.317</b>	<b>SIS (USA)</b>	<b>= 0.912</b>	<b>ICV (Poland)</b>	<b>= 6.630</b>
<b>ISI (Dubai, UAE)</b>	<b>= 1.582</b>	<b>ПИИЦ (Russia)</b>	<b>= 3.939</b>	<b>PIF (India)</b>	<b>= 1.940</b>
<b>GIF (Australia)</b>	<b>= 0.564</b>	<b>ESJI (KZ)</b>	<b>= 9.035</b>	<b>IBI (India)</b>	<b>= 4.260</b>
<b>JIF</b>	<b>= 1.500</b>	<b>SJIF (Morocco)</b>	<b>= 7.184</b>	<b>OAJI (USA)</b>	<b>= 0.350</b>

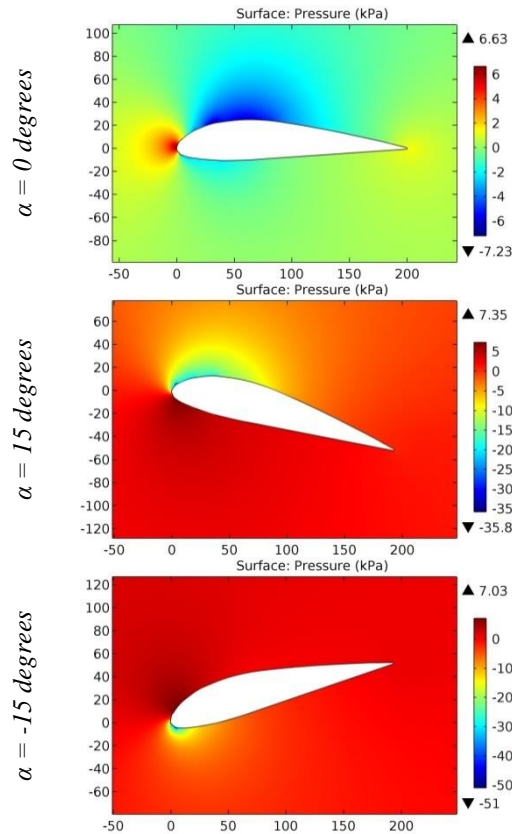


Figure 119. The pressure contours on the surfaces of the GOE 290 (MVA 290) airfoil.

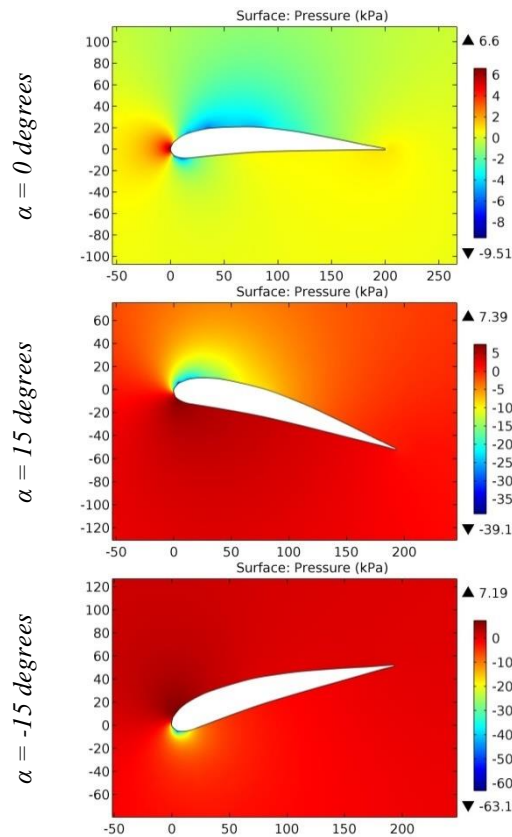


Figure 120. The pressure contours on the surfaces of the GOE 298 airfoil.

**Impact Factor:**

ISRA (India) = 6.317	SIS (USA) = 0.912	ICV (Poland) = 6.630
ISI (Dubai, UAE) = 1.582	ПИИЦ (Russia) = 3.939	PIF (India) = 1.940
GIF (Australia) = 0.564	ESJI (KZ) = 9.035	IBI (India) = 4.260
JIF = 1.500	SJIF (Morocco) = 7.184	OAJI (USA) = 0.350

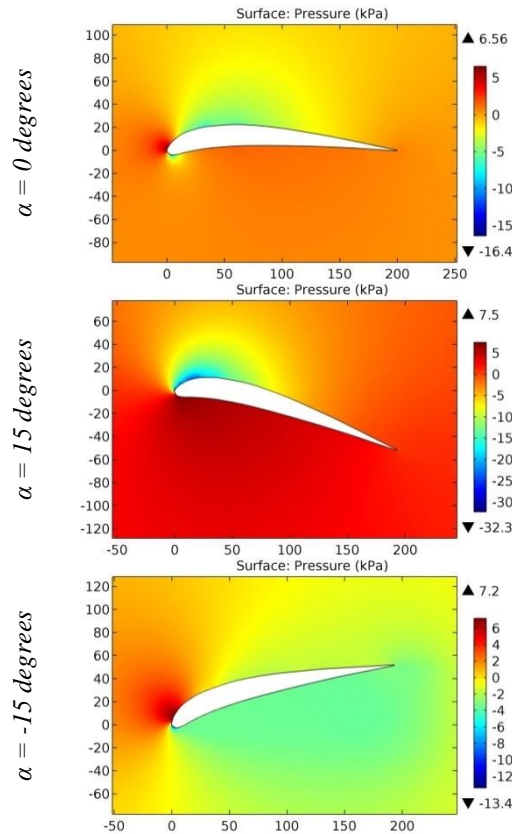


Figure 121. The pressure contours on the surfaces of the GOE 29B airfoil.

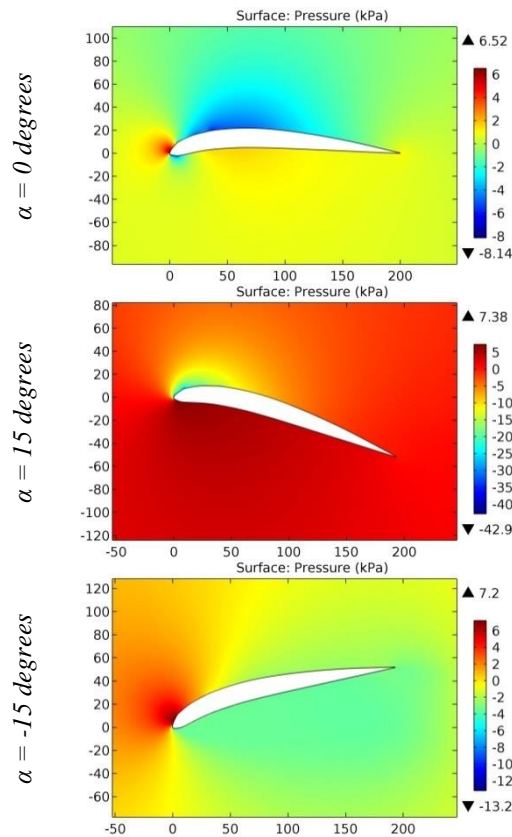


Figure 122. The pressure contours on the surfaces of the GOE 300 (FRIEDRICHSHAFEN G20) airfoil.



**Impact Factor:**

ISRA (India)	= 6.317	SIS (USA)	= 0.912	ICV (Poland)	= 6.630
ISI (Dubai, UAE)	= 1.582	ПИИЦ (Russia)	= 3.939	PIF (India)	= 1.940
GIF (Australia)	= 0.564	ESJI (KZ)	= 9.035	IBI (India)	= 4.260
JIF	= 1.500	SJIF (Morocco)	= 7.184	OAJI (USA)	= 0.350

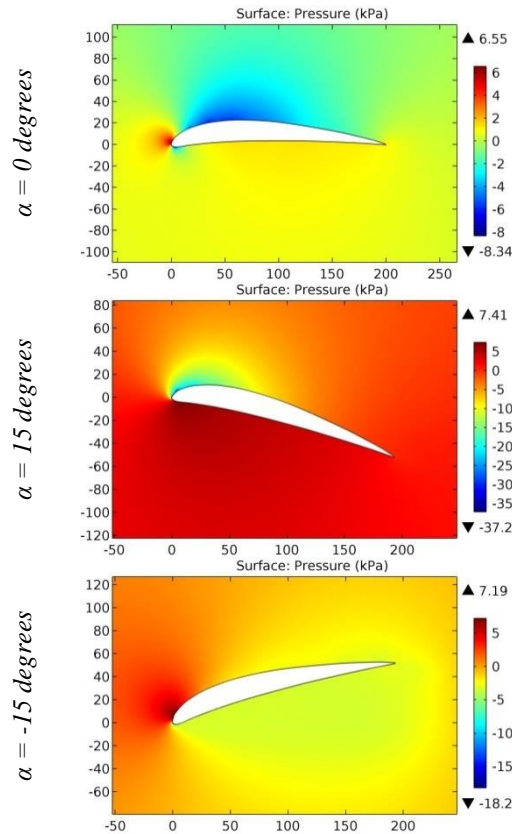


Figure 123. The pressure contours on the surfaces of the GOE 301 (FRIEDRICHSHAFEN G 13) airfoil.

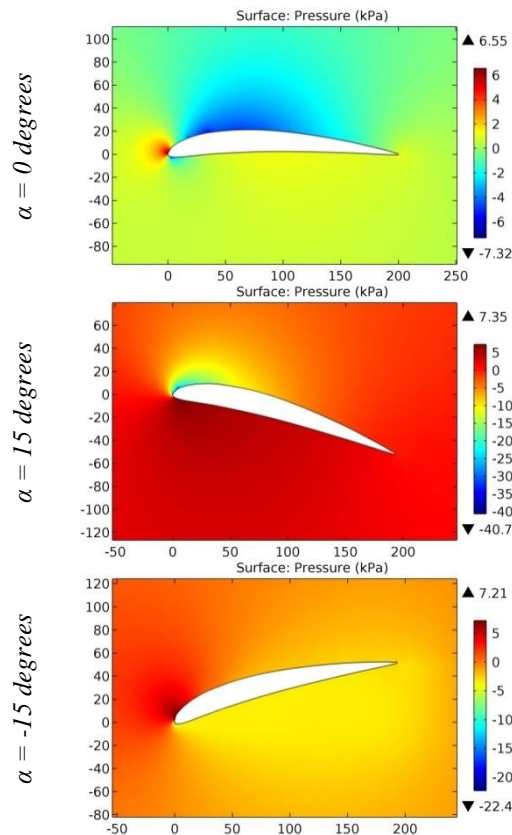


Figure 124. The pressure contours on the surfaces of the GOE 303 (FRIEDRICHSHAFEN G03) airfoil.

**Impact Factor:**

ISRA (India)	= 6.317	SIS (USA)	= 0.912	ICV (Poland)	= 6.630
ISI (Dubai, UAE)	= 1.582	ПИИЦ (Russia)	= 3.939	PIF (India)	= 1.940
GIF (Australia)	= 0.564	ESJI (KZ)	= 9.035	IBI (India)	= 4.260
JIF	= 1.500	SJIF (Morocco)	= 7.184	OAJI (USA)	= 0.350

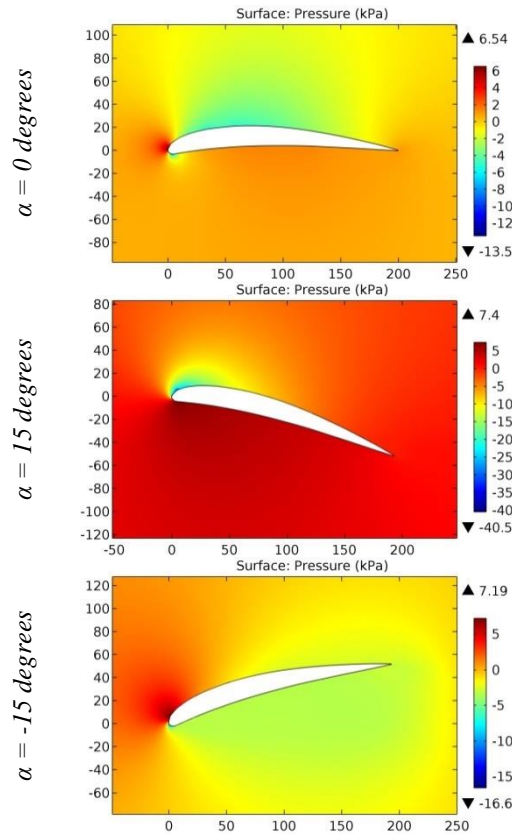


Figure 125. The pressure contours on the surfaces of the GOE 304 (FRIEDRICHSHAFEN G02) airfoil.

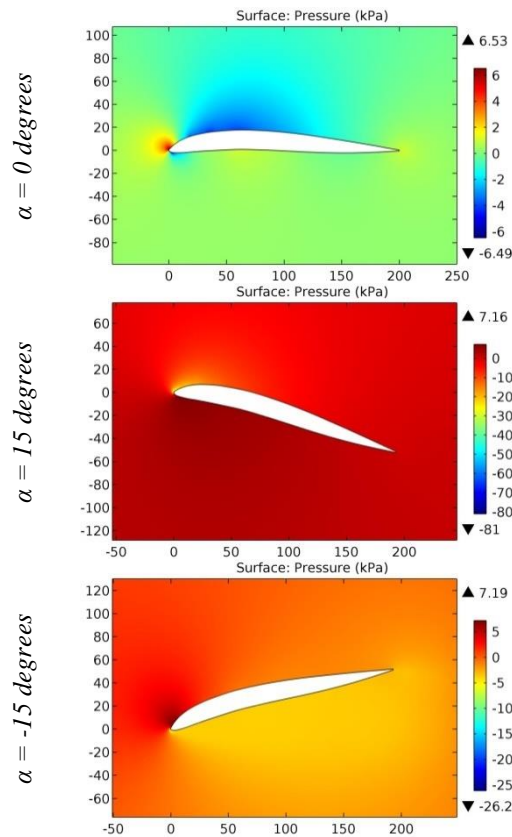


Figure 126. The pressure contours on the surfaces of the GOE 308 (MVA H,40) airfoil.

**Impact Factor:**

<b>SISRA</b> (India) = <b>6.317</b>	<b>SIS</b> (USA) = <b>0.912</b>	<b>ICV</b> (Poland) = <b>6.630</b>
<b>ISI</b> (Dubai, UAE) = <b>1.582</b>	<b>ПИИЦ</b> (Russia) = <b>3.939</b>	<b>PIF</b> (India) = <b>1.940</b>
<b>GIF</b> (Australia) = <b>0.564</b>	<b>ESJI</b> (KZ) = <b>9.035</b>	<b>IBI</b> (India) = <b>4.260</b>
<b>JIF</b> = <b>1.500</b>	<b>SJIF</b> (Morocco) = <b>7.184</b>	<b>OAJI</b> (USA) = <b>0.350</b>

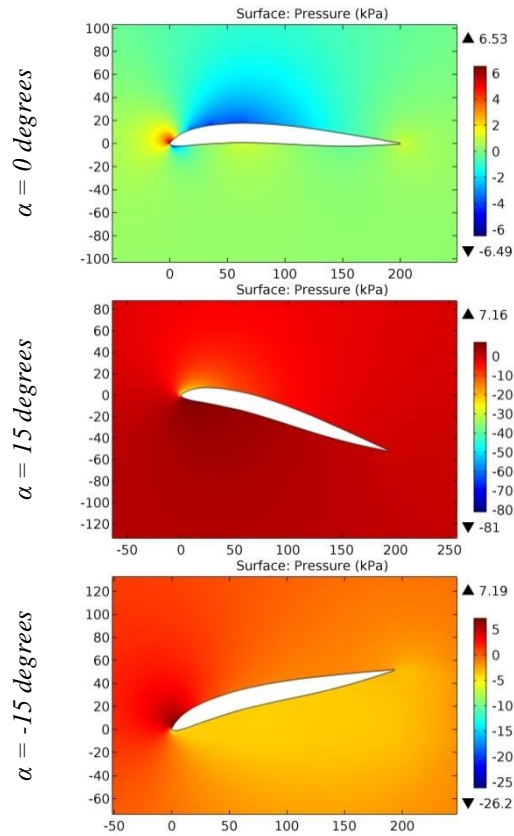


Figure 127. The pressure contours on the surfaces of the GOE 309 (MVA H,41) airfoil.

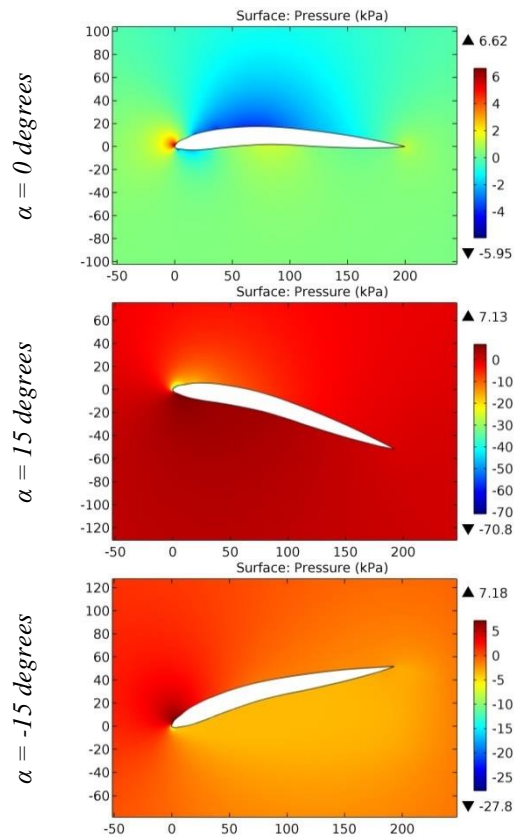


Figure 128. The pressure contours on the surfaces of the GOE 310 (MVA H,42) airfoil.

**Impact Factor:**

ISRA (India) = 6.317	SIS (USA) = 0.912	ICV (Poland) = 6.630
ISI (Dubai, UAE) = 1.582	ПИИЦ (Russia) = 3.939	PIF (India) = 1.940
GIF (Australia) = 0.564	ESJI (KZ) = 9.035	IBI (India) = 4.260
JIF = 1.500	SJIF (Morocco) = 7.184	OAJI (USA) = 0.350

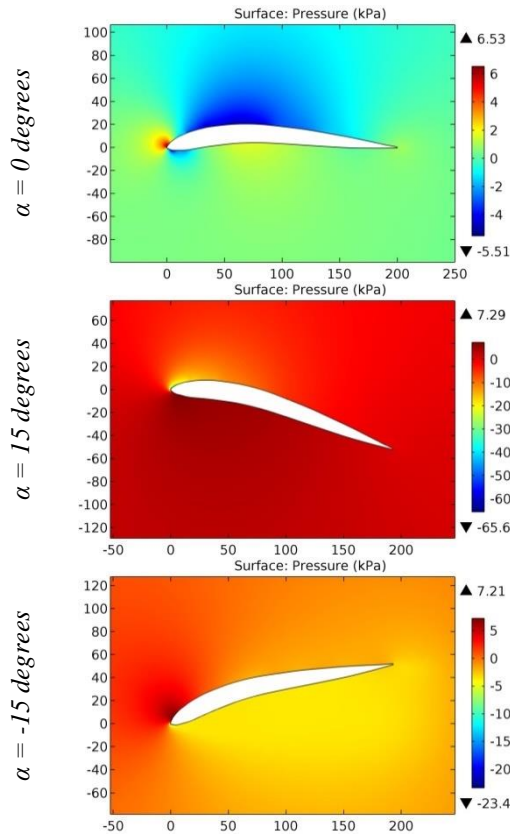


Figure 129. The pressure contours on the surfaces of the GOE 311 (MVA H,43) airfoil.

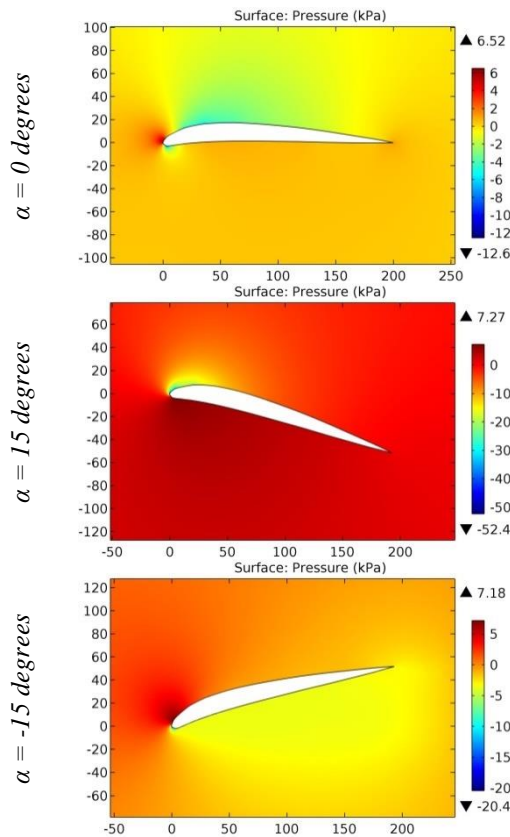


Figure 130. The pressure contours on the surfaces of the GOE 314 (HANSA-BRANDENBURG) airfoil.

**Impact Factor:**

ISRA (India) = 6.317	SIS (USA) = 0.912	ICV (Poland) = 6.630
ISI (Dubai, UAE) = 1.582	ПИИЦ (Russia) = 3.939	PIF (India) = 1.940
GIF (Australia) = 0.564	ESJI (KZ) = 9.035	IBI (India) = 4.260
JIF = 1.500	SJIF (Morocco) = 7.184	OAJI (USA) = 0.350

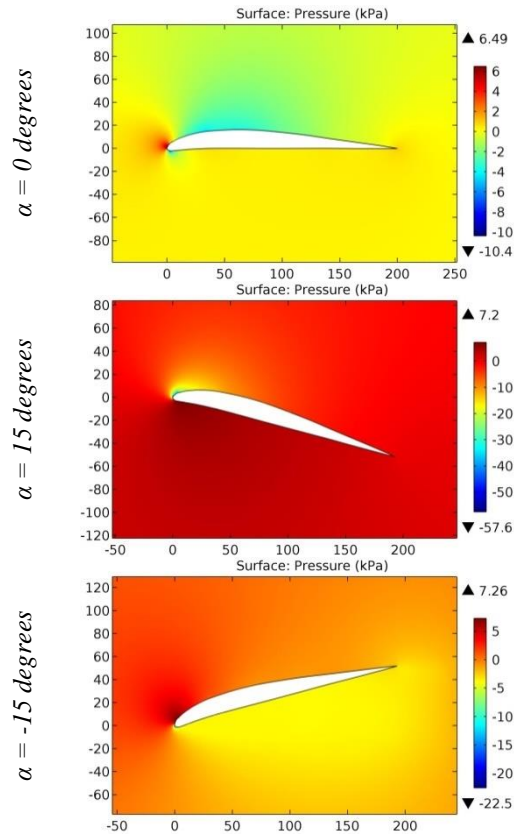


Figure 131. The pressure contours on the surfaces of the GOE 315 (HANSA-BRANDENBURG III,5) airfoil.

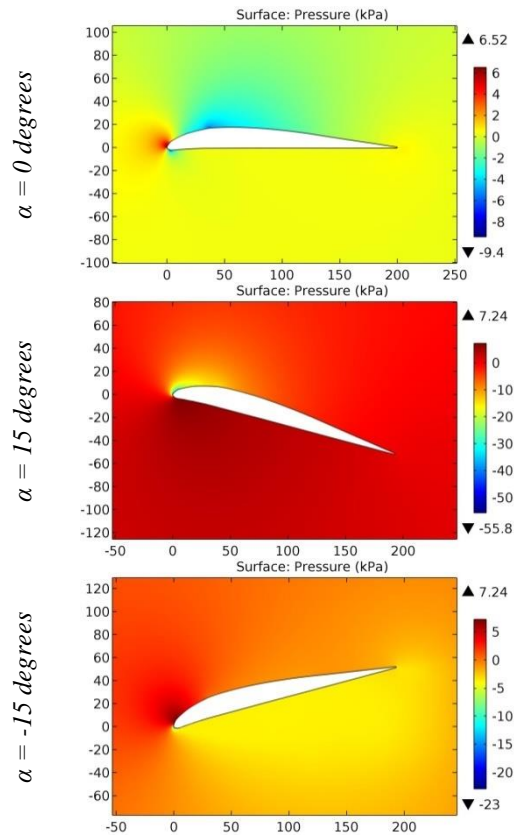


Figure 132. The pressure contours on the surfaces of the GOE 316 (HANSA-BRANDENBURG IV,5) airfoil.



**Impact Factor:**

<b>ISRA (India)</b> = <b>6.317</b>	<b>SIS (USA)</b> = <b>0.912</b>	<b>ICV (Poland)</b> = <b>6.630</b>
<b>ISI (Dubai, UAE)</b> = <b>1.582</b>	<b>ПИИЦ (Russia)</b> = <b>3.939</b>	<b>PIF (India)</b> = <b>1.940</b>
<b>GIF (Australia)</b> = <b>0.564</b>	<b>ESJI (KZ)</b> = <b>9.035</b>	<b>IBI (India)</b> = <b>4.260</b>
<b>JIF</b> = <b>1.500</b>	<b>SJIF (Morocco)</b> = <b>7.184</b>	<b>OAJI (USA)</b> = <b>0.350</b>

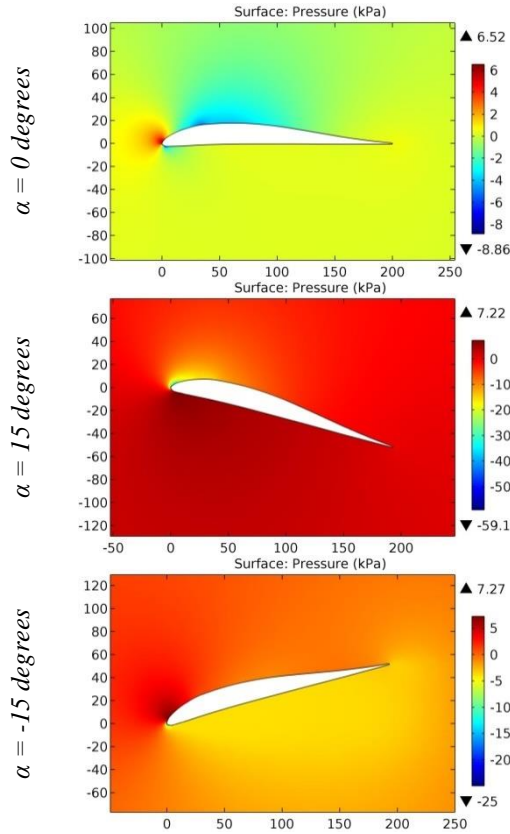


Figure 133. The pressure contours on the surfaces of the GOE 318 (HANSA-BRANDENBURG VI,5) airfoil.

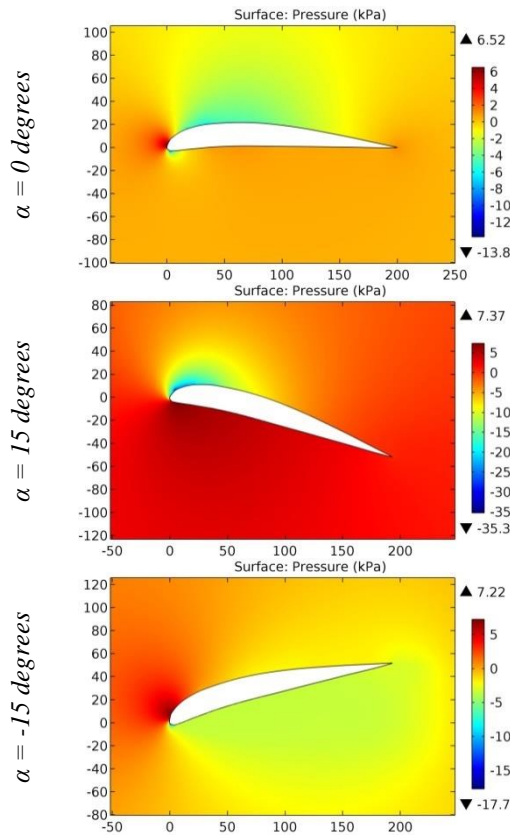


Figure 134. The pressure contours on the surfaces of the GOE 319 (HANSA-BRANDENBURG II) airfoil.

**Impact Factor:**

ISRA (India) = 6.317	SIS (USA) = 0.912	ICV (Poland) = 6.630
ISI (Dubai, UAE) = 1.582	ПИИЦ (Russia) = 3.939	PIF (India) = 1.940
GIF (Australia) = 0.564	ESJI (KZ) = 9.035	IBI (India) = 4.260
JIF = 1.500	SJIF (Morocco) = 7.184	OAJI (USA) = 0.350

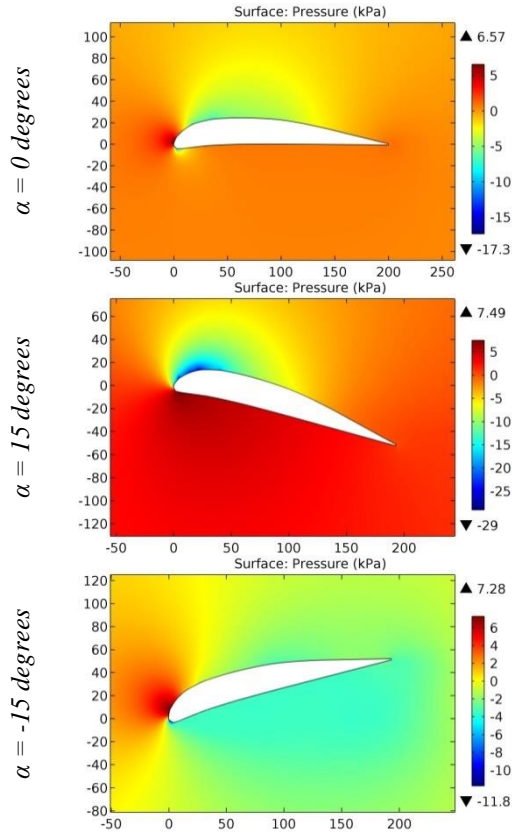


Figure 135. The pressure contours on the surfaces of the GOE 320 (HANSA-BRANDENBURG II,1) airfoil.

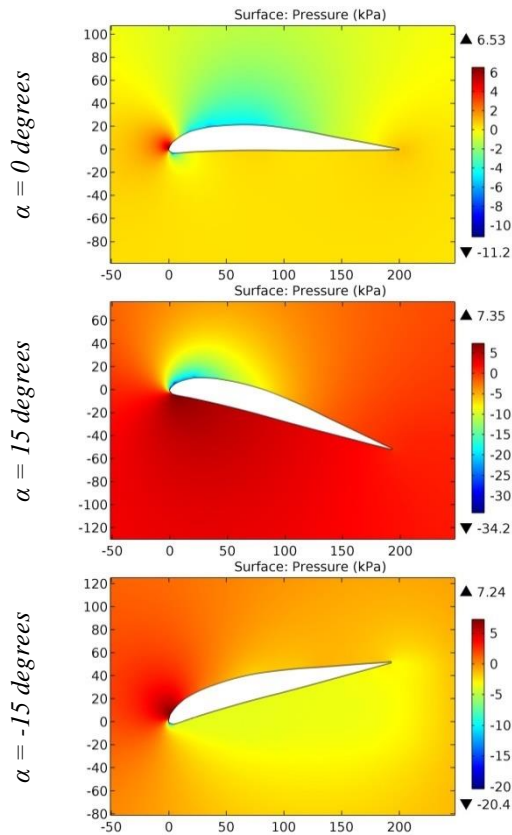


Figure 136. The pressure contours on the surfaces of the GOE 321 (HANSA-BRANDENBURG III,1) airfoil.

**Impact Factor:**

<b>SIS (India)</b> = <b>6.317</b>	<b>SIS (USA)</b> = <b>0.912</b>	<b>ICV (Poland)</b> = <b>6.630</b>
<b>ISI (Dubai, UAE)</b> = <b>1.582</b>	<b>ПИИЦ (Russia)</b> = <b>3.939</b>	<b>PIF (India)</b> = <b>1.940</b>
<b>GIF (Australia)</b> = <b>0.564</b>	<b>ESJI (KZ)</b> = <b>9.035</b>	<b>IBI (India)</b> = <b>4.260</b>
<b>JIF</b> = <b>1.500</b>	<b>SJIF (Morocco)</b> = <b>7.184</b>	<b>OAJI (USA)</b> = <b>0.350</b>

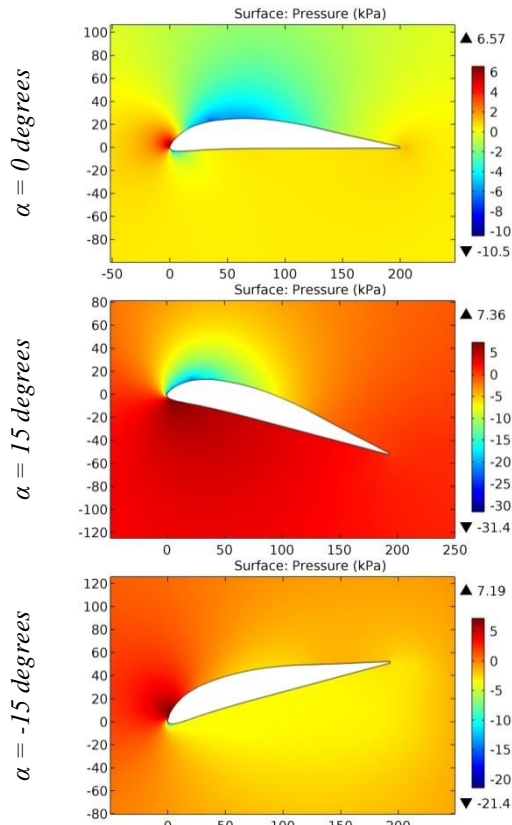


Figure 137. The pressure contours on the surfaces of the GOE 322 (HANSA-BRANDENBURG IV,1) airfoil.

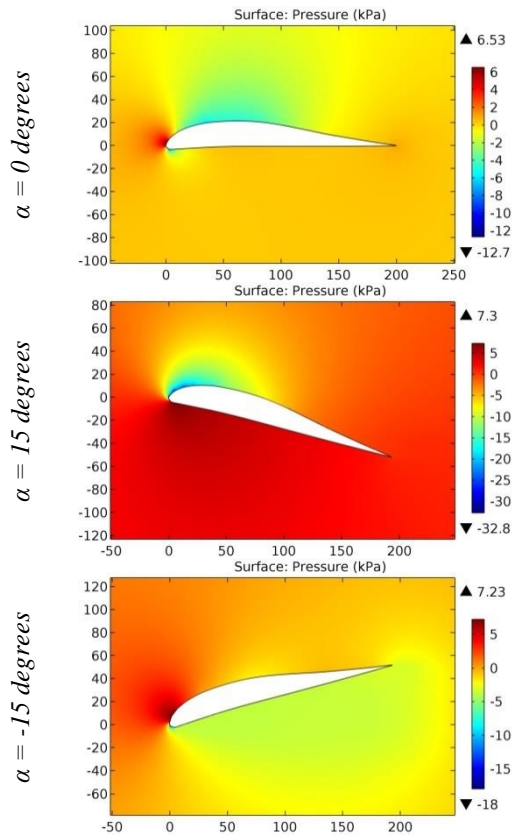


Figure 138. The pressure contours on the surfaces of the GOE 323 (HANSA-BRANDENBURG V,1) airfoil.

**Impact Factor:**

ISRA (India) = 6.317	SIS (USA) = 0.912	ICV (Poland) = 6.630
ISI (Dubai, UAE) = 1.582	ПИИЦ (Russia) = 3.939	PIF (India) = 1.940
GIF (Australia) = 0.564	ESJI (KZ) = 9.035	IBI (India) = 4.260
JIF = 1.500	SJIF (Morocco) = 7.184	OAJI (USA) = 0.350

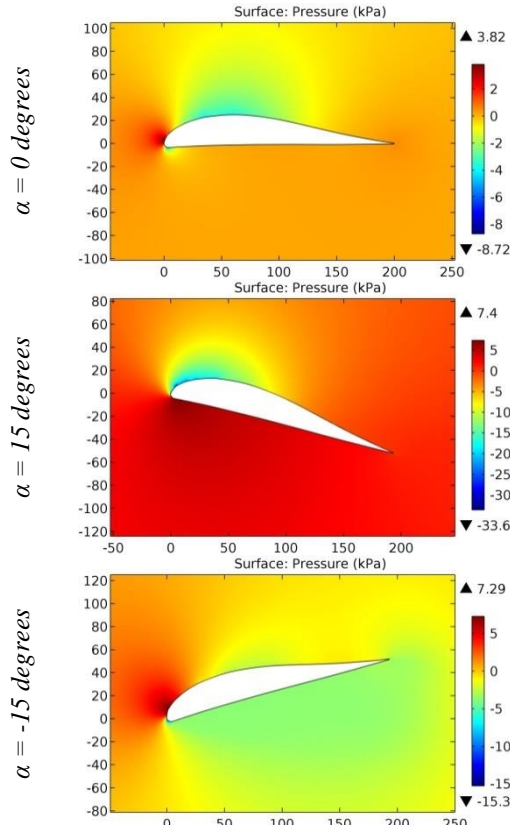


Figure 139. The pressure contours on the surfaces of the GOE 324 (HANSA-BRANDENBURG) airfoil.

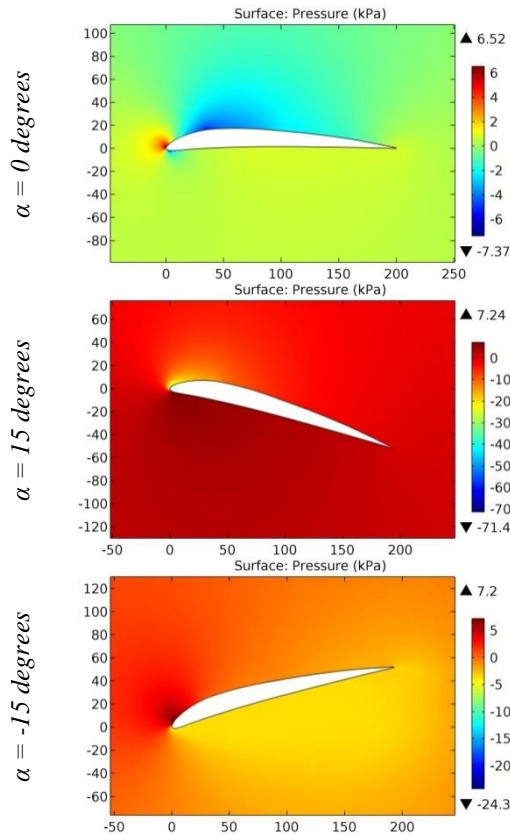


Figure 140. The pressure contours on the surfaces of the GOE 325 (PFALZ 54) airfoil.

**Impact Factor:**

ISRA (India)	= 6.317	SIS (USA)	= 0.912	ICV (Poland)	= 6.630
ISI (Dubai, UAE)	= 1.582	ПИИЦ (Russia)	= 3.939	PIF (India)	= 1.940
GIF (Australia)	= 0.564	ESJI (KZ)	= 9.035	IBI (India)	= 4.260
JIF	= 1.500	SJIF (Morocco)	= 7.184	OAJI (USA)	= 0.350

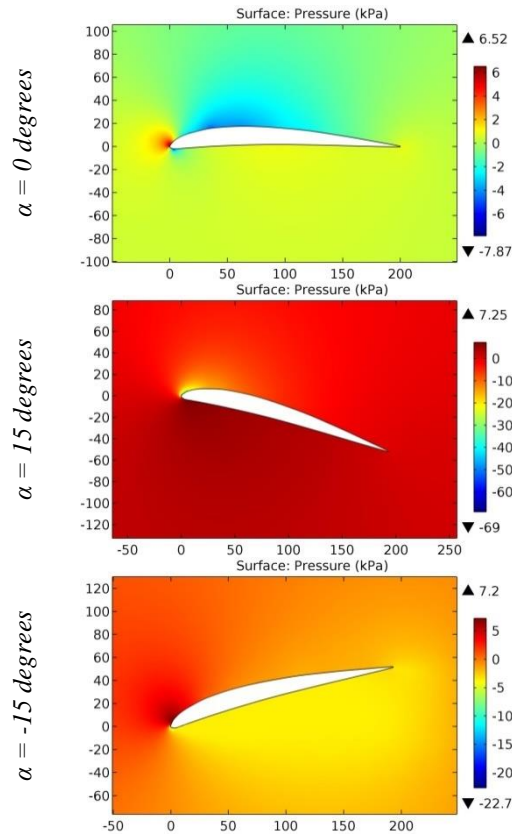


Figure 141. The pressure contours on the surfaces of the GOE 326 (PFALZ 55) airfoil.

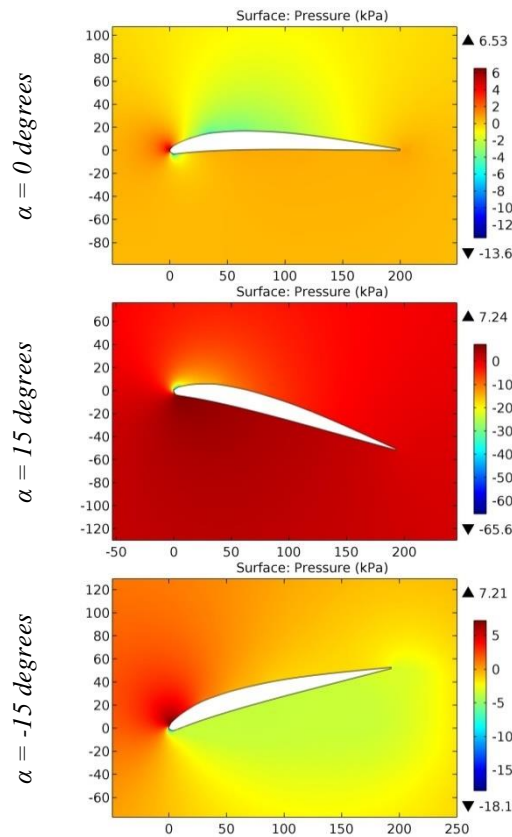


Figure 142. The pressure contours on the surfaces of the GOE 328 airfoil.



**Impact Factor:**

ISRA (India) = 6.317	SIS (USA) = 0.912	ICV (Poland) = 6.630
ISI (Dubai, UAE) = 1.582	ПИИЦ (Russia) = 3.939	PIF (India) = 1.940
GIF (Australia) = 0.564	ESJI (KZ) = 9.035	IBI (India) = 4.260
JIF = 1.500	SJIF (Morocco) = 7.184	OAJI (USA) = 0.350

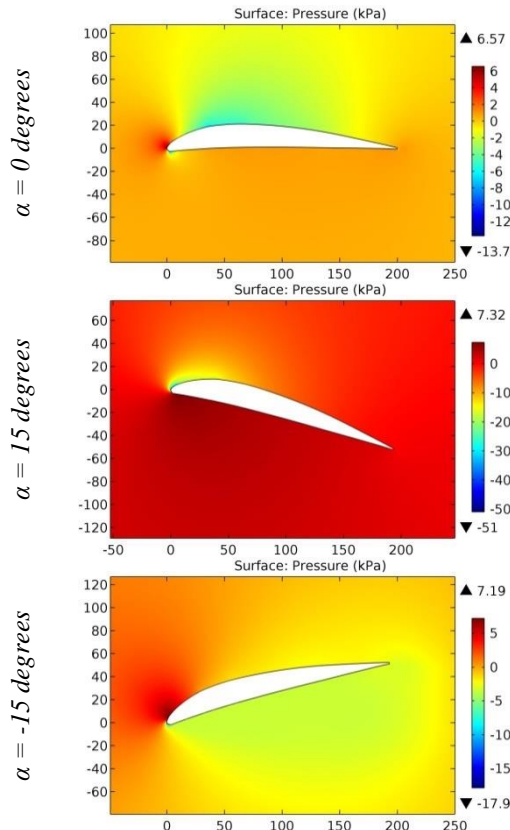


Figure 143. The pressure contours on the surfaces of the GOE 329 (PFALZ 58) airfoil.

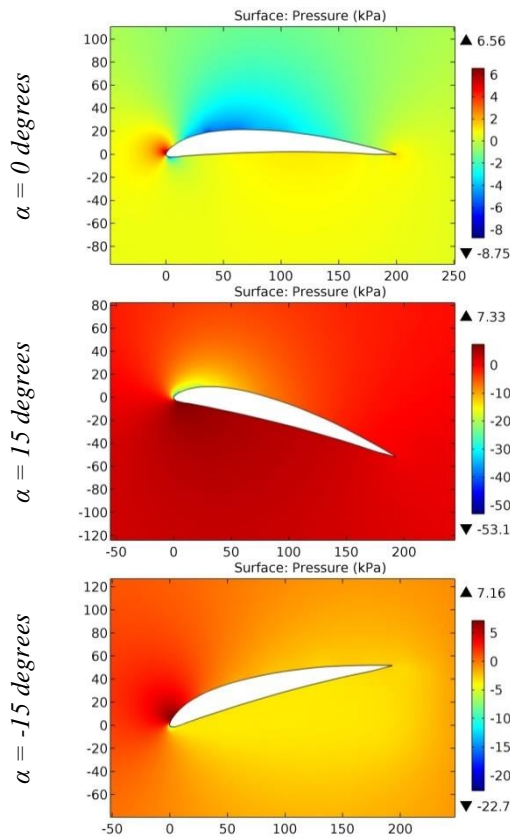


Figure 144. The pressure contours on the surfaces of the GOE 330 (PFALZ 59) airfoil.

**Impact Factor:**

ISRA (India) = 6.317	SIS (USA) = 0.912	ICV (Poland) = 6.630
ISI (Dubai, UAE) = 1.582	ПИИЦ (Russia) = 3.939	PIF (India) = 1.940
GIF (Australia) = 0.564	ESJI (KZ) = 9.035	IBI (India) = 4.260
JIF = 1.500	SJIF (Morocco) = 7.184	OAJI (USA) = 0.350

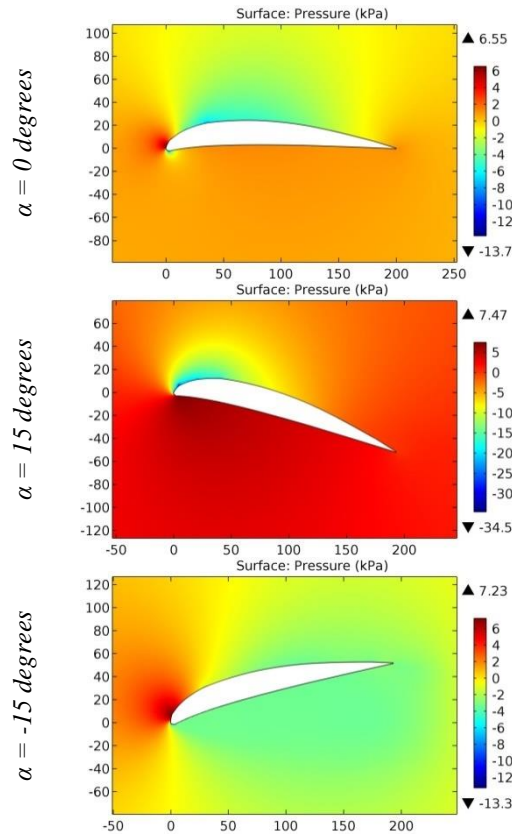


Figure 145. The pressure contours on the surfaces of the GOE 331 (PFALZ 60) airfoil.

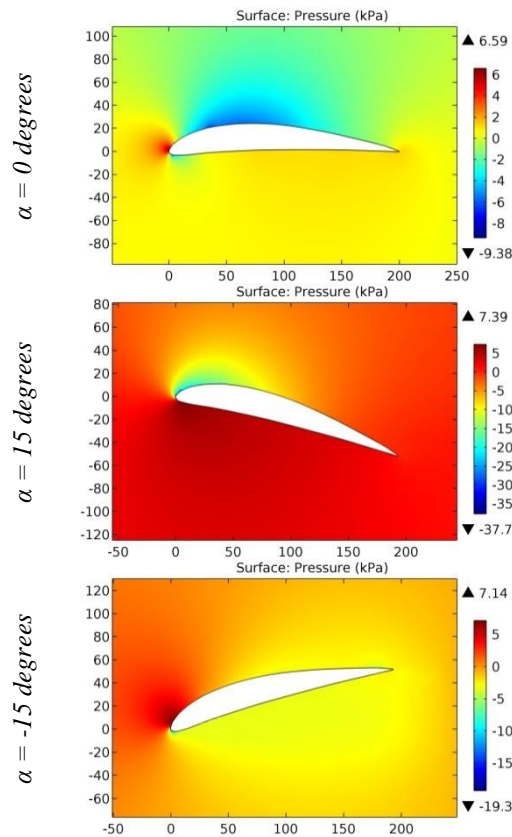


Figure 146. The pressure contours on the surfaces of the GOE 332 (PFALZ 61) airfoil.

**Impact Factor:**

ISRA (India)	= 6.317	SIS (USA)	= 0.912	ICV (Poland)	= 6.630
ISI (Dubai, UAE)	= 1.582	ПИИЦ (Russia)	= 3.939	PIF (India)	= 1.940
GIF (Australia)	= 0.564	ESJI (KZ)	= 9.035	IBI (India)	= 4.260
JIF	= 1.500	SJIF (Morocco)	= 7.184	OAJI (USA)	= 0.350

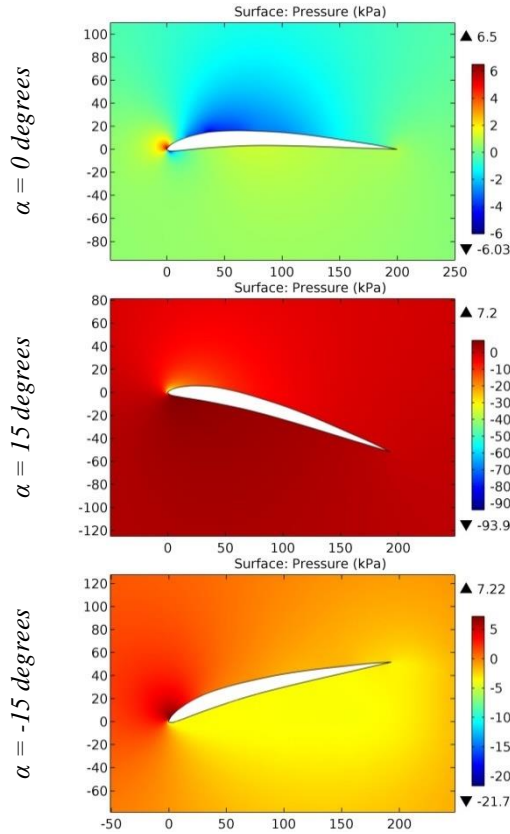


Figure 147. The pressure contours on the surfaces of the GOE 335 (D,F,W) airfoil.

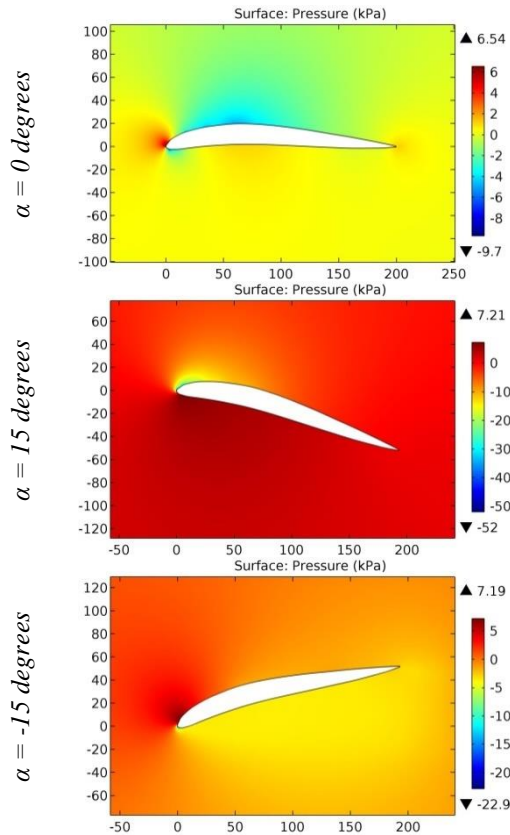


Figure 148. The pressure contours on the surfaces of the GOE 336 (MVA H,44) airfoil.

## Impact Factor:

ISRA (India) = 6.317	SIS (USA) = 0.912	ICV (Poland) = 6.630
ISI (Dubai, UAE) = 1.582	ПИИИ (Russia) = 3.939	PIF (India) = 1.940
GIF (Australia) = 0.564	ESJI (KZ) = 9.035	IBI (India) = 4.260
JIF = 1.500	SJIF (Morocco) = 7.184	OAJI (USA) = 0.350

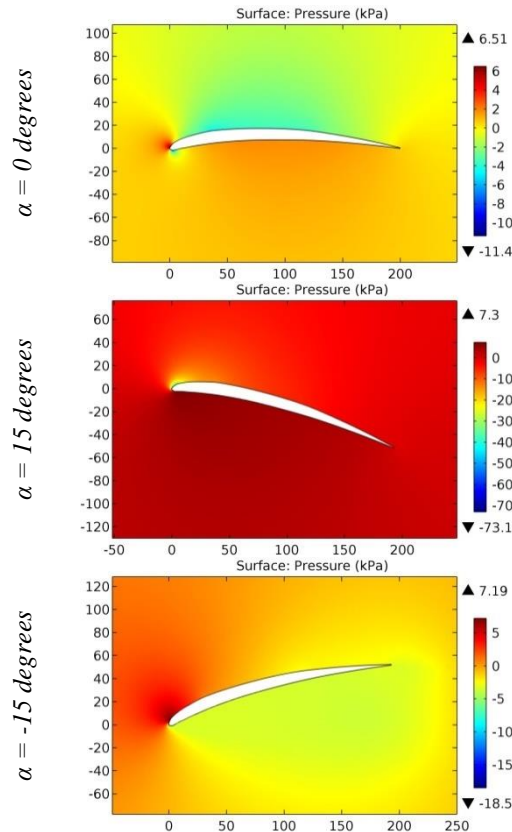


Figure 149. The pressure contours on the surfaces of the GOE 342 airfoil.

A maximum increase in pressure at the leading edge occurs at the angle of attack of -15 degrees for the following airfoils: G6, GEMINI (smoothed), GIII BL0, GIII BL45, GIII BL75, GMARTIN4, GO-436B, GO-624B, GOE 12K, GOE 13K, GOE 14K, GOE 15K, GOE 16K, GOE 190 (MVA MK,18), GOE 217 (MVA MK,12), GOE 222 (MVA H,33), GOE 223 (MVA H,34), GOE 227 (MVA H,37), GOE 228 (MVA H,38), GOE 229 (MVA H,39), GOE 234 (MVA CA5), GOE 241 (MVA PR,1), GOE 243 (MVA PR,3), GOE 255 (MVA CA,6), GOE 256 (JUNKERS E), GOE 284, GOE 285, GOE 288, GOE 289 (MVA 289), GOE 290 (MVA 290) and GOE 298. A maximum increase in pressure at the leading edge

occurs at the angle of attack of 15 degrees for the remaining airfoils.

### Conclusion

The most optimal aerodynamic characteristics have been determined for the convex-concave airfoils of the GOE series used in the subsonic airplanes wings structures. The airfoils used in the transonic airplanes wings structures are characterized by an increase in drag during climb. The wings geometry of the supersonic airplanes provides improvement of the aerodynamic characteristics during horizontal flight and the airplane descent.

### References:

1. Anderson, J. D. (2010). *Fundamentals of Aerodynamics*. McGraw-Hill, Fifth edition.
2. Shevell, R. S. (1989). *Fundamentals of Flight*. Prentice Hall, Second edition.
3. Houghton, E. L., & Carpenter, P. W. (2003). *Aerodynamics for Engineering Students*. Fifth edition, Elsevier.
4. Lan, E. C. T., & Roskam, J. (2003). *Airplane Aerodynamics and Performance*. DAR Corp.
5. Sadraey, M. (2009). *Aircraft Performance Analysis*. VDM Verlag Dr. Müller.
6. Anderson, J. D. (1999). *Aircraft Performance and Design*. McGraw-Hill.

## Impact Factor:

**ISRA (India) = 6.317**  
**ISI (Dubai, UAE) = 1.582**  
**GIF (Australia) = 0.564**  
**JIF = 1.500**

**SIS (USA) = 0.912**  
**ПИИИ (Russia) = 3.939**  
**ESJI (KZ) = 9.035**  
**SJIF (Morocco) = 7.184**

**ICV (Poland) = 6.630**  
**PIF (India) = 1.940**  
**IBI (India) = 4.260**  
**OAJI (USA) = 0.350**

7. Roskam, J. (2007). *Airplane Flight Dynamics and Automatic Flight Control, Part I*. DAR Corp.

8. Etkin, B., & Reid, L. D. (1996). *Dynamics of Flight, Stability and Control*. Third Edition, Wiley.

9. Stevens, B. L., & Lewis, F. L. (2003). *Aircraft Control and Simulation*. Second Edition, Wiley.

10. Chemezov, D., et al. (2021). Pressure distribution on the surfaces of the NACA 0012 airfoil under conditions of changing the angle of attack. *ISJ Theoretical & Applied Science*, 09 (101), 601-606.

11. Chemezov, D., et al. (2021). Stressed state of surfaces of the NACA 0012 airfoil at high angles of attack. *ISJ Theoretical & Applied Science*, 10 (102), 601-604.

12. Chemezov, D., et al. (2021). Reference data of pressure distribution on the surfaces of airfoils having the names beginning with the letter A (the first part). *ISJ Theoretical & Applied Science*, 10 (102), 943-958.

13. Chemezov, D., et al. (2021). Reference data of pressure distribution on the surfaces of airfoils having the names beginning with the letter A (the second part). *ISJ Theoretical & Applied Science*, 11 (103), 656-675.

14. Chemezov, D., et al. (2021). Reference data of pressure distribution on the surfaces of airfoils

having the names beginning with the letter B. *ISJ Theoretical & Applied Science*, 11 (103), 1001-1076.

15. Chemezov, D., et al. (2021). Reference data of pressure distribution on the surfaces of airfoils having the names beginning with the letter C. *ISJ Theoretical & Applied Science*, 12 (104), 814-844.

16. Chemezov, D., et al. (2021). Reference data of pressure distribution on the surfaces of airfoils having the names beginning with the letter D. *ISJ Theoretical & Applied Science*, 12 (104), 1244-1274.

17. Chemezov, D., et al. (2022). Reference data of pressure distribution on the surfaces of airfoils (hydrofoils) having the names beginning with the letter E (the first part). *ISJ Theoretical & Applied Science*, 01 (105), 501-569.

18. Chemezov, D., et al. (2022). Reference data of pressure distribution on the surfaces of airfoils (hydrofoils) having the names beginning with the letter E (the second part). *ISJ Theoretical & Applied Science*, 01 (105), 601-671.

19. Chemezov, D., et al. (2022). Reference data of pressure distribution on the surfaces of airfoils having the names beginning with the letter F. *ISJ Theoretical & Applied Science*, 02 (106), 101-135.